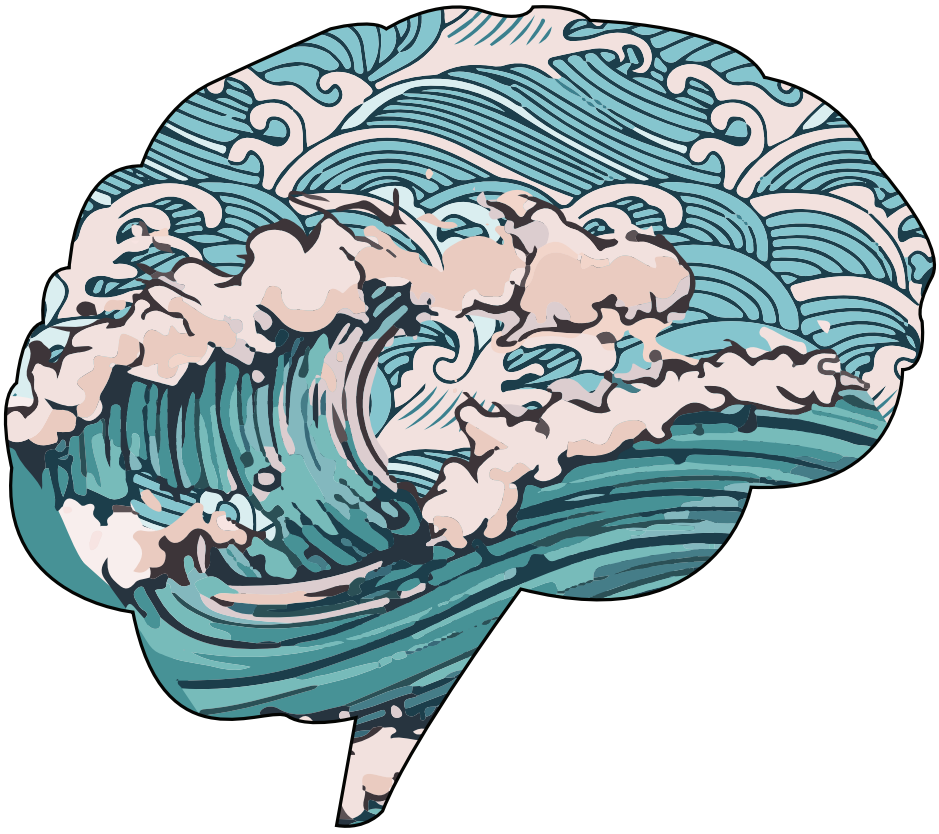

DRIVING VISUAL CORTEX TO STUDY NEURONAL OSCILLATIONS

Jim D. Herring

DONDERS
SERIES

Driving visual cortex to study neuronal oscillations

Jim D. Herring

ISBN: 978-94-6284-120-8

Printing: Ridderprint BV - www.ridderprint.nl
Lay-out: Ridderprint BV - www.ridderprint.nl
Cover: James Jardine - www.designyourthesis.com

Driving visual cortex to understand neuronal oscillations

Proefschrift

ter verkrijging van de graad van doctor
aan de Radboud Universiteit Nijmegen
op gezag van de rector magnificus prof. dr. J.H.J.M. van Krieken,
volgens besluit van het college van decanen
in het openbaar te verdedigen op 8 december 2017
om 10.30 uur precies

door
Jimmy Don Herring
geboren op 29 april 1987
te Kerkrade

Promotor
Prof. dr. O. Jensen

Copromotor
Dr. T.O. Bergmann (Eberhard Karls Universität Tübingen, Duitsland)

Manuscriptcommissie
Prof. dr. W.P. Medendorp
Prof. dr. C. Herrmann (Carl von Ossietzky Universität Oldenburg, Duitsland)
Dr. J.F.M. Jehee

Contents

CHAPTER 1

General introduction

Writing a thesis

Imagine sitting in your living room with a glass of wine or beer, while you are working on the umpteenth revision of the manuscript you wanted to submit a few weeks ago. It is late in the evening; your kid is fast asleep. Your significant other is relaxing and watching TV. You try to focus your attention on your laptop, while ignoring the sounds that originate from the TV. You are able to ignore the sounds from the TV and successfully work on your manuscript. Suddenly, you faintly hear your kid calling your name from upstairs. Although the child's voice was not as loud as the sounds from the TV, it immediately grabs your attention and your focus of attention shifts to the noises coming from upstairs. You rush upstairs and find your child sobbing in bed telling you he, or she, had a nightmare. You comfort your child, go back downstairs and continue your writing.

How were you successfully able to block the sounds from the TV, while still being able hear your child calling from upstairs? Alpha oscillations have been suggested to serve this purpose by blocking out irrelevant stimuli, while still allowing for processing information that is salient enough (Klimesch et al., 2007; Jensen and Mazaheri, 2010).

Alpha oscillations as a mechanism of functional inhibition

Traditionally, alpha oscillations were thought not to be actively involved in sensory processing (Berger, 1929; Adrian and Matthews, 1934). Up until recently, alpha oscillations were seen as a mechanism of 'cortical idling' (Pfurtscheller et al., 1996). Recent evidence has shown that alpha oscillations are very actively involved in cortical processing. For example, it has been shown that when participants are asked to retain certain items in working memory, the power of alpha oscillations increases linearly with working memory load (Jensen et al., 2002; Tuladhar et al., 2007; Scheeringa et al., 2009). Additionally, alpha oscillations have been thought to be under influence of top-down attention. Generally, alpha goes up in regions processing irrelevant (ignored, unattended) information. For example, when spatial attention is directed to the left visual field and the right visual field has to be ignored, alpha oscillations in the hemisphere ipsilateral to the attended hemifield increase in magnitude, while contralateral alpha oscillations decrease (Worden et al., 2000; Sauseng et al., 2005; Thut et al., 2006a). This is also evident from studies investigating cross-modal attentional shifts. In a classical example, alpha oscillations increase in magnitude in visual regions when attention is directed towards the auditory modality (Foxe et al., 1998). Furthermore, alpha oscillations have been shown to be modulated by attention in somatosensory regions (Haegens et al., 2011a;

Haegens et al., 2011b; van Ede et al., 2011). Importantly, these modulations in the alpha band were related to detection performance (Händel et al., 2011). However, it remains problematic to quantify the exact contribution of modulations in the alpha-band in explaining behavior (van Ede et al., 2012). In this thesis, I attempted to investigate **whether alpha oscillations are an intrinsic property of the visual system.**

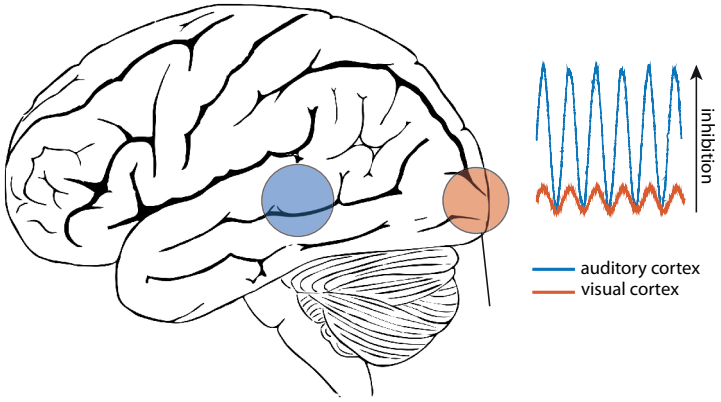

Figure 1. *Alpha oscillations block distracting input.* In this schematic example, sensory input from the auditory cortex (blue) is blocked, while sensory input from the visual cortex (red) is not. The schematic traces on the right indicate the level of inhibition for each region. For auditory cortex, sensory input must have a very high saliency for it to be processed, while visual input would easily reach the excitation threshold.

The afore mentioned studies and many similar studies have led to the hypothesis that alpha oscillations serve as a mechanism of *pulsed functional inhibition* (Figure 1; Jensen and Mazaheri, 2010). In this framework, alpha oscillations gate information flow in the brain by inhibiting task-irrelevant regions. This inhibition is thought to be phasic in that states of excitation and inhibition alternate within each cycle of alpha (Jensen et al., 2014). This notion is backed by studies showing coupling of bottom-up gamma-band activity to alpha-band oscillations (Jensen and Colgin, 2007; Osipova et al., 2008). The idea, similar to theta-phase coding in hippocampus, is that bouts of bottom-up activity, as reflected by gamma-band oscillations, are grouped and segregated by alpha-oscillations. However, evidence for the role of phase in the pulsed-inhibition framework is still sparse. In this thesis I therefore attempt to answer the question: **Do cortical alpha oscillations serve as a mechanism of functional inhibition by phasically modulating visual processing?**

In the example of you sitting on the couch writing your thesis you are using top-down attention to block distracting sensory input (the sounds from the TV). This would be reflected as an increase in alpha oscillations in the audio cortex. However, this inhibition

is pulsed: overall auditory input is suppressed, but in phases of excitability and suppression. The high saliency of your child's voice exceeds the threshold of this suppression allowing it to be processed and grab your attention.

EEG and MEG

Both electroencephalography (EEG) and magnetoencephalography (MEG) are tools used to measure neuronal firing. When neurons fire, they produce current flows. Action potentials are too short lived (~2 ms) for us to measure with EEG. With EEG, we mostly measure currents flowing as a result of synaptic excitation of dendrites. Current spread of postsynaptic potentials (~10 ms) along the apical dendrites form electrical dipoles (see Figure 2). As EEG is not sensitive enough to measure single neurons, thousands of neurons have to fire simultaneously for it to be measurable. Additionally, these neurons have to be somewhat aligned in parallel to avoid cancellation of measurable electric fields. For these reasons, we usually measure activity from large cortical pyramidal cells in deep layers. Not only the intracellular (primary currents), but also the extracellular currents (secondary, or volume currents) contribute to the magnetic field measured in the MEG.

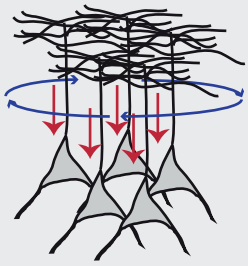

Figure 2. The electric current along the apical dendrites (in red) is measureable with EEG. While the magnetic field produced by this current flow (blue) is measurable with MEG.

In **chapter 2** I measured EEG, while in **chapters 3** through **5**, I measured MEG. Throughout this thesis, I was investigating posterior alpha oscillations. To achieve this, I usually applied a version of *time-frequency analysis* in which a fast-Fourier transform (FFT) is performed on segments of the data in a moving time-window approach. A moving time-window approach implies analyzing the raw data from beginning to end in pre-specified segments, or windows (for example, within one trial). By extracting *power* and *phase* of oscillations for each of these time windows, you can see these parameters develop over time.

With EEG and MEG, activity is typically measured at the scalp level. However, we would rather see what is going on inside the brain. Luckily, we have certain mathematical tricks that we can perform to estimate activity at the source. In **chapters 1, 2,** and **3**, I used linearly constrained minimum variance (LCMV; Van Veen et al., 1997) and dynamic imaging of coherent sources (DICS; Gross et al., 2001) beamforming techniques to estimate activity at the source level. Mathematically, LCMV and DICS are very similar. Both use a combination of a volume conduction model (a model of the head containing conductivity values of various tissue types in the head) and the covariance of the data (how does the data from each sensor relate to the data from every other sensor) to estimate activity at predefined sources. The major difference being that DICS works in the frequency domain, and LCMV in the time domain.

Non-invasive brain stimulation as a tool to study alpha oscillations

Although converging evidence exists on the role of alpha oscillations in sensory processing and memory, most of this evidence is correlational in nature. Non-invasive brain stimulation techniques such as transcranial magnetic stimulation (TMS) and transcranial current stimulation (TCS) have been used in recent years in an attempt to modulate, disrupt, and drive cortical oscillations such as posterior alpha oscillations. For example, with TMS it has been shown that stimulation in the alpha band (10-12 Hz) performance on various visual tasks could be disrupted (Romei et al., 2010; Romei et al., 2011). Additionally, illusory flashes induced by direct cortical stimulation of the visual cortex by TMS (i.e. phosphenes) showed a perceptual dependency on the phase of alpha oscillations in that phosphenes were more likely to be seen when TMS was applied at specific phases of alpha (Dugue et al., 2011). In an attempt to 'entrain' posterior alpha oscillations, (Thut et al., 2011a) applied short bursts of TMS at 10 Hz and observed an increase in alpha-band oscillations. Entrainment relies on the assumption that a network consisting out of oscillators can be externally driven so that the endogenous oscillation follows the external rhythm (Thut et al., 2011a). This same principle underlies a handful of studies attempting to drive alpha band oscillations using transcranial alternating current stimulation (TACS) (e.g. Helfrich et al., 2014; Neuling et al., 2015). Although the amount of current reaching the target cortical region is rather low, according to a physical principle called *Arnold's tongue* an external rhythm can drive any internal rhythm given that either the magnitude is strong enough or the external rhythm is close to the natural resonance frequency of the system (Ali et al., 2013). Similar to soldiers walking in rhythm on a bridge, relatively weak TACS could therefore drive endogenous alpha oscillations. This is important as the efficacy of TCS, specifically transcranial direct cur-

rent stimulation (TDCS) has recently been brought into question (Horvath et al., 2014, 2015). A study in human cadavers has suggested that the current reaching the cortex by applying TACS to scalp is too low to effectively induce spiking (Underwood, 2016). However, it was already known that TACS cannot induce action potentials, yet is able to modulate the external membrane potential of neurons slightly shifting states of excitability (Moreno-Duarte et al., 2014). Additionally, a recent study recording intracranial while TACS was applied in macaque monkeys showed the current reaching the target region is sufficient to modulate neuronal populations modulating neuronal adaption (Kar et al., 2017). It is evident that more studies are necessary to clarify the efficacy and mechanisms of TCS in modulating neuronal activity. To this extent neuroimaging techniques can be combined with brain stimulation techniques, such as TDCS and TACS, to study its effects during and after stimulation (Bergmann et al., 2016).

TMS

Transcranial magnetic stimulation (TMS) is a non-invasive brain-stimulation technique in which electrical fields can be generated inside the brain without opening the scalp. TMS works by applying a very brief (~0.1 ms), strong current through a circular coil, whose magnetic field, according to the principle of induction, induces an electric field in the target area. When stimulating nerve tissue, this electric field is strong enough to induce action potentials.

The intensity of the magnetic field produced by the TMS coil decreases exponentially with distance from the coil. For this reason, we are usually only able to stimulate the surface of the cortex. The magnetic field can be optimized by changing the shape of the coil. A typical TMS experiment uses a so-called figure-of-eight, or butterfly coil. This is basically two coils attached next to each other, in the shape of an eight. The advantage of this configuration is that the magnetic field is maximum in the center where both coils meet.

TMS can be used in various ways to probe, disrupt, and modulate activity in the brain. I used TMS in chapter 2 to probe cortical excitability and evoke alpha oscillations. To this end, I applied single pulses of TMS. Other examples of protocols are paired-pulse, rhythmic, and theta-burst TMS. Each protocol serves specific purposes and usually differs in terms of the rate of stimulation (frequency) and amount of pulses.

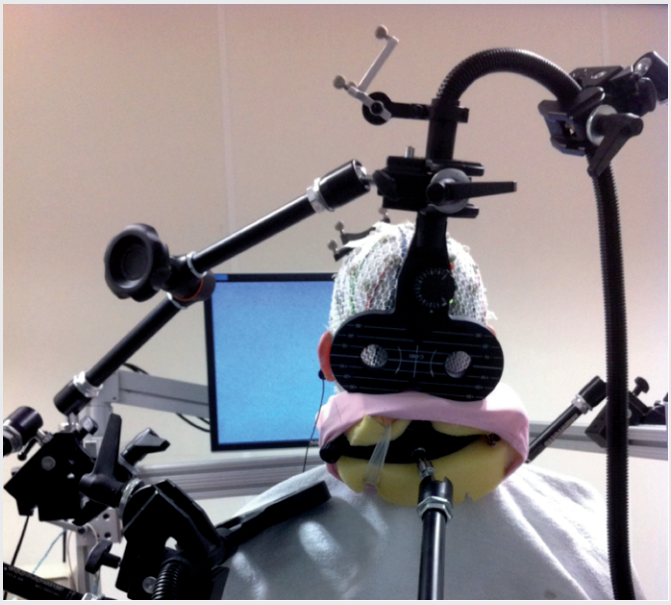

Figure 3. Experimental setup of **chapter 2**. The figure-of-eight, or butterfly, coil can be seen placed against the back of the participant's head. The coil is held in place using adjustable arms to keep a stable position throughout the experiment. In **chapter 2** I combined TMS with concurrent EEG. The EEG cap contains electrodes which are specifically suitable for combined TMS-EEG recordings; the electrodes are flat to minimize the distance from the scalp to the TMS coil and they contain a slit to avoid induction of Eddy currents. Additionally, on top of the head and attached to the coil trackers allow for real-time neuronavigation. Together with the participants anatomical MRI scan I tracked the position of the TMS coil, with respect to the subject's brain, throughout the experiment.

TACS

Transcranial alternating current stimulation is a specific form of current stimulation (next to transcranial direct current stimulation; TDCS) in which a weak alternating current is applied to the scalp using two, or more, electrodes. Unlike TMS, TACS does not induce action potentials and is thought to work by slightly modulating a neuron's resting membrane potential. This should then result in a slight change in the excitability of the neuron making it easier, or more difficult, to induce firing by other input.

Because of its rhythmic properties, TACS is thought to be suitable to modulate, or perhaps entrain, neuronal oscillations, by rhythmically changing resting membrane potentials of groups of neurons. For this reason, I applied TACS in **chapter 4** in an attempt to drive posterior alpha oscillations.

In **chapter 4**, I concurrently measured MEG while applying TACS. The artifacts produced by TACS in the MEG signal are problematic but in theory MEG is more suitable to combine with TACS than EEG. The stimulators we use in TACS experiments are current sources, not voltage sources as your typical battery is. The stimulator keeps the current constant by adjusting the voltage to the resistance of the circuit. Throughout a typical experiment the resistance fluctuates due to, for example, sweating of the participant and drying of the conductive gel. These small fluctuations are compensated by the stimulator by changes in voltage. These small potential differences will be measurable by EEG and will make artifact correction more complicated. Magnetic field, on the other hand, solely depend on the current, not the voltage, in an electric circuit, and are therefore insensitive to the small fluctuations in voltage produced by the stimulator.

Frequency tagging to probe neocortical excitability

A promising approach to study the role of neuronal oscillations in sensory processing is frequency tagging. Frequency tagging is an experimental design in which one, or more stimuli, are presented at a fixed flickering rate. This produces robust steady-state visually evoked potentials, or fields (respectively SSVEPs or SSVEFs, for EEG and MEG), with high power at the tagged frequency (Vialatte et al., 2010). Frequency tagging has been used to study the effect of attention on selective stimulus processing (Müller et al., 1998; Müller et al., 2003; Müller et al., 2006; Vialatte et al., 2010), binocular rivalry (Tononi et al., 1998; Srinivasan et al., 1999; Srinivasan, 2004), visual perception in MEG (Parkkonen et al., 2008), as well as representational selectivity in down-stream areas (Baldauf and Desimone, 2014).

The magnitude of the response to the tagged frequency is not uniform across different presentation frequencies. Both in humans (Herrmann, 2001) and animals (Rager and Singer, 1998) it was evident that stimuli tagged at frequencies close to endogenous oscillations produce higher magnitude responses. For example, Rager and Singer (1998) presented anesthetized cats with stimuli flickering between 2 Hz and 50 Hz while measuring local-field potentials (LFPs) and multi-unit activity (MUA) from the visual cortex. The authors compared the measured response to a model of superimposed VEPs to single flashes at the rate of presentation. The model predicted the data rather well, except for stimuli presented between 10 Hz and 13 Hz (α-band), and between 30 Hz and 50 Hz (γ-band). Rager and Singer (1998) argue stimulation at these frequencies cause resonance with naturally occurring oscillations. These effects can indeed be seen as 'entrainment' of cortical oscillations (Thut et al., 2011a). When using frequency tag-

ging to study bottom-up sensory processing, entrainment of neuronal oscillations is problematic as it introduces a confound by interacting with processes thought to be important in neuronal processing. With this thesis I hope to answer the question: **can rapid frequency tagging be used as a tool to study the role of neuronal oscillations in visual information processing?**

Main research aims and outline

In this thesis, I examine the functional role of posterior alpha band oscillations in visual sensory processing. Using various non-invasive brain-, and visual, stimulation techniques I examine how processing of visual information is guided by neuronal oscillations.

More specifically, with this thesis I aimed at answering the following questions:

1. Are cortical alpha oscillations an intrinsic property of the visual system (**chapter 2 and 3**)?
2. Do cortical alpha oscillations serve as a mechanism of functional inhibition by phasically modulating visual processing (**chapter 4 and 5**)?
3. Can rapid frequency tagging be used as a tool to study the role of neuronal oscillations in visual information processing (**chapter 5**)?

CHAPTER 2

Attention modulates TMS-locked alpha oscillations in the visual cortex

Appeared as:

Herring, J. D., Thut, G., Jensen, O., & Bergmann, T. O. (2015). Attention modulates TMS-locked alpha oscillations in the visual cortex. *Journal of Neuroscience*, *35*(43), 14435-14447.

Abstract

Cortical oscillations such as 8-12 Hz alpha-band activity are thought to subserve gating of information processing in the human brain. While most of the supporting evidence is correlational, causal evidence comes from attempts to externally drive ('entrain') these oscillations by transcranial magnetic stimulation (TMS). In fact, the frequency profile of TMS-evoked potentials (TEP) closely resembles that of oscillations spontaneously emerging in the same brain region. However, it is unclear whether TMS-locked and spontaneous oscillations are produced by the same neuronal mechanisms. If so, they should react in a similar manner to top-down modulation by endogenous attention. To test this prediction, we assessed the alpha-like EEG response to TMS of the visual cortex during periods of high and low visual attention while participants attended to either the visual or auditory modality in a cross-modal attention task. We observed a TMS-locked local oscillatory alpha response lasting several cycles post-TMS (but not post-Sham stimulation). Importantly, TMS-locked alpha power was suppressed during deployment of visual relative to auditory attention, mirroring spontaneous alpha amplitudes. In addition, the early N40 TEP component, located at the stimulation site, was amplified by visual attention. The extent of attentional modulation for both TMS-locked alpha power and N40 amplitude did depend, with opposite sign, on the individual ability to modulate spontaneous alpha power at the stimulation site. We therefore argue that TMS-locked and spontaneous oscillations are of common neurophysiological origin, whereas the N40 TEP component may serve as an index of current cortical excitability at the time of stimulation.

Significance Statement

Rhythmic transcranial magnetic stimulation (TMS) is a promising tool to experimentally 'entrain' cortical activity. If TMS-locked oscillatory responses actually recruit the same neuronal mechanisms as spontaneous cortical oscillations, they qualify as a valid tool to study the causal role of neuronal oscillations in cognition but also to enable new treatments targeting aberrant oscillatory activity in e.g. neurological conditions. Here, we provide first-time evidence that TMS-locked and spontaneous oscillations are indeed tightly related and are likely to rely on the same neuronal generators. In addition, we demonstrate that an early local component of the TMS-evoked potential (the N40) may serve as a new objective and non-invasive probe of visual cortex excitability, which so far was only accessible via subjective phosphene reports.

Introduction

Cortical oscillations reflect the synchronization of large neuronal populations, rhythmically shifting between states of excitability (Schroeder and Lakatos, 2009). By modulating synaptic input and synchronizing neuronal output (Varela et al., 2001; Fries, 2005) they may temporally organize information processing and communication between brain areas and thus support a variety of cognitive functions (VanRullen and Koch, 2003; Buzsaki and Draguhn, 2004; Engel and Fries, 2010; Hanslmayr et al., 2011; Jensen et al., 2014). Yet, although numerous studies have linked cortical oscillations to task performance, the causal relevance of these oscillations remains to be proven (Thut et al., 2012).

To this end, neuronal oscillations need to be experimentally manipulated to investigate their immediate impact on behaviour. Research in humans can benefit from non-invasive brain stimulation techniques like transcranial magnetic stimulation (TMS) and transcranial alternating current stimulation (tACS) to directly induce frequency-specific rhythmic activity in the brain (Thut et al., 2011a; Herrmann et al., 2013). While entrainment effects of tACS supposedly rely on subtle shifts in neurons' membrane potential, rTMS is capable of periodically triggering action potentials, and supposedly drive neuronal oscillations (Thut et al., 2011a). Accordingly, short trains of rTMS in the 8-14 Hz alpha range were found to produce frequency-specific effects on task performance (Klimesch et al., 2003; Sauseng et al., 2009; Romei et al., 2010; Romei et al., 2011; Jaegle and Ro, 2014; Ruzzoli and Soto-Faraco, 2014) in line with the supposed cognitive function of alpha oscillations as rhythmic inhibition of task-irrelevant brain regions (Klimesch et al., 2007; Jensen and Mazaheri, 2010). However, evidence for actual 'entrainment' in electrophysiology is still sparse (Thut et al., 2011b; Hanslmayr et al., 2014). The question remains open whether oscillatory responses locked to transcranial stimulation and spontaneously occurring neuronal oscillations originate from the same neuronal generator.

Supporting the notion of a common mechanism for TMS-locked and spontaneous oscillations, the frequency profile of TMS-evoked potentials (TEP) demonstrates site- and state-specificity resembling that of spontaneous oscillations: Firstly, it predominates at the frequency of neuronal oscillations naturally generated in the stimulated brain region, e.g. in the alpha range for the visual cortex (Rosanova et al., 2009; Garcia et al., 2011). Secondly, it depends on the current state of vigilance, e.g. wake vs. deep sleep (Massimini et al., 2007; Bergmann et al., 2012).

We argue that, if TMS-locked alpha oscillations in the visual cortex resemble spontaneous alpha oscillations, they should both be subject to top-down control, i.e. suppressed when visual attention is high but boosted when visual attention is low, as during endogenous crossmodal shifts of attention (Adrian, 1944; Fu et al., 2001). In contrast, early TEP components, reflecting immediate cortical excitation, should depend on visual cortex excitability itself and therefore show the opposite pattern. To test these hypotheses, we applied single-pulse TMS to the left visual cortex (intermingled with Sham TMS to the left shoulder to control for auditory and somatosensory input) while participants performed a cross-modal detection task, requiring them to attend to a visual while ignoring an auditory input stream (*High visual attention*) or vice versa (*Low visual attention*).

Materials and Methods

Participants

Participants were recruited from a participant database from the Radboud University. Twenty-four healthy subjects with normal or corrected-to-normal vision (15 females, 9 males) participated in the experiment. All subjects conformed to standard inclusion criteria for MRI, EEG, and TMS. Written informed consent was gathered at the start of the experiment according to the Declaration of Helsinki. The study was approved by the local ethics committee. Participants were compensated financially at a rate of 10 euros per hour.

Procedure

All subjects participated in an intake session and one experimental session on two separate days. During the intake session a structural MRI scan was obtained for subsequent neuronavigation of TMS. Participants were familiarized with the cross-modal attention task followed by the determination of TMS intensity and location as well as titration of visual and auditory stimulus parameters using an adaptive staircase procedure (see below). During the experimental session, subjects were first prepared for EEG recordings and TMS neuronavigation. Then, resting state EEG was recorded for two minutes with eyes open and two minutes with eyes closed, before participants performed a 5 minute training session of the cross-modal attention task while the EEG was recorded but without applying TMS. Afterward, the cross-modal attention task was performed in short blocks of 15-60 seconds alternating between conditions (see below) while EEG was recoded and TMS was applied (main experiment). Every 5 minutes, short breaks were introduced (Fig. 1A).

Attention task

Participants performed a blocked cross-modal attention task (Figure 1A). Each block began with a brief audio-visual cue, i.e. the spoken and written words 'Listen' or 'Look', instructing the participants to pay attention to either the visual or the auditory background noise stream. They were presented simultaneously via a 17" TFT-monitor (resolution: 1024 x 768, refresh rate: 60Hz, viewing distance: 60 cm) and earphones, respectively. In addition, the color of a central fixation dot indicated the block type throughout the entire experiment (green: Attend visual, red: Attend auditory) to prevent potential confusion. Participants had to detect subtle 'targets' only in the attended background noise stream while ignoring changes in the other as distracting stimuli have been shown to increase alpha modulation (Haegens et al., 2012). Cue validity was thus always 100 %. For the visual background noise, the grayscale value of each pixel on the screen was randomly drawn from a uniform distribution. Visual targets consisted of small circular patches, 4 degrees visual angle in size, whose pixels were increased in contrast compared to the background (Figure 1B) for a period of 500 ms. The patches could appear at any location on the screen (except for a one patch-wide margin, 4 degrees visual angle, along the edge of the display and around the fixation dot), i.e. between 4 to 8 degrees vertically and 4 to 13 degrees horizontally relative to the fixation dot. Participants were informed that the patches could appear anywhere on the screen to encourage attention to the entire display. The auditory background noise stream was constructed from the discrete Fourier transform of an audio sample (48 kHz, stereo) of one TMS click. To this end, the phase of each resulting frequency bin was first randomly shuffled. The phase-shuffled frequency domain data was then back-transformed to the time domain using an inverse Fourier transform. Finally, these phase-shuffled TMS click sounds were randomly concatenated, resulting in a constant stream of noise which contained the same frequency band power as the TMS clicks and was therefore particularly suited to attenuate the sound from the actual TMS pulses. Auditory targets consisted of transient fluctuations in noise volume for 500 ms at a 30 Hz rate (Figure 1B). In other words, the volume of the noise was reduced and increased 30 times per second. Magnitudes of contrast (visual targets relative to noise) and volume (auditory targets relative to noise) were titrated individually in the intake-session to 80 % detection accuracy. Titration was performed using an adaptive staircase procedure following a one-up, three-down staircase in which three consecutive hits resulted in an increase in difficulty. The step-size of the change in difficulty decreased over trials converging to a level of 80 % detection accuracy in 40 trials. The task was presented using Matlab2012b (Mathworks) and the Psychophysics Toolbox (Kleiner et al, 2007). Blocks were of varying length (range = 15 to 60 s; mean = 37 s; SD = 13 s), unpredictable in duration for the participant, and were alternated between visual and auditory attention. The number of blocks per condition varied per subject as the length

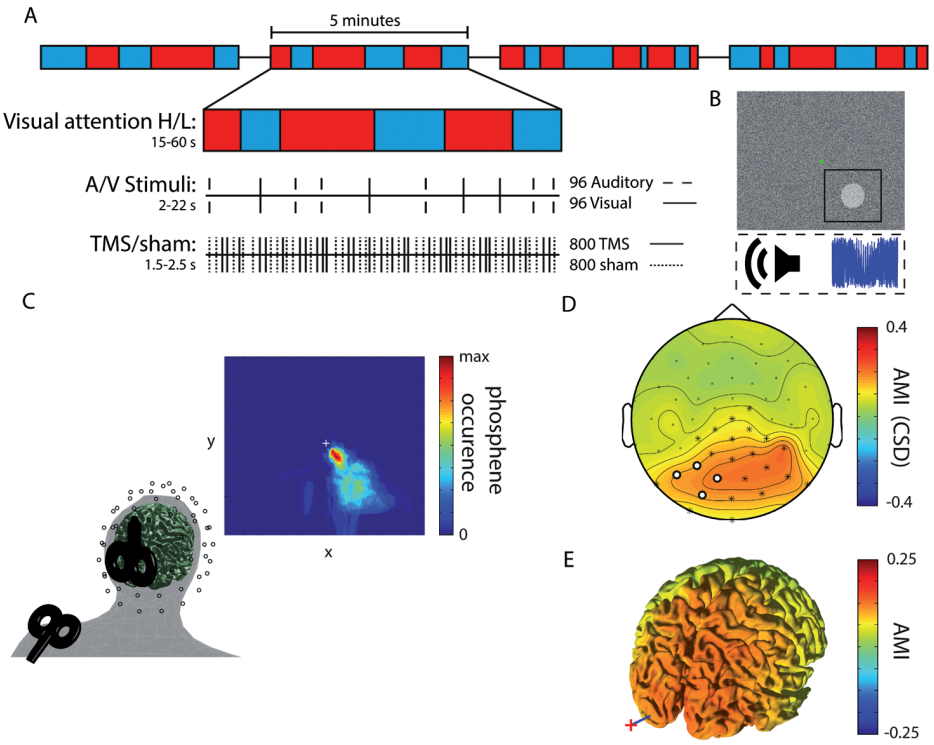

Figure 1. Experimental paradigm and setup. **A,** Experimental paradigm. Each run of 5 minutes consisted of 'attend auditory' or 'attend visual' blocks of varying length. Before the onset of each block, an audio-visual cue ("Look" or "Listen") indicated whether subjects had to attend to the visual modality (High visual attention) or to the auditory modality (Low visual attention). Both target (attended modality) and distractor (unattended modality) stimuli (500 ms duration) appeared unpredictably at a very low rate forcing participants to attend throughout the block. TMS and Sham pulses (shoulder TMS) were delivered randomly intermingled independently of the attentional task. **B,** Participants had to maintain fixation while detecting near-threshold changes in simultaneously ongoing streams of auditory and visual background noise. Visual target stimuli were brief transient increases in contrast within a circular patch at an unpredictable location within 4° to maximally 13° visual angle around the fixation dot. Auditory target stimuli were brief fluctuations in noise volume. **C,** Site of stimulation and anatomical coregistration. EEG electrode and TMS-coil positions were coregistered to individual MRIs. The TMS target site was determined by a phosphene tracing procedure within the left visual cortex resulting in the depicted average phosphene probability map (note that stimulation intensity during the experiment was below phosphene threshold). The Sham site at the left shoulder was matched with regard to subjective auditory and somatosensory perception to control for multisensory evoked EEG responses. **D,** CSD Topographical plot of the alpha modulation index (AMI): Low - High visual attention) / (Low + High visual attention). Channels indicated in white were used for analyses. Channels indicated in white and channels indicated with an asterisk showed significant alpha modulation at $p < 0.001$ (corrected for False Discovery Rate (Benjamini and Hochberg, 1995)). **E,** Source analysis of the alpha modulation index (AMI). The red cross and blue line indicates position of the TMS coil and target, respectively.

of each block was varied randomly (mean = 86 blocks, SD = 4 blocks). The order of trials and blocks were generated prior to onset of the experiment such that an equal number of blocks were presented for both attentional conditions. A visual or auditory stimulus could appear every 2 – 22 seconds with a 50 % chance of appearing in the attended modality. Participants were instructed to ignore stimuli in the unattended modality. In total, 48 auditory (24 targets), and 48 visual (targets) stimuli were presented. In total, 48 auditory, and 48 visual stimuli were presented.

TMS

TMS was applied with biphasic pulse configuration using a MagVenture C-B60 Butterfly coil connected to a MagPro-X100 stimulator (MagVenture, Farum, Denmark). The coil position and orientation was kept constant during the experiment using a frameless stereotactic neuronavigation system (Localite TMS Navigator, St. Augustin, Germany) after coregistration of individual MRI scans. Coregistration was achieved (using the Localite software) in a two-step procedure by first marking the position of three anatomical locations on the participant's head with a digitizing pen; nasion, left, and right outer canthus corresponding to markers set in the individual's MRI. Secondly, a scalp surface registration was performed to further improve the coregistration by tracing the scalp surface using a digitizing pen followed by a fitting of the individual MRI to the traced scalp surface. The coregistration was accepted if the root mean squared error of the fitting procedure was below 3 mm.

The coil position, orientation, and stimulation intensity were individually determined in the intake session using a phosphene thresholding procedure (Dugue et al., 2011). During this procedure the room was darkened and subjects adapted to darkness for about 10 min. Starting 2 cm left of the inion with the handle pointing upward; trains of 7 pulses at 20 Hz were applied at 70 % maximum stimulator output (MSO) with the most significant induced current (i.e. 1st flank of 2nd half wave) in the brain tissue flowing in the anterior-posterior direction. The coil was moved around in small steps until a location was found that reliably produced a phosphene in the lower right visual field. This procedure ensured that we effectively targeted the visual cortex. After a location was found, five trains of pulses were given after which subjects were asked to draw the outline of the phosphene percept with a mouse on the screen (Figure 1C provides a map for the phosphenes across subjects). Following this procedure we assessed the intensity at which subjects would perceive phosphenes in 50% of trials (phosphene threshold) with single-pulse TMS using a manual staircase procedure. Starting at 70 % MSO, the intensity was increased in steps of 5 % per TMS pulse until the participant reported seeing a phosphene. The intensity was then decreased in steps of 1 % until no phosphene was perceived anymore. 6 pulses were applied to assess whether

phosphenes were perceived in 50 % of trials. Depending on whether a phosphene was perceived in more or less than 50 % of trials the intensity was decreased or increased by 1 %, respectively, until the 50 % threshold was found. To ensure the determined phosphene threshold was not confounded by participants' expectancy due to the regularity of the staircase procedure we always pretended to change the intensity of the 6 consecutive pulses while actually keeping it constant. On average, phosphene threshold was 68 % (SD = 8 %) of the MSO. Stimulation intensity during the experiment was set at 80 % of phosphene threshold (mean = 55 % MSO, SD = 6 % MSO).

Since auditory stimulation alone can cause phase reset in the visual cortex (Romei et al., 2012) a multisensory Sham condition served as control. To reproduce the auditory and somatosensory sensation associated with the TMS pulse without stimulating the brain, a second TMS coil (Sham) was placed on the left shoulder blade on the superior border of the scapula (Figure 1C). For the Sham coil, stimulation intensity was matched to occipital TMS in terms of equal subjective loudness and reported sensory perception (mean = 59 % MSO, SD = 8 % MSO). Superimposed on the phase-shuffled TMS sound noise, we also presented a stream of randomly and densely packed (50 pulses per second) TMS click samples samples to further mask the sound of the actual TMS and Sham clicks.

Throughout the experiment, participants received 400 TMS and 400 Sham pulses per attention condition, randomly intermingled with an inter-pulse interval uniformly jittered between 1.5 and 2.5 s, resulting in a total of 800 TMS and 800 Sham pulses.

MRI data acquisition

A high-resolution T1-weighted image (TR = 2250 ms, TE = 2.58 ms, flip angle = 15°, 208 sagittal slices, in plane voxel size = 1×1×1 mm, FoV = 224×224 mm) was acquired using a 1.5T Avanto MRI scanner (Siemens, Erlangen, Germany) for TMS neuronavigation and EEG source analysis.

EEG data acquisition

The EEG was recorded from 61-channels and digitized at 5 kHz (filter: DC to 1000Hz) with 0.1μV/bit resolution using two battery-driven 32-channel BrainAmp DC amplifiers (BrainProducts) connected to a custom equidistant electrode cap (EasyCap M10) with TMS-compatible, extra flat Ag-AgCl ring electrodes with a slit in the ring to avoid magneto-induction (TMS Multitrodes, EasyCap). Skin resistance was kept below 5 kOhm by thorough preparation using abrasive Abralyt HiCl electrode paste (EasyCap). Recording reference was at the vertex while a separate ground electrode was placed on the right collarbone. Electrode positions were digitized and co-registered to the

individual anatomical MRI using a frameless stereotactic neuronavigation system (TMS Navigator, Localite).

EEG data analysis

EEG data were analyzed using Matlab2014a (Mathworks) and the FieldTrip Matlab toolbox (http://www.fieldtriptoolbox.org) (Oostenveld et al., 2011). EEG data were preprocessed blind to the experimental conditions. First, EEG data were re-referenced to the common grand average of all EEG channels and epoched to -1.5 to 2.5 s intervals around the onset of the TMS pulse. (Note that this time-window extended into preceding and following trials and was chosen for the purpose of filtering and time-frequency analysis only. Later this time-window was shortened to -0.2 to 1 s around the onset of TMS). The following steps are specific to TMS-EEG datasets and should be performed before any other forms of processing to avoid introducing additional artifacts. We have included a schematic pipeline (Figure 2A) to aid researchers in dealing with TMS-EEG datasets. This pipeline has been worked out in detail on a different dataset presented as a tutorial on http://www.fieldtriptoolbox.org/tutorial/tms-eeg. A period of -1 to 7 ms relative to the TMS pulse was cut out (Figure 2D) and excluded from the following steps in the artifact removal process to remove the initial 'ringing artifact' (0-7 ms) resulting from the step response of the hardware filter of the EEG amplifier (Figure 2B,D, red line). Pre- and post-'ringing' epochs were subsequently subjected to an independent component analysis (FastICA) to remove components reflecting (i) the 'exponential decay artifact' (Figure 2F) caused by electrode movements due to contraction of underlying muscles possibly in combination with concomitant depolarization of the electrode-electrolyte-skin interface (Ilmoniemi and Kicic, 2010), (ii) residual muscle artifacts (Korhonen et al., 2011) and (iii) to clean the data from eye-blinks, eye-movements, line noise, and other muscle artifacts unrelated to TMS (Jung et al., 2000). The 'exponential decay artifact' was identified in the ICA components after time-locking to the TMS pulse (Figure 2E). All ICA components were removed that clearly showed an exponential decay and or a sinusoidal waveform (single cycle upwards of 67 Hz, ending at 15 ms, see Figure 2C for an example) reflecting the muscle artifact starting at the TMS pulse and a topography that corresponded to the site of stimulation (Figure 2F). On average, 12 (range; 12 ± 2.5 M±SD) out of 60 components were rejected, of which 1 to 2 (range; 1.75 ± 0.75 M±SD) were related to the exponential decay and/or muscle artifact, 2 to 3 (range; 2.45 ± 0.88 M±SD) related to eye-artifacts (blinks/saccades), 1 to 2 (range; 1.83 ± 0.76 M±SD) related to line-noise, and 6 (range; 6.08 ± 2.20 M±SD) related to other muscle artifacts unrelated to TMS. As ICA was not always able to fully capture the sinusoidal muscle artifact, cubic interpolation was used subsequently to replace the -1 to 15 ms period of the ICA-cleaned signal in all subjects (see Figure 2G for a TMS-locked average cleaned solely of TMS-related artifacts). Following TMS-artifact removal, the data were downsampled

to 1 kHz. Prior to downsampling, a two-pass 4th order Butterworth low-pass filter with a cut-off frequency of 200 Hz was applied to prevent aliasing. Subsequently the data were z-transformed with the mean and standard deviation calculated over all time and

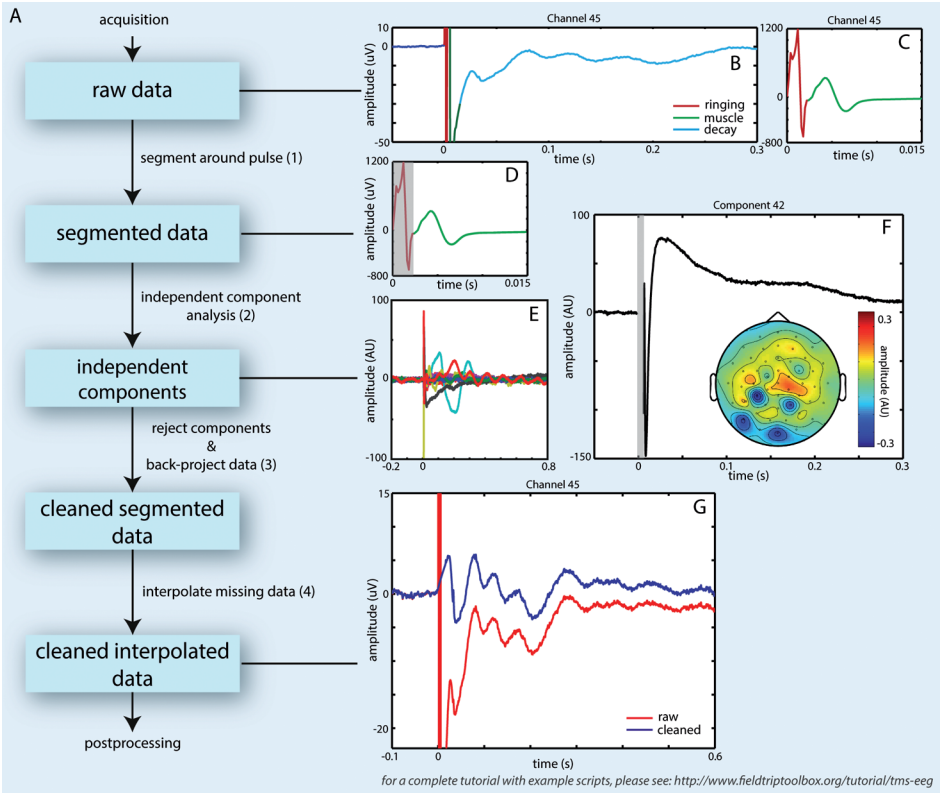

Figure 2. A, Processing pipeline for handling artifacts in TMS-EEG datasets. When dealing with TMS-EEG datasets it is important to remove the TMS-related artifacts as early as possible in the processing pipeline (prior to any filtering preceding downsampling) to avoid introduction of additional "ringing artifacts" due to interaction of filter kernels with existing artifacts. First, the types and extent of artifacts was assessed from TMS-locked averages (**B**,**C**). Artifacts are indicated by colored lines. The data were then (1) segmented to exclude the 'initial ringing' artifact (**B**,**C**, red line, **D**, shaded area) prior to conducting an *independent component analysis* (2). Time-locked averages of independent components (ICs) were used to identify ICs capturing TMS-related artifacts (**E**,**F**) taking into account topographical representations with extrema close to the stimulation site and adjacent cranial muscles. At this stage other components related to non-TMS artifacts were identified as well. Then the data was back-projected to channel space (3) without the artifactual components. At this stage the gap around the TMS pulse was interpolated. If the muscle artifact was not removed completely, this period was interpolated as well. TMS-locked averages were inspected afterwards to check that the cleaning was successful (**G**). (For a tutorial with example scripts on how to deal with TMS-EEG datasets, please see *http://www.fieldtriptoolbox.org/tutorial/tms-eeg*.")

trials. Trials containing values deviating more than 5 standard deviations were removed. Visual inspection was then performed on the remaining trials to remove trials containing residual muscle contractions. Additionally, trials that contained visual or auditory target stimuli were removed. This resulted in rejection of on average 418 (26%) ± 23 (2%) trials of which 96 trials due to the presence of an auditory or visual stimulus. After trial rejection 296 trials remained per condition, on average. Subsequently, data were band-pass filtered between 3 Hz and 45 Hz using a two-pass 4^{th} order Butterworth filter (104 dB/octave). Filtering was applied to the initial epochs (-1.5 to 2.5 s), but only the -0.2 to 1.0 s interval around the TMS pulse was considered for later analyses. The cut-off frequency of the high-pass filter was chosen relatively high to suppress contributions of slow fluctuations to the variance of faster components.

TMS-locked oscillations were analyzed based on time-frequency representations (TFRs) of power of the averaged TEPs by means of Fast Fourier Transform. The TEPs were multiplied with a Hanning tapered sliding time window moving in steps of 20 ms. The length of the time-window varied with frequency (T = 3 cycles = 3/f,). The mean and linear trends of the trial were subtracted from each time-window prior to the time-frequency analysis in case of residual offsets and trends after filtering (Luck, 2005). An absolute baseline correction was performed for each TFR by subtracting power estimates of the pre-TMS period (-0.5 to -0.2 s, to avoid overlap with the onset of the TEP) from the post-TMS interval. This was to avoid non-phase locked alpha activity surviving averaging from influencing the post-TMS power estimates.

To assess individual ability to modulate the power of alpha oscillations during cross-modal shifts of attention (i.e. Low vs. High visual attention), oscillatory activity was estimated in the baseline interval at -0.5 to -0.001 s relative to the TMS pulse by applying a fixed time-window to avoid confounding by the evoked response when using a sliding window. An *alpha modulation index* (AMI) was calculated for the pre-TMS interval (see Figure 1D):

$$\frac{Power_{Low\ visual\ attention} - Power_{High\ visual\ attention}}{Power_{Low\ visual\ attention} + Power_{High\ visual\ attention}}$$

Where indicated, topographical plots of scalp current source density (CSD) were calculated by fitting 4^{th} order spherical splines (first 9 Legendre polynomials, λ=1e-5) to the data at the last stage before plotting surface maps for the TMS-evoked potentials (Perrin et al., 1989, 1990). CSD maps of power values were calculated by estimating the CSD on the individual trials before performing Fourier analysis.

To localize the source of the alpha modulation due to the cross-modal shifts in attention prior to TMS onset we used a DICS beamformer approach (Gross et al., 2001). The DICS algorithm uses the cross-spectral density (CSD) matrix from the data and a lead field matrix to calculate a spatial filter. The CSD was calculated from a 500 ms pre-TMS time period (-0.5 s to -0.001 s) pooled across attention conditions by calculating the FFT centered at 8 Hz of the data multiplied by a Hanning taper. A realistic three-layer volume conduction model was constructed using the individual MRI using the boundary element method (BEM; Oostendorp et al., 1989). A grid with $1cm^2$ resolution was created per individual, which was subsequently normalized to MNI space. The lead field was calculated for each point in this grid. The spatial filter was then used to estimate power distributions for the attention conditions separately averaged over trials. The source of the TMS-locked alpha oscillations was similarly estimated with a spatial filter calculated on the single trial data (-0.5 s to 1 s) pooled over all conditions. The calculated spatial filter was then applied to the power estimates from the 0.4 s to 0.8 s period of the TEP for all conditions separately. Subsequently, an absolute baseline correction (-0.5 s to -0.1 s, to have an equal length of data for baseline and post-TMS period) was performed to account for any alpha power not-related to TMS surviving averaging. Similar to the sensor level data, an *alpha modulation index* was calculated for the source level data (see formula above).

Results

To test whether TMS-locked alpha oscillations in the visual cortex reflect the same neuronal processes as spontaneous alpha oscillations, we investigated whether they are modulated in a similar manner by endogenous top-down attentional control, i.e. decreased during high and increased during low visual visual attention (Figure 1A and B). To this end, we simultaneously applied either TMS to the visual cortex or Sham stimulation to the shoulder and recorded 61-channel EEG while participants attended to either the visual (High visual attention) or auditory (Low visual attention) modality.

Behaviour and attention manipulation

Performance in the cross-modal attention task remained close to 80 %: participants detected 84 % (SEM = 2 %) of the attended auditory targets and 81 % (SEM = 2 %) of the attended visual targets. Performance did not differ between conditions ($p > 0.2$; paired sample t-test).

The topographical distribution of the alpha modulation index (AMI) in Figure 1D clearly shows that top-down attention did indeed modulate pre-TMS alpha power as intended.

Low visual (i.e. high auditory) attention compared to High visual (i.e. low auditory) attention produced relative alpha power increases over posterior regions. The increase included the four channels close to the stimulation site (t_{23} = 2.35, p = 0.0137, one-sided). Furthermore, source analysis allowed us to identify cross-modal alpha power modulation to bilateral visual and parietal cortices (Figure 1E). We could not observe a clear alpha power modulation in auditory cortices, which may be due to difficulties in localizing alpha activity from audio cortices (Frey et al., 2014).

Visual attention enhanced early TEP N40 component

If top-down visual attention gates stimulus processing by up-and down-regulation of visual cortex excitability (Gilbert and Li, 2013), this should be reflected by the immediate responsiveness of the visual cortex to transcranial stimulation, i.e. larger early evoked potentials during epochs of High compared to Low visual attention. Figure 3A shows the TMS-evoked potentials (TEPs) for all experimental conditions for the four channels closest to the TMS coil (marked in insert).

TMS evoked potentials (TEPs) were calculated by averaging trials time-locked to the TMS pulse separately for each condition. Unless specified otherwise, data were averaged from electrodes closest to the stimulation site (channel no. 28, 29, 44, 45, see Fig. 1D, roughly corresponding to PO8, P3, O1, and PO7 in the 10-20 system) and baseline corrected (-0.05 to -0.01 s). We observed seven clearly identifiable components, i.e. P20, N40, P80, N90, P120, N200 and P300 (Figure 3A; note that other components may be prominent at other channels). Amplitudes of TEP components were extracted individually from the largest peak or trough, respectively, in the following time windows relative to the TMS pulse: 15-25 ms, 25-45 ms, 70-85 ms, 85-110 ms, 110-120 ms, 150-250 ms, and 250-350 ms. All components (i.e. P80-P300) after 50 ms were present not only for TMS but also Sham (albeit to a lesser degree, see Figure 3A), suggesting that a considerable part of the TEP may in fact be superimposed with multisensory evoked potentials related to the auditory and somatosensory stimulation. The early N40 component, a large negative deflection over the left visual cortex (Figure 3B,C), could only be observed during TMS, but not during Sham. Indeed, the deflection was significantly larger for TMS than for Sham (main effect of STIMULATION; $F_{1,22}$ = 32.21, p = 9 x 10^{-6}). In addition, there was a significant interaction between STIMULATION and VISUAL ATTENTION ($F_{1,22}$ = 12.84, p = 0.002), as the TMS-evoked N40 component was significantly larger during High than Low visual attention (t_{23} = 3.41, p = 0.0024), whereas there was no attentional modulation during this time interval for Sham (p > 0.2). Notably, the topography of the attentional modulation of the TMS-evoked N40 was clearly restricted to the stimulation site (inset in Figure 3B). An earlier positive deflection, the P20, also observed at the site of stimulation was also visible for TMS only and was significantly larger for TMS

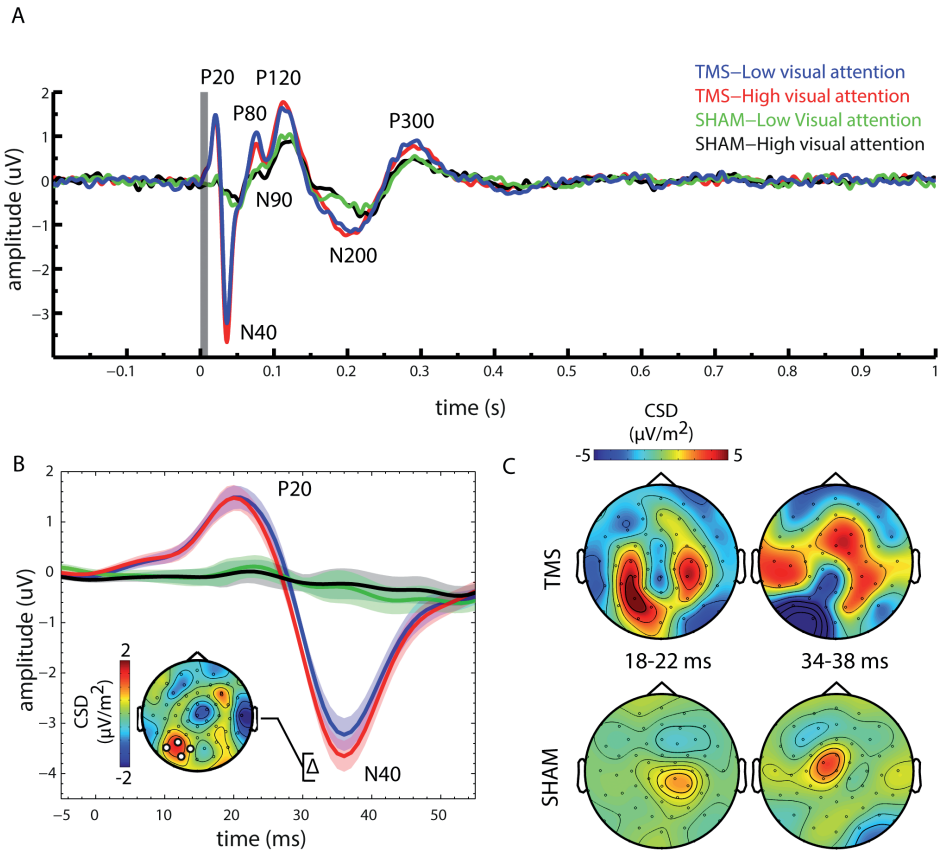

Figure 3. Attention modulated TMS-evoked potentials (TEP). **A,** TEPs (average of the four channels at the site of stimulation) are shown for TMS and Sham and separately for the High- and Low visual attention conditions. **B,** A magnified view of the P20 and N40 TEP components for all conditions. The shaded areas represent the within-subject standard error of the mean (SEM; Loftus and Masson, 1994). The inset displays a topographical plot of the difference between Low and High visual attention for TMS, highlighting the increased early N40 amplitude for High vs. Low visual attention. **C,** Topographical plots (current source density, CSD) are shown for early TEP components, separately for TMS and Sham but averaged across attention conditions, revealing clear differences in topography for TMS and Sham.

than for Sham (main effect of STIMULATION; $F_{1,22} = 16.09$, $p = 5 \times 10^{-4}$), however, it was not modulated by visual attention (no main effect of VISUAL ATTENTION; $p > 0.2$; no interaction effect; $p > 0.7$). For Sham (but not for TMS), analysis of a central channel cluster (seven channels centered around Cz) showed a negative deflection at 117 ms, which was significantly larger for low than for high visual attention. The topography of the difference is commensurate either with the N100 component of the auditory or somatosensory evoked potential. Thus, either an imperfect masking of the Sham click

sound or sensation of left shoulder stimulation during Sham may be responsible for this component. Importantly, this did not affect the time window of our TMS-related findings, and no such difference around the N100 was observed for low-high visual attention for TMS. In summary, the P20 and N40 deflections of the TEP appeared for TMS only, and the N40 was significantly modulated by visual attention, being larger during High than during Low visual attention.

Visual attention suppressed TMS-locked alpha power

We hypothesized that if TMS-locked alpha oscillations are generated by the same neuronal mechanisms as spontaneous alpha oscillations, TMS-locked occipital alpha power should be decreased by High but increased by Low visual attention. Since we assumed alpha oscillations to be phase-locked to the TMS pulse, we calculated time-frequency representation (TFRs) of power for the individually averaged TEPs. Unless specified otherwise, data were averaged from electrodes closest to the stimulation site (channel no. 28, 29, 44, 45, see Fig. 1D). To avoid any potential confounds by multisensory (audio-tactile) evoked potentials within the first 400 ms, TMS-locked alpha power was compared between experimental conditions in the window 0.4 to 1.0 s post-stimulus between 8 and 12 Hz. The TFRs were calculated per subject and averaged. No overlap with pre-TMS intervals or with the removed TMS pulse occurred. Based on the TFR for TMS pooled over Low and High visual attention we determined the TMS-locked alpha power to be centered at 8 Hz and tapered off towards 0.8 s, which determined the upper bound of our analysis window. Please note that, due to spectral leakage depending on the characteristics of the FFT, contributions of neighboring frequencies will leak into the estimation at 8 Hz. Given the frequency resolution due to the length of the sliding time window at 8 Hz (3 cycles, or 375 ms) and the use of a Hanning taper, estimates at 8 Hz will be biased towards contributions from frequencies at 8 Hz ± 1.33 Hz. In accordance with our hypothesis, topographical representations of TMS-locked alpha power (centered at 8 Hz) in the 0.4 to 0.8 s post-TMS interval (i.e. after the early evoked potentials) show a clear attentional modulation: Low compared to High visual attention caused a local increase in TMS-locked alpha power at the site of stimulation (t_{23}= 1.87, p = 0.037, one-sided t-test, Figure 4A). This modulation did not occur for the Sham condition (p > 0.6, Figure 4B). Importantly, this effect was corroborated by the directed interaction contrast ($TMS_{Low\text{-}High}$ – $Sham_{Low\text{-}High}$) comparing attentional modulation of TMS- and Sham-locked alpha power (t_{23} = 1.7317, p = 0.048, one-sided t-test). Note that, TMS-locked alpha oscillations are not readily visible in the grand average TEP (Figure 3A) probably due to phase cancellation over subjects. They were however observable in individual subjects. Figure 4D shows TEPs of three representative subjects for whom TMS-locked alpha oscillations are clearly visible (low visual attention conditions) with voltage maps for one subject centered on a selection of peaks and troughs of the TMS-

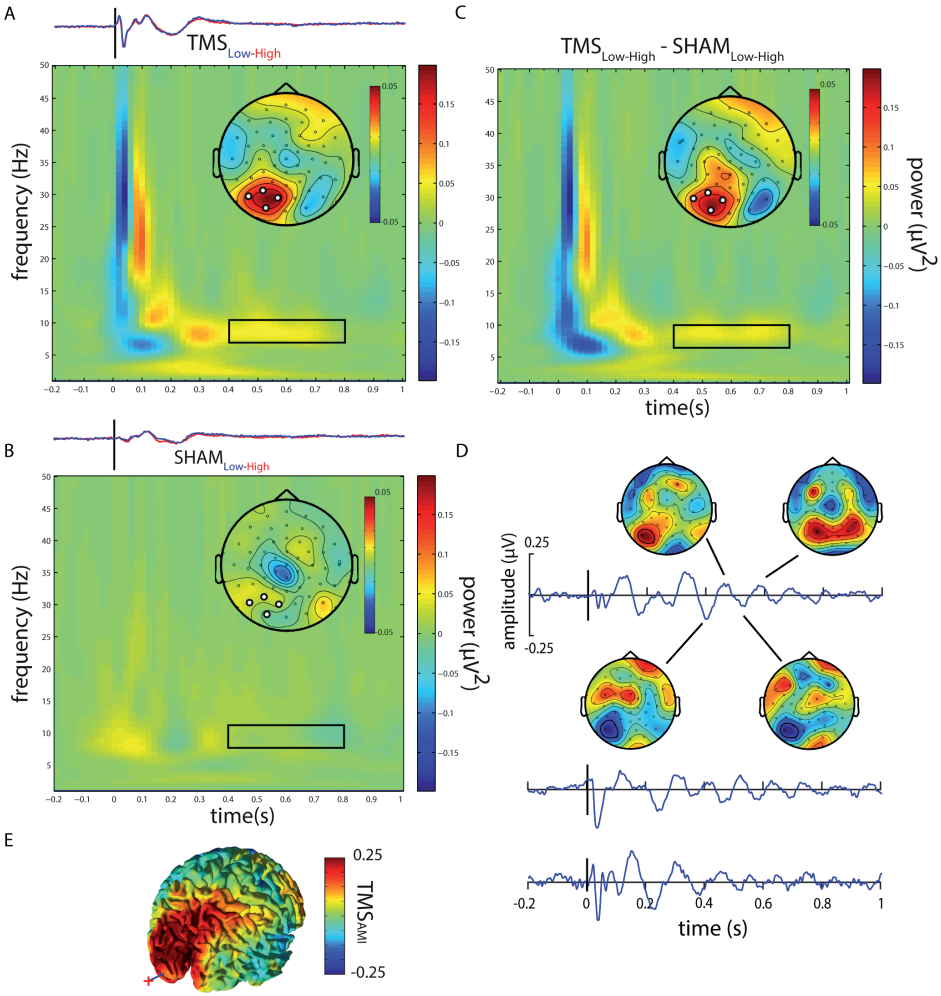

locked oscillation. The voltage maps highlight that the oscillating activity is strongest at the site of stimulation. Additionally, source analysis allowed us to identify the attention modulation of TMS-locked alpha activity to the left visual cortex overlapping both with the site of stimulation as well as the area in which alpha activity was modulated by attention prior to TMS onset (Figure 4E).

To further quantify the TMS-locked alpha oscillation in the 0.4-0.8 s interval we calculated the phase-locking factor (PLF) to assess inter-trial phase coherence in the alpha band Phase-locking analysis was performed using an equal amount of trials for each condition by random sampling, without replacement such that the amount of trials per condition was equated to the condition with the least amount of trials. As expected,

Figure 4. Attention modulates TMS-locked alpha power. **A,** Time-frequency representations (TFRs) show the attentional modulation (Low - High visual attention) of TMS-locked oscillatory power for TMS and **B,** Sham (bottom row). Topographical maps represent the average power from the time-frequency region of interest (0.4-0.8 s post-TMS, centered at 8 Hz, FFT window size: 375 ms) indicated by black rectangles within each TFR. The FFT window was multiplied with a Hanning taper thereby biasing spectral estimation towards the center of the window. No overlap with pre-TMS intervals or with the removed TMS pulse occurred. Note the increased TMS-locked alpha power in the stimulated left visual cortex for TMS but not for Sham. For direct comparison with the TMS-locked power, TEPs separately for low (blue) and high (red) visual attention, are depicted above each TFR. **C,** The difference in attentional modulation (Low - High) between TMS and Sham, i.e. the interaction ($TMS_{Low\text{-}High} - Sham_{Low\text{-}High}$). **D,** TEPs for three representative subjects in the Low visual attention condition. Individual TMS-locked alpha oscillations are clearly visible but not perfectly phase-aligned across subjects, thus averaging out at the group TEP. Topographical voltage maps for several half-waves of the TMS-locked alpha oscillation demonstrate an oscillatory pattern mainly restricted to the stimulated left visual cortex. **E,** Source analysis of the normalized ($TMS_{Low\text{-}High\ /\ }TMS_{Low+High}$) attention modulation of TMS-locked alpha power demonstrates the modulation of TMS-locked alpha power by attention to be localized to the visual cortex in the stimulated left hemisphere. The red cross and blue line indicates position of the TMS coil and target, respectively.

TMS resulted in higher phase-locking than Sham ($F_{1,23} = 7.79$, $p = 0.01$; Figure 5A). The PLF was not modulated by attention ($F_{1,23} = 0.17$, $p = 0.69$). This is expected as attention mainly modulates power but not the phase of alpha oscillations (Mathewson et al., 2009; Mathewson et al., 2011). To verify that phase-locking was limited to the alpha-band we calculated a time-frequency representation of the difference in phase-locking factor between TMS and Sham. We indeed found a time-frequency region of increased phase-locking in the alpha range, extending from the late TEP components and tapering off towards the end of the trial (Figure 4B). Interestingly, we also found a decrease in phase-locking compared to Sham in the delta theta band (3 Hz) starting 0.5 s after TMS onset. As this is not within the scope of the current study, we do not further discuss this observation.

In sum, these findings demonstrate that the amplitude of TMS-locked alpha oscillations is indeed modulated by visual attention the same way as spontaneous alpha oscillations are.

Attentional modulation of spontaneous alpha power predicts attentional modulation of both TMS-locked alpha power and amplitude of the N40

If TMS-locked alpha oscillations are actually reflecting a recruitment of the same neuronal mechanisms that constitute spontaneous alpha oscillations, the individual ability to modulate spontaneous alpha oscillations by visual attention should be predictive for the ability to modulate the TMS-locked alpha oscillations. Indeed, the normal-

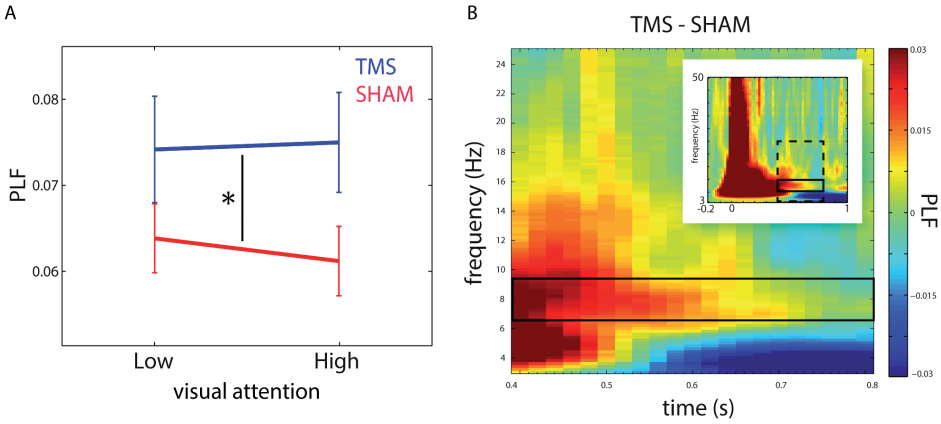

Figure 5. TMS caused increased phase-locking in the alpha band. **A,** Line plot indicating the PLF for the 0.4 – 0.8 s alpha response (centered at 8 Hz) to TMS (blue) and Sham (red), separately for both levels of VISUAL ATTENTION (Low vs. High). A 2x2 ANOVA of VISUAL ATTENTION (Low vs. High) and STIMULATION (TMS vs. Sham) revealed a main-effect of STIMULATION only. Error-bars indicate standard error of the mean (SEM). **B,** Time-frequency representation (TFR) of the phase-locking factor (PLF) shows the comparison of TMS versus Sham, pooled over Low and High visual attention from 0.4 – 0.8 s for 3 – 25 Hz (dashed box in insert). The solid box represents the analysis window. Insert shows TFR of PLF for the entire trial (-0.2 – 1 s), for 3 – 50 Hz.

ized individual alpha modulation index, AMI = (High – Low visual attention) / (High + Low visual attention), at the site of stimulation during intervals directly preceding the TMS pulse predicted the attentional modulation of TMS-locked alpha power (i.e. $TMS_{Low-High}$-$Sham_{Low-High}$): Pearson $r_{22} = 0.70$, $p = 0.00014$ (Figure 6A). Figure 6B shows the topographical distribution of channel-wise correlation coefficients between pre-TMS AMI at a given channel and attentional modulation of TMS-locked alpha power (i.e. $TMS_{Low-High}$-$Sham_{Low-High}$) at the same channel. Notably, the relationship appears to be particularly strong at the site of stimulation (Figure 6B). In short, the subjects for whom spontaneous visual alpha power was stronger modulated by top-down attention also were the subjects in which the TMS-locked alpha power was stronger modulated by attention. Interestingly, there was no such relationship between the attentional modulation of spontaneous alpha power and the strength of non-phase-locked alpha activity for the same time-frequency window ($r_{23} = 0.17$, $p > 0.4$, spearman correlation). Together with observed phase-locking analysis this clearly shows that this relationship cannot be explained by a rebound of endogenous alpha activity into the state prior to TMS.

Taking into account the individual differences in attentional alpha power modulation at the stimulation site, we performed a 2x2 repeated-measures analysis of covariance

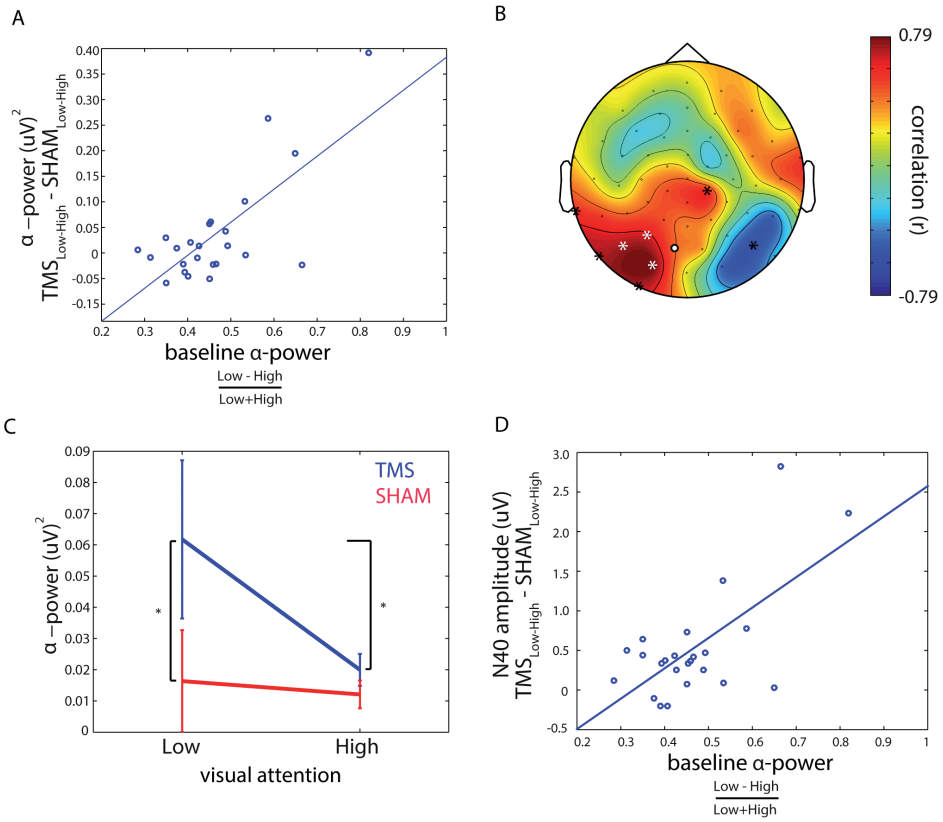

Figure 6. Impact of pre-TMS alpha visual attention modulation on TMS-locked alpha power modulation. **A,** Participant's ability to modulate spontaneous alpha at the stimulation site during pre-TMS intervals by top-down visual attention predicts the strength of attentional TMS-locked alpha power modulation at the stimulation site (i.e. white channels in panel B). The differential modulation of TMS-locked alpha power by TMS and Sham (i.e. $TMS_{Low-High}$-$Sham_{Low-High}$) is predicted by alpha modulation index (AMI) at pre-TMS baseline. **B,** Topographical plot depicts all correlation coefficients between pre-TMS alpha power modulation at a given channel and the attentional modulation of TMS-locked alpha power (i.e. $TMS_{Low-High}$-$Sham_{Low-High}$) at the same channel. Note: the better spontaneous alpha power could be modulated by top-down attention in the left (stimulated) visual cortex, the stronger also TMS-locked alpha power was modulated in that region by attention. Channels indicated by an asterisk showed a significant correlation ($p < 0.05$, corrected for False Discovery Rate (Benjamini and Hochberg, 1995). Channels indicated by a white asterisk, or white dot with black outline represent the channels used in the analyses throughout the study. **C,** Visual attention modulated TMS-locked alpha power for TMS but not for Sham. Asterisks indicate significant ($p < 0.05$) post-hoc comparisons following significant interaction of the STIMULATION x VISUAL ATTENTION ANCOVA using attentional alpha power modulation (AMI) prior to TMS as covariate. **D,** Participant's ability to modulate spontaneous alpha at the stimulation site during pre-TMS intervals by top-down attention predicts the strength of the attentional modulation of the N40 TEP component. Please note that due to the negative sign of the N40 component, positive here means a stronger negative deflection for High visual attention than for Low visual attention.

(ANVOCA) for TMS-locked alpha power with the factors VISUAL ATTENTION (Low vs. High) and STIMULATION (TMS vs. Sham) and pre-TMS AMI as covariate. As shown in Figure 6C, the ANCOVA revealed a significant two-way interaction between VISUAL ATTENTION and STIMULATION ($F_{1,22}$ = 18.80, p = 0.00027), reflecting that visual attention modulated TMS- but not Sham-locked alpha power. Importantly, the magnitude of this attentional modulation effect on TMS-locked alpha power depended on the magnitude of attentional alpha power modulation prior to TMS, as indicated by the highly significant three-way interaction between AMI, VISUAL ATTENTION, and STIMULATION ($F_{1,22}$ = 26.153, p = 0.00004). That is, subjects that were better able to modulate spontaneous alpha power during pre-TMS intervals by visual attention also showed stronger attentional modulation of the TMS-locked alpha power consistent with the correlation analysis in Figure 6A. Importantly, the results of the ANCOVA additionally show that attention has an effect on TMS-locked alpha activity over and above that of the pre-TMS alpha modulation as this is corrected for in the two-way interaction.

In addition, we assessed similarities in peak frequency. To maximize frequency resolution while keeping estimation similar across data segments we estimated peak frequency in the alpha band from 0.4 s data segments (as this is the largest uncorrupted segment obtainable from the post-TMS interval) multiplied by a Hanning taper, zero-padded to 10 seconds (Figure 7A). We found that the peak frequency of TMS-locked alpha correlated significantly with the peak frequency during the training session (r_{24}=.44, p=0.038, Figure 7B). While the peak frequency of TMS locked alpha did not correlate with the alpha frequency during the resting state measurement, or the pre-TMS interval, average peak frequency of the attentional modulation of TMS-locked alpha (9.34 ± 0.49 Hz) did not significantly differ from 1) spontaneous alpha frequency in the TMS-free training session (9.47 ± 0.41 Hz), 2) alpha frequency during the resting state measurement (10.01 ± 0.30 Hz), and 3) alpha frequency in the pre-TMS interval (10.11 ± 0.29 Hz), (paired t-tests; resp. p > 0.4, p > 0.1, p > 0.2; Figure 7A).

We also tested whether the magnitude of attentional modulation of the N40 TEP component was predicted by the extent to which attention did modulate spontaneous alpha power prior to TMS. We found that the interaction effect between STIMULATION and VISUAL ATTENTION in the N40 was correlated with pre-TMS AMI (r_{22} = 0.65, p = 5 x 10^{-4}) demonstrating that the modulation of the N40 by attention was stronger in subjects who showed higher AMI prior to TMS (Figure 6D).

To test whether it is pre-TMS alpha power itself, irrespective of visual attention, that predicts TMS-locked alpha power we pooled the data of both attention conditions and binned them into High and Low pre-TMS alpha power by means of a median split of

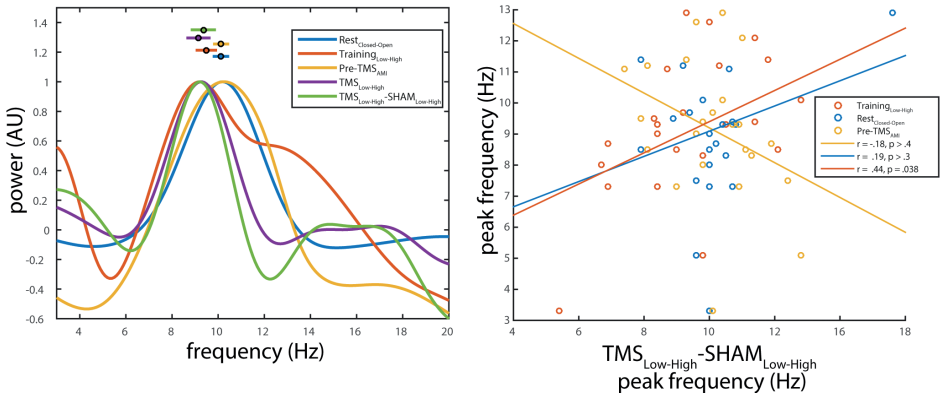

Figure 7. A, Average power spectra showing peak alpha frequency for all attentional contrasts. Each line represents the normalized power spectrum (all values divided by maximum power within condition) for the attentional contrasts shown in the legend. Data points with error bars represent mean and SEM individual peak frequencies for each contrast. **B,** Peak frequency of attentionally modulated TMS-locked alpha correlates with peak frequency of attentionally modulated spontaneous alpha in the training session (but not in the main experiment or for eyes closed-open). Each circle represents the peak frequency of the attentionally modulated TMS-locked alpha (x-axis) versus the peak frequency of attentionally modulated spontaneous alpha during training (gold) and pre-TMS intervals (blue), as well as of the closed-open eyes contrast at rest (orange). The lines represent least-squares regression lines for the separate correlations (see figure legend for Pearson r, and p-values).

all trials with respect to alpha power during the -0.5 s to -0.001 s interval, separately for TMS and Sham. The N40 component was indeed larger (more negative) when evoked during Low compared to High alpha power (t_{23}=2.32, p=0.03) for TMS, but not for Sham (p>0.7). Furthermore, a significant main effect of STIMULATION could be observed ($F_{1,23}$ = 32.5, p = 8 x 10^-6), but no significant interaction between STIMULATION and ALPHA POWER (p > 0.1). In contrast, TMS-locked alpha power was not significantly higher for High compared to Low alpha power trials, neither for TMS (p > 0.1, one-sided paired t-test), nor for Sham (p > 0.5, paired t-test), although, a directed interaction test did reveal a significant interaction between stimulation condition and level of pre-TMS alpha power (t_{23} = 2.14, p = 0.04).

Together, these findings demonstrate that the individual ability to top-down modulate spontaneous alpha power by attention predicts the amount of attentional modulation of both TMS-locked alpha power and the N40 TEP component, but in opposite direction. Therefore, TMS-locked and spontaneous alpha oscillations are likely reflecting recruitment of the same neuronal mechanisms, whereas the N40 TEP component rather reflects cortical excitability.

Discussion

Single-pulse TMS (but not Sham) evoked an early TEP component (N40) as well as subsequent alpha-like oscillations (400-800 ms post-TMS) that were both localized to the stimulated left visual cortex. Top-down visual attention increased the amplitude of the N40 TEP component but decreased the power of the TMS-locked alpha-like oscillation. Moreover, the extent to which attention modulated TMS-locked alpha power was predicted by the extent to which it modulated spontaneous alpha power in the stimulated cortical region during pre-TMS intervals. We thus provide new evidence that TMS-locked alpha responses rely on the same neuronal processes as spontaneous alpha activity.

TMS-locked alpha oscillations 'behave' like spontaneous alpha oscillations

First and foremost, the power of TMS-locked alpha was top-down modulated by endogenous visual attention in the same way as the power of spontaneous alpha. As shown by our own (Figure 1D) as well as previous work using an audio-visual cross-modal attention task (Adrian, 1944; Fu et al., 2001; Mazaheri et al., 2014), spontaneous alpha power in the visual cortex is increased during periods of low visual attention (when subjects attend the auditory input stream) but decreased during periods of high visual attention (when subjects attend the visual input stream). This is believed to reflect the inhibitory nature of alpha oscillations, up-regulated in task-irrelevant brain regions to suppress and down-regulated in task-relevant regions to facilitate information processing (Klimesch et al., 2007; Jensen and Mazaheri, 2010). The TMS-locked alpha oscillation at 400-800 ms is not readily evident in the grand average TEP (Figure 3A) because its onset and frequency (and thus phase) are coherent within but not across subjects (Figure 4D), causing phase cancelation when averaging. However, grand averages of individual TEP time-frequency representations clearly reveal that TMS but not Sham evokes an alpha oscillation of several cycles in the analyzed post-ERP period from 400 to 800 ms (Figure 4A-C). Importantly, phase-locking analysis confirmed that this alpha oscillatory response is phase-locked to the TMS pulse (stronger than for Sham; Figure 5A) and thus not a mere TMS-related power modulation. For instance, it cannot be explained by a rebound of pre-TMS alpha after a TMS-induced alpha desynchronization (with alpha merely surviving averaging due to its high amplitude despite a lack of phase-locking). As for spontaneous alpha, endogenous attention modulated the power but not the phase-locking of TMS-locked alpha oscillations. The reason for TMS-locked alpha not being visible before 400 ms is unclear. Possibly, TMS elicited distinct episodes of excitation and suppression (Moliadze et al., 2003). Alternatively, TMS-locked alpha started earlier but got masked by the TEPs and multisensory ERP components during the early post-TMS period. In fact, TMS-locked alpha power seems to be modulated by

attention already 250 to 400 ms post-TMS (Figure 4A) but did not yet differ significantly from Sham during that period (Figure 4B).

The second finding supporting the notion that TMS-locked alpha resembles spontaneous alpha comes from the inter-individual correlation of their respective attentional modulation effects. The extent to which endogenous attention modulated TMS-locked alpha power was predicted by the amount of attentional modulation of spontaneous alpha power in the stimulated cortical region during pre-TMS intervals (Figure 6A&B). These inter-individual differences are possibly linked to structural differences in white matter tracts (Marshall et al., 2015). Two complementary interpretations are commensurate with this finding, but cannot be disentangled based on the current experimental design. The first possibility is that TMS triggers a new alpha oscillation in the stimulated neuron population, which is independent of the global spontaneous alpha oscillation at the time of stimulation. This would characterize an evoked response in the classical sense. Yet, both oscillations would be top-down modulated to the same degree by visual attention according to the current task condition and depending on the subjects' individual ability. Alternatively, TMS may actually reset the ongoing spontaneous alpha oscillation, but only in the stimulated neuron population. Again, its amplitude modulation would directly depend on the amplitude modulation of the global spontaneous alpha oscillation that has been reset. This would explain the evoked potential as emerging from phase-resetting of a spontaneous oscillation. Interestingly, the size of TMS-locked alpha power could not be fully explained by pre-TMS alpha power. The size of the TMS-locked alpha response seems to rather depend on the strength of top-down attentional modulation of alpha power than on the mere level of spontaneous alpha power randomly fluctuating at the stimulation site.

The peak frequencies of the attentional modulation of TMS-locked and spontaneous alpha power during the TMS-free training session were comparable and even correlated across participants. The frequency of TMS-locked alpha power did not correlate with that of attention modulated alpha power during pre-TMS intervals of the main task or during rest. Importantly however, they did not differ significantly either. Thus, while attentional modulation of TMS-locked alpha power was at the lower boundary of the typical alpha band (8-9 Hz, depending on the method of estimation), it was well within the range of spontaneous alpha power modulation observed in our sample. In fact, considerable inter- but also intra-individual differences in peak alpha frequency have been reported, varying between subjects by a standard deviation of 2.8 Hz and within subjects by a standard deviation of 0.9 Hz, interestingly increasing with task engagement (Haegens et al., 2014). It is thus possible that attentional modulation in the presence of TMS in the main task required more engagement than in the TMS-free training session.

Although we found no significant differences between TMS-locked and spontaneous alpha in the current study, they are principally conceivable. While spontaneous alpha may be constantly driven by a neuronal generator, e.g. a thalamic pacemaker, a single TMS pulse may evoke transient resonance in the same circuits but slow down quickly due to progressive phase-desynchronization in the absence of repetitive synchronizing input. In summary, roughly comparable peak frequencies together with the correlation of peak frequencies for attentional modulation of TMS-locked alpha and spontaneous alpha during the training session provide additional evidence for common mechanistical grounds. Yet, the lack of correlation with the frequency of spontaneous alpha power modulation during the main task remains unexplained.

TMS-locked alpha oscillations cannot be explained by multisensory stimulation artefacts

The application of TMS is inevitably accompanied by multisensory stimulation. Auditory stimulation is caused by the typical "click" sound of the discharging TMS coil, somatosensory stimulation by the co-stimulation of cranial muscles and peripheral nerves in the skin, and visual perceptions (i.e. phosphenes) maybe triggered when stimulating the visual cortex. All these inputs cause evoked potentials in the respective sensory systems, overlaying transcranially evoked brain potentials within the first ~400 ms. As demonstrated for auditory stimuli (Romei et al., 2012), they may even cause cross-modal phase resetting of alpha oscillations in the visual cortex, which can be mistaken for TMS-locked alpha oscillations. We prevented phosphene perception by adjusting stimulation intensity to 80% phosphene threshold. In addition, we designed a multisensory extracranial Sham stimulation controlling for audio-tactile input but lacking actual brain stimulation. Perfectly matching the subjective experience of cranial TMS is hardly possible. Nevertheless, stimulation of the ipsilateral shoulder blade, individually matched for auditory and somatosensory perception, at least produced a left-lateralized audio-tactile input of comparable intensity and resulted in a strikingly similar "TEP" (Figure 3). In fact, TMS and Sham TEPs shared most of their components (except the N40 and P20), albeit with slightly lower amplitude for Sham, emphasizing the necessity of appropriate control conditions in TMS-EEG research.

Importantly, we observed TMS-locked alpha oscillations as well as their attentional modulation only for visual cortex TMS but not for Sham, rendering it unlikely that these effects resulted from multisensory stimulation or cross-modal phase-resetting. Moreover, the effects we observed were restricted to the stimulated left visual cortex (Figure 4) and emerged in the analysed time interval of 400-800 ms (unaffected by multisensory ERPs), whereas Romei et al. (2012) observed more shorter-lasting cross-modal phase-resetting effects (< 300 ms) throughout the entire visual cortex.

Taken together, we are confident that the observed TMS-locked alpha oscillation did actually result from transcranial stimulation of cortical neurons in the left visual cortex rather than any kind of accompanying sensory stimulation. If properly controlled, TMS-EEG thus provides a suitable tool not only to study but also to manipulate cortical oscillations (e.g. via 'entrainment').

N40 reflects excitability of the visual cortex

TMS to the visual cortex evoked a response consisting of several components (P20, N40, P80, N90, P120, N200, P300; Figure 3). While most component were visible for both TMS and Sham, and are thus most likely attributable to unspecific multisensory stimulation effects, the N40 component was evident for TMS only and was additionally modulated by attention. As expected for early TEP components, its amplitude was larger during periods of high compared to low visual attention, a pattern already known from the attentional amplification of visual evoked potentials (Rajagovindan and Ding, 2011). Interestingly, the N40 amplitude also correlated with the individual extent to which spontaneous alpha power was modulated by attention during pre-TMS intervals, thus paralleling the correlation with TMS-locked oscillations but in opposite direction. As a strong link has been established between pre-TMS alpha power and the level of visual cortex excitability (Thut et al., 2006b; Romei et al., 2008b; Romei et al., 2008a), the N40 amplitude appears to index the level of visual cortex excitability at the time of stimulation. This finding is in line with TMS-EEG work targeting the primary motor cortex, where the N40/45 was localized to the stimulation site and its amplitude correlated with stimulation intensity and conditioning pulse intensity in a paired-pulse design (Paus et al., 2001; Premoli et al., 2014). Also during deep sleep, the amplitude of a positive component of comparable latency (P40) indexed motor cortical excitability fluctuations during the sleep slow oscillation (Bergmann et al., 2012). However, since the motor cortex N45 has been recently linked to GABA-A-ergic inhibition (Premoli et al., 2014), it may reflect the inhibitory feedback in response to TMS-induced cortical excitation (which nevertheless scales with the amount of excitation), rather than the initial excitation itself. Future research is needed to further evaluate the N40 component as an index for cortical excitability and inhibition.

Conclusion

Our findings strongly suggest that TMS-locked alpha oscillations do indeed rely on the same neuronal mechanisms as spontaneous alpha oscillations. They are top-down modulated by endogenous attention in the same way and are tightly linked to the extent subjects are able to modulate spontaneous alpha power in the stimulated brain

region. Importantly, these effects cannot be explained by mere multisensory stimulation as ruled out by comparison to a high-level audio-tactile Sham condition. However, it remains to be explained why the peak frequency of TMS-locked alpha did not perfectly match that during pre-TMS intervals. Conversely, the early N40 TEP component is also modulated by attention, but in the opposite direction, presumably indexing visual cortex excitability at the time of stimulation. Therefore, a local alpha response to single-pulse TMS, possibly reflecting phase-rest of spontaneous alpha, may be the basis for the effectiveness of transcranial entrainment protocols.

CHAPTER 3

Complex interplay between perceptual echoes and cross-modal attention

Adapted from:

Herring, J.D., Chota, S., Bergmann, T.O., VanRullen, R., & Jensen, O. (2017) Complex interplay between perceptual echoes and cross-modal attention (in preparation) & Chota, S. (2017) Effect of attention on perceptual echoes (master's thesis)

Abstract

Alpha oscillations have been shown to subserve neuronal processing by, for example, organizing information flow between regions. The generation of alpha band activity seems to underlie the dynamics of the visual system. This is partially evident from studies by VanRullen et al. attempting to estimate the 'impulse response function' of the brain when visually stimulated with a randomly flickering disk. When estimating these so-called 'perceptual echoes' long-lasting (up to 1 second) alpha-like responses were observed that were enhanced by spatial attention. Conversely, Herring et al. observed long-lasting alpha-like responses to single-pulse TMS in early visual cortex. These impulse responses, however, were enhanced with low visual attention in a cross-modal cued attention design, as would be expected from endogenous alpha oscillations. In the current study, we investigated the effects of cross-modal attention on perceptual echoes. We found an increase in baseline and task-related endogenous alpha power when attention is directed towards the auditory modality; however, no robust effects were found for perceptual echo alpha power. In an explorative follow-up analysis, we found an early N70 component to be related to the modulation of attention on perceptual echo alpha power. Together with baseline alpha power modulation of attention we propose a complex model in which visual attention increases the effectivity of the visual stimulation, while at the same time reducing alpha power. Alpha oscillations, on the other hand, suppress visual input. Depending on individual variability in effectivity of respectively attention and alpha power, perceptual echo power was influenced more by attention (i.e. enhanced with visual attention) or alpha (i.e. increased with increased alpha power).

Introduction

In the recent years evidence has accumulated for the role of cortical oscillations in supporting various cognitive functions, organizing information processing and commucation between cortical reguions (VanRullen and Koch, 2003; Buzsaki and Draguhn, 2004; Engel and Fries, 2010; Hanslmayr et al., 2011; Jensen et al., 2014) (Bonnefond et al., 2017). Alpha is thought to have a supporting role in allocating attention to relevant stimuli and inhibiting distractors. Alpha oscillations reflect shifting between states of excitability and inhibition (Klimesch et al., 2007). This so-called 'pulsed-inhibition' (Jensen and Mazaheri, 2010) is evident in studies where perception of near-threshold visual stimuli can be predicited by the phase of the alpha rhythm at time of stimulus onset (Van Dijk et al., 2008; Busch et al., 2009; Mathewson et al., 2009; Drewes and VanRullen, 2011; Dugue et al., 2011).

The dynamics supporting the generation of spontenous alpha oscillations appear to be a property of the visual system. Among others, this is evident from a study by VanRullen and Macdonald (2012) revealing so-called perceptual echoes. VanRullen and Macdonald (2012) presented participants with disks that randomly varied in luminance while measuring the neuronal responses using EEG. Following, they estimated the impulse resposes, i.e. the function that allows for best to account for the measured EEG when convolved with the time-course of the luminance (VanRullen and Macdonald (2012); Figure 1A). Surprisingly, they found a strong alpha-like response lasting for more than one second.

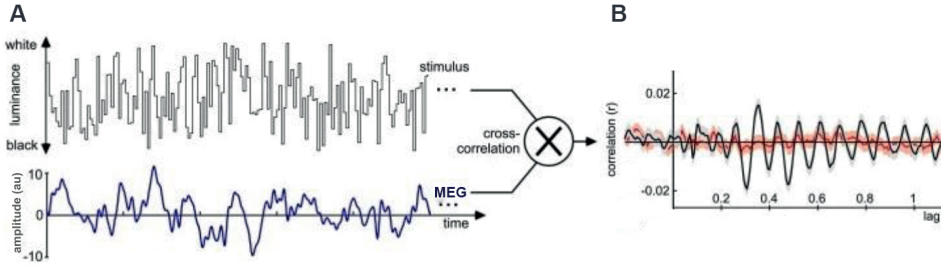

Figure 1. *Illustration of the paradigm and the perceptual echo functions.* **A**, The cross-correlation is computed by multiplying the two signals for every time point and summating the result, then shifting one signal by one time point and repeating the first step. This operation estimates the impulse response function (IRF); i.e. the function that best help to reconstruct the MEG data when convolved to the visual input. **B**, Time course of the cross-correlation (the IRF in black) and the IRF calculated for the surrogate data (red) for lags from 0 to1 s (example from representative subject). Adapted with permission from VanRullen and Mcdonald (2012).

In a different study, Herring et al. (2015), studied the effect of transcranial magnetic stimulation (TMS) and how they affected the oscillatory brain responses. They applied single-pulse TMS to the left occipital cortex while simultaneously measuring EEG. Interestingly, they found similar alpha-like responses not too different from the percetual echo. Additionally, the subjects performed a cross-modal attention task resulting in an increased alpha-like response when participants attended away from the visual modality. VanRullen and Macdonald (2012), however, had participants perform a cued spatial attention task where subjects attended to a disk in either the left and right visual field. They found the alpha-like response in the IRF to be highest contraleral to the attended disk.

It remains to be further explored to what extend the perceptual echo increases or decreases with the allocation of attention. It is well estblished that alpha oscillations in visual and parietal regions increase with the allocation of auditory attention (Adrian, 1944; Fu et al., 2001; Mazaheri et al., 2014). We exploit this finding in the current study in which participants performed a cross-modal attention task, while recording whole-head MEG, where they attended either a centrally presented disks varying in luminance or an auditory tone that was randomly modulated in amplitude. We calculated the impulse response functions and compared both attentional conditions on the sensor level.

Methods

Participants

Participants were recruited from a database at Radboud University Nijmegen. Twenty-one healthy (8 Female, Age: 21.7 +/- 0.28; Mean +/- SEM) participants completed the study. Written informed-consent was acquired before the start of the experiment. All subjects conformed to standard inclusion criteria for MRI and MEG experiments. Subjects had normal, or corrected-to-normal vision. The study was approved by the local ethics committee. Subjects received financial compensation at a rate of 8 Euros per hour or were compensated in course credits.

Procedure

In the experimental session, subjects were first prepared for MEG recordings by changing into clothes free of ferromagnetic materials. Following, the head shape of the participants was digitized using a 3D digitizer (Polhemus, Colchester, USA). Next, participants were brought into the magnetically shielded room and placed in the MEG. An EyeLink 1000 Plus eye tracker (SR Research, Ottawa, Canada) with a sampling rate

of 1000 Hz was used to monitor the gaze of the participants. After calibrating the eye-tracker participants were familiarized with the experimental task. The spatial attention task was performed in five blocks of 12 minutes with short breaks in between. In total, the task lasted 60 minutes. On a separate occasion a structural MRI was acquired for subsequent source localization of the MEG data.

Task and Stimuli

Participants performed a cross-modal attention task in which they were cued to attend to the visual, or auditory modality (Figure 2). In the visual modality, participants had to attend to a disk presented in the lower visual field, randomly varying in luminance. Auditory stimuli were amplitude modulated tones. At the beginning of each trial a letter was presented indicating the condition ("V" for visual and "A" for auditory). Trials were self-paced by button-press. At trial onset, a baseline period of one second was followed by presentation of both auditory and visual stimuli for 6.25 seconds. In the attended modality, frequent (80 %) targets appeared, which the participant had to detect, while ignoring infrequent (20 %) distractors in the unattended modality. On average, three stimuli (targets, or distractors) appeared per trial (range: 2 to 4). The task was divided into 5 blocks of 60 trials.

Visual and auditory random sequences

Visual random sequences consisted of a spherical disc (5.7° visual angle) presented in the center of the lower visual field for 6.25 s (see Figure 2). The luminance of the disc

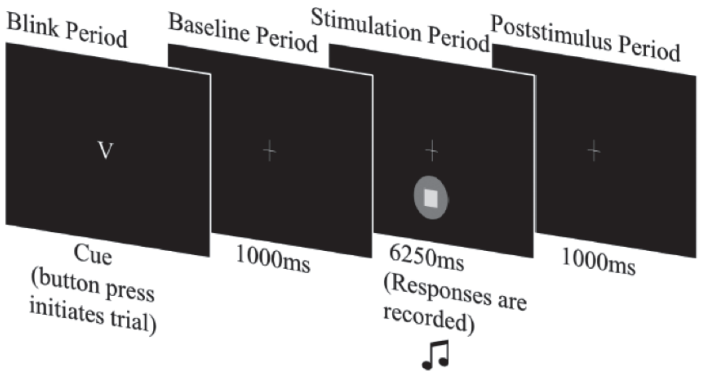

Figure 2. *The task.* Trials began with a letter indicating the attentional condition. After a 1000 ms baseline the stimulation period began in which the luminance disc was presented in the lower central visual field for 6.25 s. Simultaneously, the auditory random sequence was presented. Depending on condition, participants had to covertly attend to visual or auditory random sequence and detect faint visual or auditory targets that were infrequently presented. Visual targets were presented as squares within the disc while auditory targets were short changes in pitch.

was randomly varied over time (min: 0.56 – 7.85 cd/m^2; min - max) so that the power spectrum of the luminance over time was flat between 1 and 80 Hz. Random auditory sequences were generated similarly to the visual random sequences and lasted 6.25 s. The amplitude envelope of a 1000 Hz carrier wave was randomly modulated to contain equal power in frequencies between 1 and 80 Hz. The auditory sequence was then up-sampled to 44100 Hz.

Visual and auditory targets/distractors

Between two and four visual and auditory stimuli were presented during each trial. Visual target stimuli were presented as a square (2.5° visual angle) in the center of the disc and lasted 25 ms. The luminance difference between stimulus and disc was determined by a QUEST adaptive staircase procedure (Watson and Pelli, 1983) to ensure a detection performance of 80 %. The average luminance difference was 60 %, of the total luminance (± 0.05 SEM). Auditory stimuli were 25 ms long changes in the pitch of the auditory sequence. Similar to the visual stimuli the amount of reduction was determined by the QUEST algorithm.

MEG Data Analysis

Preprocessing

The acquired MEG data sets were analyzed using the Fieldtrip Toolbox (version 20160605; Oostenveld et al., 2011) implemented in MATLAB R2015a (Mathworks Inc, Natrick, USA). The data was segmented into trials with 0.5 s baseline and 7.45 s post-stimulus intervals. Jump artifacts originating from the MEG system where removed by calculating the z-transform of the raw data and discarding all trials where the z value exceeded a predefined threshold of 20. A band-pass filter between 1 and 100 Hz was applied and the data was baseline-corrected. We performed an independent component analysis (ICA) on the resulting datasets to remove eye blinks and other muscle-related artifacts (Bell and Sejnowski, 1995; Jung, 2000). The cleaned datasets were then used to estimate the impulse response (see section Cross-correlation function). On average 258 trials were recorded per subject of which 128.2 ± 4.9 (SEM) attend-visual and 128.7 ± 4.9 (SEM) attend-auditory trials were used for further processing (0.4 % loss).

Sensor-level frequency analysis

We divided the peri-stimulus period in an early and late segment to be able to analyze the early evoked components and the time windows during ongoing stimulation separately. A frequency analysis at the sensor level data was performed in the -0.5 – 0 s baseline period, in the 0 – 1 s early post-stimulus period and in the late 1 – 6.25

s post-stimulus period. Synthetic planar gradients were calculated (Bastiaansen and Knösche, 2000). A Hanning taper was applied and power spectra were computed separately in the baseline-period, early, and late post-stimulus periods. Each segment was zero-padded to 10 s prior to the Fast Fourier Transform resulting in a 0.1 Hz frequency resolution. Time-frequency representations (TFRs) of power were computed or the full time-course using a sliding time window approach (dT = 400 ms) multiplied by a hanning-taper. Single subject TFRs were baseline corrected by dividing the post-stimulus onset period by a 400 ms baseline from -0.6 – -0.2 s. TFRs for the 30 to 50 Hz band were calculated by applying 7 tapers (multitaper approach (Mitra and Pesaran, 1999)) to the sliding time window data.

Cross- correlation functions

Impulse Response Functions (IRFs) were calculated using the filtered and artifact-free datasets and the respective visual luminance and auditory amplitude modulated sequences. The IRFs were calculated using a cross-correlation approach (VanRullen and Macdonald, 2012). Visual luminance sequences were up-sampled from 160 Hz to 1200 Hz to match the MEG datasets. Auditory random sequences were down-sampled from 44100 Hz to 1200 Hz. We included the MEG data between 1 s and 6.25 s after stimulus onset in calculating the cross-correlation to avoid inclusion the evoked response due to onset and offset of the stimulus. The cross-correlation was then computed to estimate the IRF(t) for each sensor with respect to the luminance- and auditory sequences for -1.5 – 1.5 s lags:

$$IRF\,(\mathrm{t}) = \sum_{-1.5 < t' < 1.5} stim\,(t').MEG(t' + t)$$

Where stim and meg denote the stimulus sequence and the corresponding EEG response, respectively (adapted from VanRullen and Macdonald (2012)). The calculated IRF(t) were averaged over trials resulting in one perceptual echo per participant, sensor, and condition. The averaged IRF(t) with the luminance and auditory sequence will be referred to as respectively perceptual and auditory echoes.

Similar to VanRullen and Macdonald (2012), we used shuffled stimuli to statistically access the reliability of the IRFs. The IRF(t) from the shuffled data will be referred to as surrogate data. A frequency analysis was performed on the perceptual echoes. Power spectra were calculated for the perceptual echoes between 0 s and 1.2 s. Time-frequency analyses power of the perceptual echoes were calculated from -1.5 s to 1.5 s with the same parameters as described in the section sensor level frequency analysis.

Source localization of perceptual echoes

We used Dynamical Imaging of Coherent Sources (DICS) (Gross et al., 2001) to localize the source of the perceptual echoes. We calculated coherence between visual stimulus time course and the MEG data at the individual's peak alpha frequency for both the perceptual echo, as well as the surrogate data. To this end, cross spectral density (CSD) matrices were calculated on the data concatenated over conditions. Peak alpha frequency was determined as the peak alpha power in the perceptual echo for the time lags from 0 to 1 s. Single-shell head models (Nolte, 2003) were created based on individual anatomical MRIs. Spatial filters were calculated on a 1 cm resolution grid warped to an MNI template brain.

Results

We recorded the ongoing MEG while participants performed a cued cross-modal detection task. Participants had to detect a square within a randomly flickering disk (attend visual condition), or an auditory tone within a stream of amplitude modulated white-noise (attend auditory condition) (Figure 2). We then derived the impulse response function (VanRullen and Macdonald, 2012) with respect to the visual and auditory stimuli; i.e. the impulse response that best reproduced the MEG data when convolved to sensory input stream (Figure 1).

Behavioral data

Behavioral measurements showed an average hit rate of 67.6 % (+/- 0.4 %) in the visual condition and 67.1 % (+/- 0.4 %) in the auditory condition. The false alarm rate in the visual condition was 8.6 % (+/- 1 %) and in the auditory condition 8.9 % (+/- 1 %). The hit rate and false alarm rate indicate that attention was successfully manipulated during the experiment. The average reaction time to visual targets was 476 ms (+/- 9.9 ms) and to auditory targets was 449 ms (+/- 9.5 ms). As the hit rate was adaptively titrated to be around 70 % correct, we also recorded a value reflecting the decrease in luminance of the target square with respect to the visual stimulus to keep track of individual differences in task performance. Target luminance difference reflects the percent change in luminance from a grey background. Target luminance difference was on average 60 % (+/- 5%).

Visual attention decreases Baseline and Late ongoing alpha power

The group average of time-frequency representations (TFRs) of the entire trial is shown in Figure 3A for the attend auditory condition and in Figure 3B for the attend visual condition. Sensors of interest were selected based on the strongest decrease in the 7

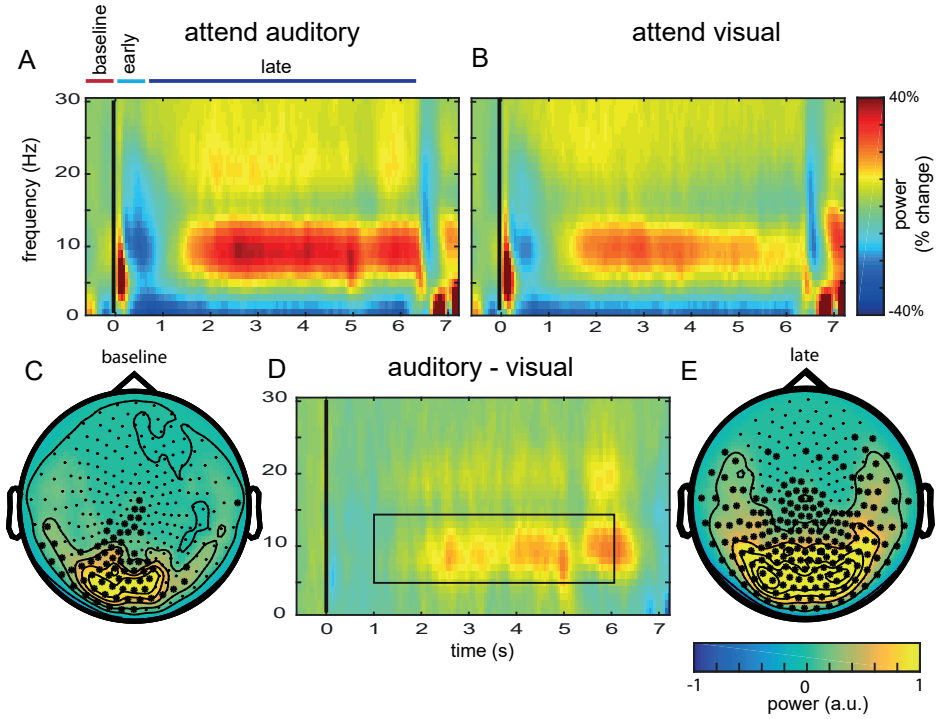

Figure 3. *Time-frequency representations (TFRs) of power* **A,** TFRs of power of the MEG data from -1 – 7 s in the attend auditory condition. **B,** Same as A for the attend visual condition. **C,** Topography of the attentional contrast (auditory minus visual) during the xx – yy s baseline. 54 sensors (asterisk) showed a significant difference in alpha power ($p < 0.05$; controlled for False Discovery Rate). **D,** TFRs of power of the difference between attend-auditory and attend-visual condition (auditory minus visual). The contrast shows increased alpha power during the late time interval (1 – 6.25 s) in the attend-auditory condition. **E,** Statistical comparison of 7 – 14 Hz power in the late time-window reveals significant differences between conditions in 199 sensors ($p<0.05$; controlled for False Discovery Rate; *'s indicate significant channels).

and 14 Hz alpha band comparing in early stimulation interval compared to the baseline interval (Figure 3A and B). A dependent samples T-test revealed a significant decrease in alpha power in 43 posterior sensors ($p < 0.05$; controlled For False Discovery Rate with respect to sensors; Benjamini and Hochberg (1995)). The *baseline period* is defined as the interval up until stimulus onset (-0.5 – 0 s). The *early period* is defined as the interval dominated by the evoked response to the onset of the stimuli (0 – 0.5 s). The *late period* is defined as the 1.5 s – 6.25 s interval and is characterized by an increase in alpha power.

In the baseline interval, alpha power (7 – 14 Hz) is significantly higher in the attend auditory compared to the attend visual condition ($p < 0.05$; corrected for False Discovery Rate; Figure 3C). During stimulation, the late period (Figure 3D) shows a significant increase in alpha power for the attend auditory compared to the attend visual condition ($p < 0.05$; corrected for False Discovery Rate; Figure 3E). Topographical representations of this difference show an increase in alpha power for posterior and parietal sensors (Figure 3E). This is in line with previous findings that showed an increase in alpha power when attention is allocated to the auditory domain (Adrian, 1944; Fu et al., 2001; Mazaheri et al., 2014). No significant effects of attention on the alpha peak frequency was observed. Alpha peak frequencies during baseline and late stimulation were significantly correlated over subjects ($r_{20} = 0.93$, $p < 0.0001$).

Perceptual echoes at 10 Hz

The main focus of our project was to examine the effects of top-down attention on the perceptual echoes. Perceptual echoes were computed by calculating the cross-correlation between the MEG and the time-course of the visual luminance and auditory stimulation respectively (Figure 1). The resulting impulse response functions (or perceptual echoes) were analyzed for spectral content and compared between conditions. We calculated the impulse response functions by cross-correlating the MEG with randomly shuffled trials (Surrogate).

As in İlhan and VanRullen (2012), no counterpart to visual perceptual echoes were found in the auditory domain, using MEG. We were not able to identify any qualitative differences between the auditory echoes and the respective surrogate functions at 7 to 14 Hz.

As in VanRullen and Macdonald (2012), we observed a strong, alpha-like response in the perceptual echoes in the visual domain, lasting for at least 1 s (Figure 4A; representative subject). We computed TFRs of the perceptual echo and compared them to the TFRs of the echoes of the surrogate data (Figure 4B; grand average over subject and sensors of interest). The contrast revealed significant differences in the 0 – 1 s interval. ($p < 0.05$; controlled for False Discovery Rate over time).

Alpha (7 – 14 Hz) power was significantly higher for the perceptual echo for the visual stimulus compared to the surrogate data in all 271 channels of the MEG i.e. this was a highly robust effect ($p < 0.05$ - controlled for False Discovery Rate). We therefore only included the top 15 % of the sensors showing the strongest echo in the alpha band. This resulted it 40 sensors of interest (see topographical plot in Figure 4B). In order to relate the perceptual echoes to the ongoing oscillations we averaged the time-frequency

representations over sensors of interest and then subjects (Figure 4B). We concluded that robust perceptual echoes in response to visual stimuli can be identified using MEG.

To examine to what extent endogenous alpha oscillations were related to the alpha component in the perceptual echo, we correlated perceptual echo with endogenous alpha peak frequency. Perceptual echo peak frequency was correlated with alpha peak

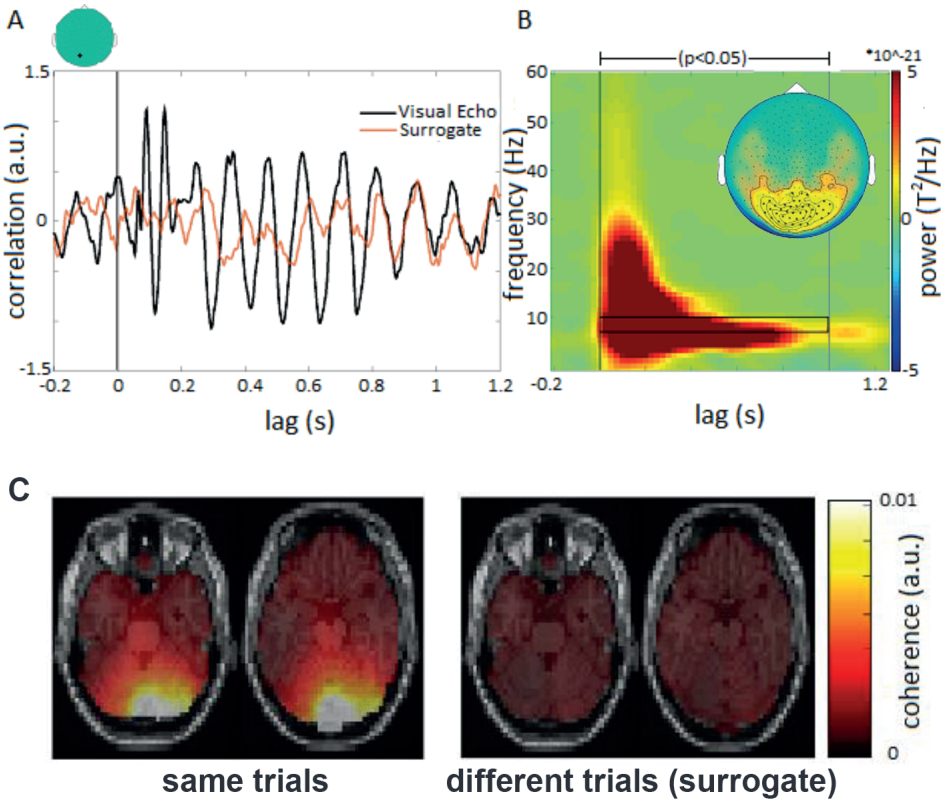

Figure 4. *The perceptual echo calculated from the MEG data.* **A.** The perceptual echo (black line) of a single subject and sensor MLO22 (medial left occipital). The perceptual echo for the time shuffled data (surrogate) is depicted in red. **B.** The TFR of the perceptual echo reveals a strong oscillatory 10 Hz component in sensors marked in the topographical insert. Statistical tests show that the power difference at 10 Hz between perceptual echo and surrogate is significant for up to 1 s. ($p<0.05$; controlled for False Discovery Rate). The topographical plot represents the topography of the perceptual echo in the alpha band (7 – 14Hz; difference between Perceptual Echo and Surrogate Echo). All sensors showed a significant difference ($p < 0.05$; controlled for False Discovery Rate). The 40 sensors (15 % of all sensors) showing the strongest differences were chosen as the 'sensors of interest'. **C,** coherence (DICS) at individual peak alpha frequency between the MEG data and the visual stimulus trace where the MEG and visual stimulus data came from the same (left), or different (right) trials. Coherence is maximal for posterior regions.

frequency during baseline ($r_{19} = 0.66$, $p < 0.01$). Additionally, echo alpha peak frequency was correlated with peak frequency during visual stimulation ($r_{19} = 0.59$, $p < 0.01$). The alpha component in the perceptual echo indeed seems to be related to endogenous alpha activity, however, only 44% of variance in alpha peak frequency during baseline and visual stimulation could be explained by alpha peak frequency in the perceptual echo.

To localize the source of the perceptual echoes we calculated coherence using DICS between the MEG data and visual stimulus time courses at individual's echo alpha peak frequency. We found coherence to be maximal at posterior regions in visual cortex

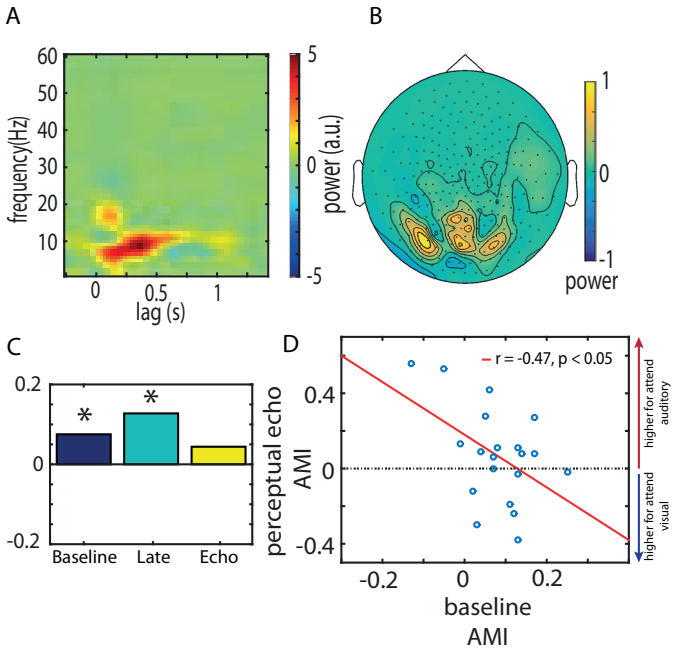

Figure 5. *Alpha modulation indices.* **A**, Time frequency representation of the difference between attend-auditory and attend- visual perceptual echo. Differences in power seem to be confined to the alpha band for lags up to 500 ms. **B**, Topography of the 7 to 14 Hz power differences between attend-visual and attend-auditory echo. No channel revealed a significant difference in the power between 7 and 14Hz. **C,** Group averages of the alpha modulation index (AMI) of the channel level data during baseline (-0.5 s to 0 s), late stimulation (1 s to 6.25 s) and the perceptual echo. Baseline and Late AMI show significant positive modulations as a result of auditory attention. The effect is not significant for the perceptual echo AMI (one sample t-test: baseline: t19 = 4.1, p<0.001; late: t19 = 4.8, p<0.001; echo: t19 = 0.791, p>0.05). **D,** Correlation between perceptual echo AMI and baseline endogenous AMI. The significant correlation suggests attentional modulation in perceptual echo reflects modulation of alpha power at baseline.

(Figure 4C – *same trials*). For the surrogate data (Figure 4C – *different trials*), coherence at individual's echo alpha peak frequency was not localized to any particular region.

Attention does not significantly modulate the perceptual echoes in the alpha band

To test whether attention modulated the perceptual echo in the alpha band, we compared time-frequency representations of power while subjects attended to the auditory versus the visual modality. while alpha power did appear stronger for the attend-auditory compared to the attend-visual condition, the difference was not significant (See Figure 5A and 5B).

To normalize for differences in alpha power across subjects, we calculated the alpha modulation index (AMI) for each participant:

$$AMI = \frac{Power_{attend\ auditory} - Power_{attend\ visual}}{Power_{attend\ auditory} + Power_{attend\ visual}}$$

The AMI was calculated based on the power at each participant's peak alpha frequency identified in the MEG data recorded during the baseline. The AMI allows us to quantify the normalized change in alpha power. We were able to show that alpha power was positively modulated in both baseline and the late time window of the TFRs of power. However, the alpha power of the perceptual echoes differed not differ between auditory and visual attention (Figure 5C; one sample t-test: baseline: $t_{19} = 4.1$, $p < 0.001$; late: $t_{19} = 4.8$, $p < 0.001$; echo: $t_{19} = 0.791$, $p > 0.5$).

To further investigate the relationship between ongoing alpha oscillations and the perceptual echoes we correlated the AMI during the baseline and during late stimulation with the AMI of the perceptual echoes. The alpha power modulation during the baseline period was significantly, negatively correlated with the AMI of the perceptual echo ($r_{19} = -0.47$, $p < 0.05$; Figure 5D). Moreover, the alpha modulation during the late stimulation was significantly and positively correlated with the alpha power modulation of the perceptual echo ($r_{19} = 0.51$, $p < 0.05$). The negative correlation between the baseline AMI and the perceptual echo AMI suggests that the baseline AMI might influence alpha modulation of the perceptual echoes. We therefore conducted an analysis of covariance (ANCOVA) in order to investigate the effect of attention on the perceptual echo (dependent variable) while taking into account the variance explained by the baseline AMI (covariate). The ANCOVA revealed a significant main effect of attention ($F_{1,19} = 6.8$, $p < 0.05$) as well as an interaction effect between alpha modulation at baseline and alpha modulation in the perceptual echo ($F_{1,18} = 5.3$, $p < 0.05$). These results suggest that subjects which stronger alpha power for auditory compared to

visual attention, are subjects that has less alpha power in the perceptual echoes for auditory compared to visual attention.

The correlations between the target contrast and average reaction times, reflecting performance, - and the AMIs of the baseline, late stimulation and the perceptual echoes did not reveal significant relationships ($p > 0.05$ respectively).

Early components of perceptual echo enhanced by visual attention

As the perceptual echo reflects the response of the visual system, we expected the early components of the response to be partially enhanced by visual attention (Gilbert and Li, 2013). In an explorative analysis, we detected peaks and troughs in the early part of the perceptual echo (< 150 ms; see Figure 6; cf. Herring et al. (2015)). We then calculated the attention modulation index (AMI) of the peak amplitudes. We did not find any significant modulation by attention in any of the detected peaks, nor a significant difference between peak amplitudes of both conditions. However, we did find the modulation by attention (AMI) of the N70 component to be significantly correlated with our measure of individual differences in task performance, the target luminance difference ($r_{19} = 0.68$, $p = 0.001$).

We considered the performance on the task to reflect the amount of attention, or effort, the participant invested in the task. We expected this would influence alpha

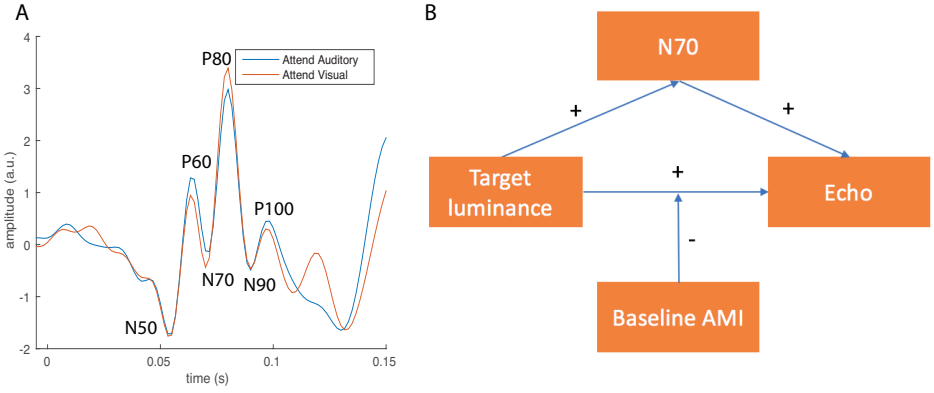

Figure 6. *Attention modulates early components in perceptual echo.* **A**, Early evoked components in perceptual echo for both attentional conditions. Attention did not modulate early components in perceptual echo. **B**, Model of moderation analysis between baseline AMI, AMI during visual stimulation, echo AMI, Target luminance, and N70 alpha power during visual stimulation. Attention (or effort), as indicated by target luminance difference, increases echo alpha power while attending to the visual domain, but this relationship is moderated by alpha modulation at baseline.

modulation at baseline and, consequently, alpha modulation in the perceptual echo. Figure 6B characterize the complex interplay between the effect of attention, alpha power, the presence of a visual stimulus, and the perceptual echo. As the perceptual echo is evoked by visual input, we expected visual attention to have a strong influence on the magnitude of the response. However, visual attention also modulates alpha power, which in turn serves as functional inhibition of sensory input. We tested this model using a mediated moderation analysis with 95% bias-corrected bootstrapped confidence interval (CI) based on 5000 bootstrap samples, performed via PROCESS (Model 6, (Hayes, 2013); Figure 6C; $F_{4,15} = 4.33$, $p < 0.05$, $r^2 = 0.54$). This analysis revealed that our behavioral measure of attention (target luminance difference), predicted the attention modulation in the N70 component ($F_{1,18} = 15.08$, $p = 0.001$), which in turn predicted the attention modulation in the perceptual echo. Target luminance also had a direct effect on the alpha power modulation in the echo, which was moderated by the alpha power modulation at baseline. What this suggests is that attention increases both the alpha power (in line with VanRullen and Macdonald (2012)), as well as the N70 component in the perceptual echo, but that alpha power at baseline suppresses this relationship. Together with the correlation between alpha modulation at baseline and alpha modulation in the perceptual echo (Figure 5D), this suggests that alpha at baseline only predicts the magnitude of the alpha response in the perceptual echo when attention is not modulated that strongly. When attention is modulated strongly, as reflected by high task performance and a high alpha modulation index at baseline, alpha power in the perceptual echo is stronger for the attend visual condition than the attend auditory condition. However, when attention is modulated moderately, the alpha power in the perceptual echo depends on the alpha power at baseline and is thus larger when attending to the auditory domain.

Discussion

In the current study, we aimed at investigating the effect of top-down attention on perceptual echoes. These were obtained by estimating the impulse response function of the MEG data for visual stimulus sequences randomly varying in luminance. Alpha power increased when attention was allocated to the auditory compared to the visual modality in occipital sensors. However, the perceptual echoes were not robustly different when comparing the attention conditions. Interestingly, the attentional alpha power modulation during baseline was negatively correlated with the modulations of the perceptual echos in the alpha band. Subsequent post-hoc analysis of covariance revealed a decrease of perceptual echo alpha power as a result of visual attention as well as an interaction effect between the alpha modulation in the baseline and the

alpha modulation of the perceptual echoes. Furthermore, we found that the peak frequency of ongoing alpha oscillations was significantly correlated with the peak frequency of the perceptual echoes. Additionally, we found that performance on the task was related to the early N70 component of the perceptual echoes and affected alpha power in the perceptual echo. This relationship was further modulated by alpha power in the baseline.

Perceptual echoes not increased with low visual attention

We were able to reproduce the perceptual echoes from MEG data earlier reported from EEG data (VanRullen and Macdonald, 2012). The perceptual echoes showed significantly stronger alpha power compared to the surrogate data. However, our initial hypothesis that the perceptual echoes would show higher alpha power in the attend auditory condition, compared to the attend visual condition, was not confirmed. Although alpha power was, on average, higher in the attend auditory condition than in the attend visual condition, this difference was not significant. Interestingly, VanRullen and Macdonald (2012) reported larger alpha power with high levels of attention in a spatial attention task. This effect was surprising given their additional finding that the magnitude of alpha power at rest was correlated to the magnitude of alpha power in the perceptual echo. They therefore concluded that while the perceptual echoes are related to endogenous alpha oscillations, they possess distinct properties. Indeed, in the current study the frequency of the alpha activity was correlated between the perceptual echo and the alpha oscillations prior to ($r_{19} = 0.66$, $p < 0.01$), and during ($r_{19} = 0.59$, $p < 0.01$) visual stimulation as was reported by VanRullen and Macdonald (2012). This suggests that the same neuronal mechanisms are responsible for generating spontaneous alpha oscillations and the perceptual echo. The study by Herring et al. (2015) showed TMS-evoked responses very similar to the perceptual echoes. As TMS can be seen as an impulse, this confirms the idea that the perceptual echoes reflect the impulse response of the visual system.

N70 reflects excitability of early visual cortex

Similar to Herring et al. (2015), we expected attention to modulate the amplitude of the early components of the perceptual echo. We did not find any early components to be modulated by attention. However, the attentional modulation in the N70 component predicted performance on the task as measured by the titrated luminance of the target stimuli.

Herring et al. (2015) found a component around 40 ms after TMS onset that was significantly enhanced by visual attention. Given an approximation of the retino-thalamocortical delay, the N70 component found in this study could be similar. The

N70 component has been previously described in the ERP literature (for a review, see: Riela (1990)). The component has been under discussion for being unreliable, however, according to Riela (1990) studies have shown this to be due to the nature of the stimuli used to illicit the VEP. The N70 component could most reliably be triggered by finer, foveal stimulation, rather than whole-field stimulation, which is often used in classical VEP studies. In the current study, we did not make use of whole-field stimulation, which makes it plausible the N70 component in the perceptual echo is related to the N70 component occasionally found in the classical VEP. Indeed, (VanRullen and Macdonald, 2012) also reported that comparing foveal to peripheral stimulation, only the early part of the perceptual echo changes in terms of time course and topography. This suggests that the perceptual echo itself has distinct components: one VEP-like early part, mostly dependent on the current excitability state of the visual cortex and a later oscillatory part, mostly dependent on the resonant properties of the visual cortex.

Complex interplay between alpha power at baseline, alpha power in perceptual echoes and attention

In the current study, we did not find a relationship between modulation of perceptual echos in the alpha band and attention. In contrast to the study by Herring et al. (2015), the current study stimulated visual cortex visual the visual stimulus stream. This complicates the effect of attention. The perceptual echoes are caused by visual stimulation and are thought to be related to endogenous alpha oscillations. The response to visual stimulation, however, is enhanced by visual attention (Gilbert and Li, 2013), while at the same time alpha is decreased (Worden et al., 2000; Fu et al., 2001). We observed that the direction and magnitude of the effect of attention on perceptual echo alpha power was quite variable across participants. We therefore explored the possibility of individual differences in ability to modulate alpha power, and attention, at baseline to explain these differences.

To test this complex interplay, we created a mediation/moderation model with the attention moderation of the N70 component as our electrophysiological measure of the level of excitability, the target luminance difference as our behavioural measure of attention, the alpha power modulation at baseline and in the perceptual echo. We found this model to significantly explain a large portion of variance of the data. In lieu of better alternatives, this model would suggest that attention increases excitability, which in turn increases the effect of the visual stimulus in producing a perceptual echo. However, the effect of attention on the perceptual echo is modulated by the alpha modulation at baseline in that alpha suppresses the enhancing effect of attention on the stimulus response. In short, both attention, as well as alpha power, can enhance the perceptual echo, but individual differences in modulation of alpha power and the

effect of attention on excitability determine the size of the perceptual echo. High levels of visual attention increase the magnitude of the perceptual echo, while under moderate levels of visual attention alpha power at baseline determines the magnitude of the perceptual echo. Regardless, our results suggest that the perceptual echo is indeed a reflection of the mechanisms underlying visual processing. Additionally, although alpha oscillations may be under the influence of top-down control by attention, both seem to operate on visual processing by distinct mechanisms. Where visual attention enhances input by increasing excitability, alpha oscillations suppress by pulsed-inhibition.

This raises the question to what extent perceptual echoes reflect alpha oscillations, or perhaps a separate mechanism. One might even wonder whether the results presented in this study provide evidence for a dissociation between endogenous alpha on the one hand, and perceptual echo alpha on the other.

Sustained alpha response during visual stimulation

After onset of the visual stimulus we observed a decrease in alpha power relative to baseline. After this initial desynchronization, however, we observed a sustained alpha response lasting up until the offset of the visual stimulus. This alpha response cannot be explained by simple entrainment as the visual stimulus had frequency content evenly distributed over the entire spectrum. However, a recent study by (Keitel et al., 2017) has shown the possibility of entrainment using so-called quasi-rhythmic stimuli (i.e. Stimuli flickering in a band, rather than at a fixed frequency). It is therefore possible that the sustained alpha-band response is a reflection of low-level entrainment of endogenous alpha oscillations in the visual cortex.

From a signal-processing point of view, the perceptual echo can be seen reflecting the filter kernel (10 Hz pass-band) of the visual system (VanRullen and Macdonald, 2012). In this view, the sustained alpha-band response reflects the filtered visual input. Interestingly, the sustained alpha band response was modulated significantly by attention, in that the power was higher when subjects attended to the auditory domain. This raises the question to what extent the alpha activity predicted by filtering the visual stimulus with the perceptual echo, explains variance in endogenous alpha activity. If the sustained alpha-band response was purely a reflection of the visual stimulus filtered with the kernel as represented by the perceptual echo, one would not predict a difference in the sustained alpha-band response between attending to the visual or auditory modality as there was no difference in the perceptual echo between conditions. To test this, one could indeed filter (or convolve), the visual stimulus time course with the perceptual echo for each condition, and compare resulting alpha power between condition, or calculate explained variance with endogenous alpha oscillations.

Conclusion

In the current study, we were able to replicate the perceptual echoes found by VanRullen and Macdonald (2012) using MEG. We did not find these echoes to be modulated by attention. However, in an explorative analysis we found task performance and alpha modulation at baseline to predict the magnitude of the perceptual echo. We proposed a model to explain the complex interaction between top-down visual attention and posterior alpha oscillations to explain these results. Also, we found an early N70 component that was related to performance on the task and served as a moderator to explain the attention modulation in the perceptual echo. In conclusion, we have shown the perceptual echo to reflect two key aspects of visual processing: (i) excitability as a function of attention, (ii) neuronal alpha-band oscillations as a mechanism of top-down functional inhibition.

CHAPTER 4

Low-frequency transcranial alternating current stimulation rhythmically suppresses stimulus-induced gamma-band oscillations in early visual cortex and impairs perceptual performance

Adapted from:

Herring, J.D., Esterer, S., Marshall, T.R., Jensen, O., & Bergmann, T.O. (2017). Low-frequency transcranial alternating current stimulation rhythmically suppresses stimulus-induced gamma-band oscillations in early visual cortex and impairs perceptual performance (in preparation).

Abstract

Alpha oscillations (8-12 Hz) are hypothesized to rhythmically gate active sensory processing - indicated by activity in the 40-100 Hz gamma band - by a process of pulsed inhibition. We applied transcranial alternating current stimulation (TACS) at individual alpha frequency (IAF) and flanking frequencies (IAF-4 Hz, IAF+4 Hz) to the occipital or frontal cortex in humans during concurrent magnetoencephalography (MEG), while participants performed a visual detection task inducing strong gamma-band responses. Occipital but not frontal TACS phasically suppressed stimulus-induced gamma oscillations in the visual cortex and impaired visual target detection, with stronger phase-to- amplitude coupling predicting behavioral impairments. Frontal control stimulation ruled out retino-thalamo-cortical entrainment resulting from (subthreshold) retinal stimulation. All TACS frequencies were equally effective, suggesting that visual gamma-band responses can be modulated by a range of low frequency oscillations and TACS entrainment is not constrained to the alpha-band. In summary, TACS can produce behaviorally relevant rhythmic modulations of gamma-band oscillations during visual stimulus processing.
Keywords: TACS, early visual cortex, gamma, alpha, oscillations, phase, inhibition

Introduction

Cortical oscillations and their cross-frequency interaction constitute important mechanisms for the organization of neuronal processing. Alpha-band oscillations (8 – 12 Hz) are hypothesized to rhythmically gate information flow in the brain via the pulsed inhibition of sensory processing, reflected by local gamma-band oscillations (40 – 100 Hz). Primarily, we aimed to test the specific hypothesis that the well-described stimulus-induced increase in gamma-band power in the visual cortex, associated with bottom-up visual processing (Bastos et al., 2015; Fries, 2015), can be actively modulated by the phase of slower oscillations, in the alpha band (Klimesch et al., 2007; Jensen and Mazaheri, 2010). While correlational data from MEG studies in humans (Osipova et al., 2008) and intralaminar recordings in monkeys (Spaak et al., 2012) has revealed coupling between alpha phase and gamma amplitude, the causal role of alpha oscillations in modulating gamma-band power remains unresolved. We therefore applied transcranial alternating current stimulation (TACS) at individual alpha frequency (IAF) to the visual cortex (Oz-Cz montage) in human volunteers performing a visual detection task to mimic the impact of alpha oscillatory phase on endogenous gamma activity during visual stimulus processing. At the same time, we sought to test (i) whether TACS is capable of modulating behaviorally relevant neuronal activity in the human brain at commonly used stimulation intensities, an assumption recently called into question by modelling work (Opitz et al., 2016) and cadaver studies (Underwood, 2016) (but see Opitz et al. (2017)), and (ii) whether its effect can be attributed to transcranial, as opposed to mere retinal, stimulation (Schutter, 2015). The novel approach of concurrently combining TCS and MEG (Soekadar et al., 2013; Neuling et al., 2015; Marshall et al., 2016) allowed us to transcranially impose oscillating currents on the visual cortex, while at the same time assessing stimulus-induced gamma power modulation in the visual cortex directly underlying the TACS electrodes (Oz-Cz montage). Whilst it is also technically possible to combine TACS with EEG, spatial interference of stimulation and recording electrodes (both affixed to the scalp) limit the usefulness of this approach (Bergmann et al., 2016). Using a combination of spatial filtering and TACS artifact suppression techniques we were able to extract gamma-band oscillatory signals from the visual cortex during TACS and estimate cross-frequency TACS-phase-to-gamma-amplitude-coupling. To control for the potential impact of electrical stimulation of the retina and resulting retino-thalamo-cortical entrainment, we also applied TACS with a frontal stimulation montage (Fpz-Cz). To further assess the frequency-specificity of TACS-phase-gamma-amplitude-coupling, we applied TACS also the two flanker frequencies of IAF -4 Hz and IAF +4 Hz.

Results and Discussion

Participants performed a forced-choice visual discrimination task in which they had to report the rotation direction of a foveally presented asterisk inside an inward moving high-contrast grating, known to produce a pronounced gamma oscillatory response in early visual cortex (Hoogenboom et al., 2006). Data from 15 of the 17 participants is reported here, as two showed no detectable gamma band response even in TACS-free trials. During each trial, we applied TACS in either a visual (Oz-Cz) or a frontal (Fpz-Cz) montage and at either of three frequencies (i.e., IAF -4 Hz, IAF, +4 Hz; Figure 1B,C) while recording ongoing brain data using concurrent whole-head magnetoencephalography (Figure 1).

Occipital TACS suppressed average gamma power

Gamma power was extracted at individual's gamma peak frequency (see Methods; see Figure 1D for group average gamma power). Average gamma peak frequency was 57.6 Hz +/- 2.2 Hz (mean +/- SEM). In all conditions, a significant increase in gamma-band power was observed during visual stimulus presentation (one-sample t-tests, all $p < 0.005$; Table S1). However, gamma responses differed between TACS montages ($F_{1,14} = 4.84$; $p = 0.045$), with occipital TACS causing a stronger suppression of the gamma response than frontal TACS (Figure 2A), while both were associated with decreased gamma power compared to TACS-free trials (all $p < 0.001$; Table S1). The relative suppression of gamma power by (particularly occipital) TACS supports the idea of occipital alpha-band oscillations reflecting functional inhibition via gamma–band suppression. There was also a main effect for TACS frequency ($F_{1,14} = 7.96$; $p = 0.02$) and a non-significant interaction between the factors ($p = 0.075$). The frequency effect, i.e., smaller gamma power values for faster TACS frequencies (IAF -4 Hz vs IAF: $t_{14} = 3.84$, $p < 0.005$; IAF vs IAF +4 Hz: $t_{14} = 5.07$, $p < 0.001$), was also observed for the TACS-free trials (see Figure S2; note the decreased scaling with increased frequency) and is presumably related to the FFT interpolation approach used to suppress TACS artifacts. Interpolation is done at the stimulation frequency and its harmonics, which resulted in higher gamma power for lower stimulation frequencies. When the number of harmonics increased (with lower stimulation frequency), more interpolation was performed resulting in more suppression of the overall signal after artifact correction. We assume that the interpolation did not affect the absolute difference between baseline and the peri-stimulus period, but rather caused an overall reduction in gamma power. With equal absolute difference between baseline and peri-stimulus period, dividing by lower baseline gamma power (IAF -4 Hz) results in a higher 'relative change from baseline' measure.

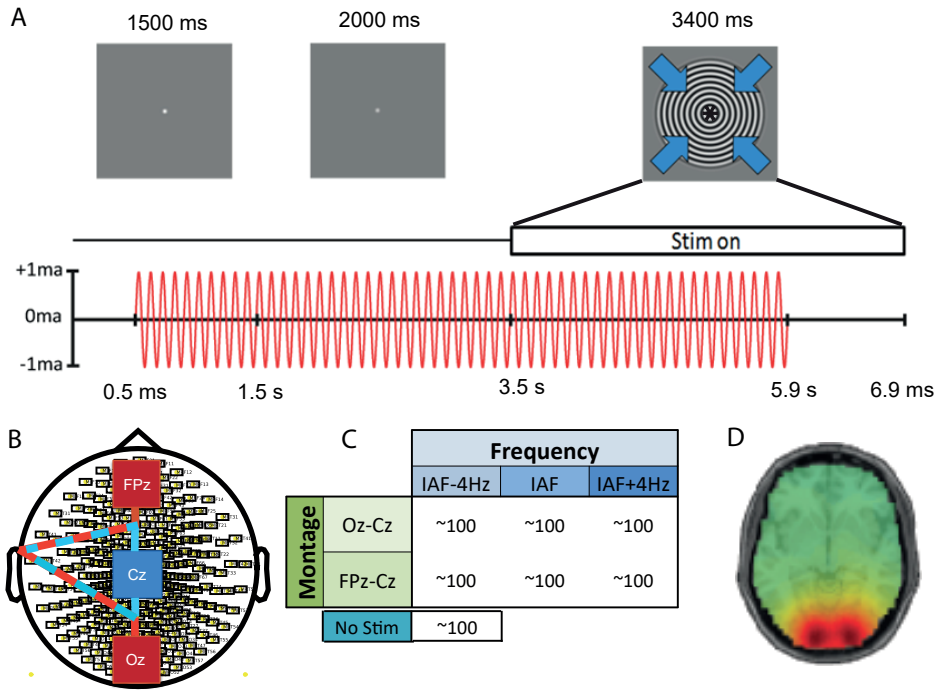

Figure 1. Experimental paradigm and setup. A, Time line of a single trial. Participants fixated a small white dot in the center of the screen and were allowed to blink, until 1500 ms later the white dot turned grey, indicating the end of the blink period. At 3500 ms an inward-moving grating appeared around the fixation dot, which contained a very slowly rotating asterisk in its center. Participants had to report the direction of rotation, by button-press, as soon as the visual stimulus disappeared after at 5900 ms and before the next trial started at 6900 ms. TACS was turned on 500 ms into the blink period and turned off 2400 ms after visual stimulus onset and 1000 ms before visual stimulus offset, thus lasting for 5400 ms each trial. **B**, TACS electrode montage. TACS was applied via three 5 x 5 cm rubber electrodes attached in a dual-montage setup: an occipital montage with electrodes located at Oz and Cz, and a frontal montage with electrodes at Fpz and Cz, with electrode Cz used in both montages. The cables connected to the electrodes were twisted at the shortest possible distance and lead left-ward away from the head towards the shoulder and out of the MEG helmet. **C,** Experimental design matrix. Seven different trial conditions were pseudorandomly intermingled: 2 montages (frontal, occipital) x 3 frequencies (IAF, IAF -4 Hz, IAF + 4 Hz) plus one stimulation-free condition), with ~100 trials per condition, i.e. ~700 trials in total. Due to limitations in total stimulation duration per day (defined by the local ethics committee) the experiment was split into two sessions of ~350 trials each, separated by at least 1 day. **D,** Group average topography of stimulus-induced gamma-band power in source space (DICS frequency domain beamforming). Virtual channels were extracted (LCMV time domain beamforming) from the 10 voxels in visual cortex showing the highest relative increase in gamma-band power from baseline.

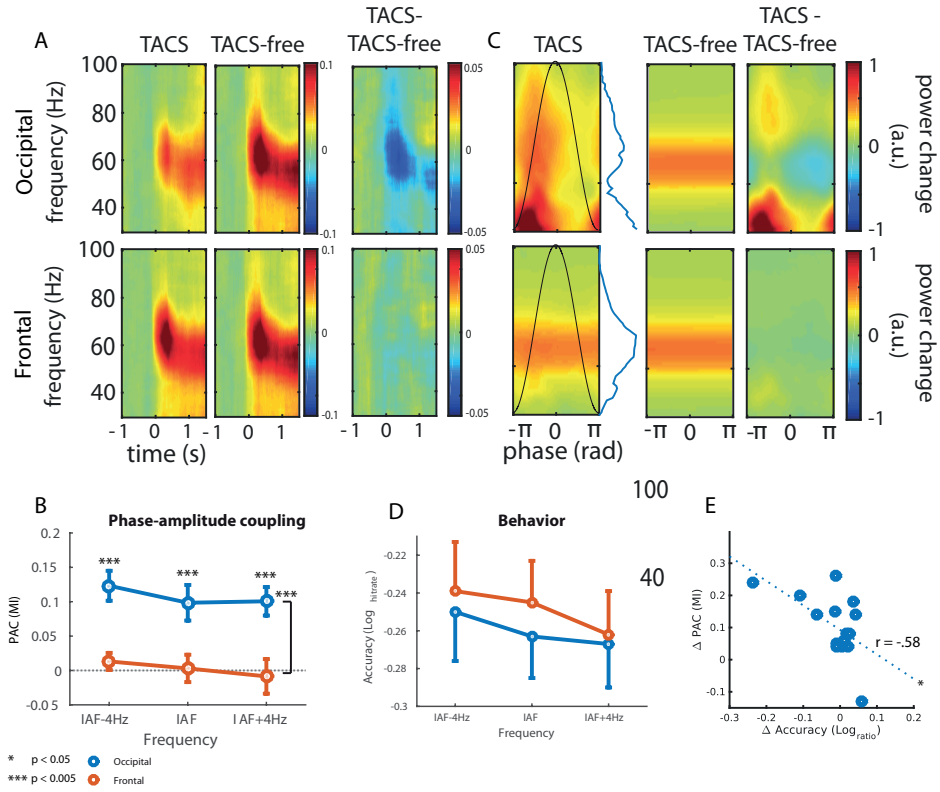

Figure 2. Occipital TACS rhythmically suppressed stimulus-induced gamma oscillations. A, Time-frequency representations (TFR) of oscillatory power timelocked to visual stimulus onset for IAF TACS (TACS) vs. stimulation free trials (TACS-free) (see Supplementary Figure S2 for all frequencies). Gamma responses differed between TACS montages ($F_{1,14}$ = 4.84; p = 0.045), with occipital TACS causing a stronger suppression of the gamma response than frontal TACS, while both were associated with decreased gamma power compared to TACS-free trials (all p < 0.001; Table S1). **B,** Phase-amplitude coupling (PAC, as indexed by the 'modulation index', MI; Tort et al., 2006) between the phase of TACS and the amplitude of the stimulus-induced gamma power during visual stimulus presentation (after subtraction of PAC during TACS in pre-visual-stimulus baseline to control for the potential impact of residual TACS artefacts on PAC). PAC was larger for occipital TACS (blue) than frontal TACS (orange) and surrogates for all TACS frequencies (all p < 0.005), whereas frontal TACS did not differ from surrogates (p > 0.3). **C,** TFRs as in A, but timelocked to TACS peaks and with the x-axis normalized to phase-angles in radians (see Supplementary Figure S4 for all frequencies). Inserted curves represent the TACS cycle. Again, occipital TACS phasically suppressed stimulus-induced gamma-band activity relative to frontal control TACS and surrogates (all p < 0.005), whereas frontal TACS did not show any PAC relative to surrogates. **D,** Accuracy on the rotation- detection task was reduced for occipital compared to frontal TACS, irrespective of TACS frequency (p < 0.05). **E,** The more the individual TACS-phase-gamma-amplitude-coupling differed between for occipital and frontal TACS, the stronger was the individual performance decrease in rotation detection for occipital relative to frontal TACS (r_{16} = -.58; p < 0.05).

Occipital TACS phase rhythmically modulated gamma power

To quantify the phasic modulation of gamma-band power by TACS, we assessed phase-amplitude coupling (PAC) between TACS phase and gamma-band power in the visual cortex, calculating Tort's Modulation Index (MI) (Tort et al., 2010) both before and during visual stimulus presentation. We calculated the MI for each TACS condition at the peak-gamma frequency determined earlier. For comparison, montage- and frequency-specific surrogate samples were created by phase-shifting the TACS signal from the respective TACS condition. PAC was significantly larger for occipital than for frontal TACS, as reflected by a significant main effect of montage (Figure 2B), during visual stimulation ($F_{1,14} = 64.53$, $p < 0.001$), but neither a main effect of frequency ($p > 0.2$) nor an interaction ($p > 0.6$). Importantly, this effect remained significant after correcting for spurious phase-amplitude coupling by subtracting both the respective PAC values at baseline (with TACS but without visual stimulus-induced gamma response) and the respective during-pre change for the surrogate PAC data ($F_{1,14} = 17.06$, $p < 0.001$). In fact, only occipital ($t_{14} = 5.23$, $p < 0.001$) but not frontal TACS ($t_{14} = 0.168$, $p > 0.8$) showed significant PAC during visual stimulus presentation relative to baseline and relative to the respective effect in the PAC surrogates.

To illustrate the phasic modulation of gamma-band power by TACS phase, we calculated TACS peak-locked TFRs (Figure 2C; Figure S4). Here a clear modulation of visually induced gamma-band power can be observed for occipital but not frontal TACS. In line with the general TACS-related gamma-power suppression, also here gamma-band activity appears to be rhythmically suppressed rather than enhanced for certain phases of the TACS cycle. This is strongly suggestive of periodic suppression of stimulus processing at particular phases of the low-frequency cycle, consistent with the notion of inhibitory gating (Jensen and Mazaheri, 2010). In addition, there also seems a rhythmic increase around 40 Hz for occipital, but not for frontal TACS. Although activity in the 40 Hz range is visible in the non-peak-locked TFRs as well (Figure 2A), it is outside the range of the main gamma-band response.

TACS decreases rotation discrimination

Participants correctly identified the rotation direction in 78% of trials (SEM = 2%) with an average reaction time of 409 ms (SEM = 11 ms), for correct trials. There was a small but significant decrease in performance for occipital (77.98% ± 2.66%) compared to frontal TACS (78.33% ± 2.26%) when taking into account the participant's baseline performance in TACS-free trials in a 2 x 3 repeated-measures ANCOVA (see Figure 2D, Figure S5). We observed a main effect of montage ($F_{1,15} = 5.81$, $p < 0.05$) and an interaction between montage and performance in the TACS-free trials ($F_{1,15} = 11.69$ $p < 0.01$). Indeed, subjects performing better in the rotation discrimination task showed

more suppression by TACS than weak performing subjects as reflected by a positive correlation between the performance during TACS-free trials and the difference in performance between frontal and occipital stimulation ($r_{16} = 0.66$, $p < 0.01$).

Interestingly, we found the effect of TACS montage on behavioral performance to be correlated to the effect of TACS montage on phase-amplitude coupling (Figure 2E; r_{13}=-.5753, $p < 0.05$). In other words, subjects showing stronger coupling of stimulus-induced gamma-band activity with TACS showed a stronger decrease in performance on the rotation discrimination task for occipital versus frontal stimulation (Figure 2E). When splitting the data according to montage we found that the modulation index (MI) for the occipital montage was correlated more strongly with the performance on the rotation discrimination task, but not significantly (Figure S6C; r_{13}=-.50, $p = 0.059$).

Effects of TACS cannot be explained by subthreshold retinal entrainment

One of the key issues in TCS research is the current flow to unintended areas such as the retina, which can produce indirect cortical effects (Schutter, 2015). To exclude the potential confound of entrainment through retinal stimulation we added a control montage (see Methods) in which we stimulated through electrodes placed on Cz and Fpz, according to the international 10-20 system. The stimulation intensity was matched according to subject's individual phosphene threshold; i.e., The intensity was adjusted to 80% of the intensity at which retinal phosphenes were induced. This ensured that (i) no retinal phosphenes were induced throughout the experiment, and (ii) the amount of current reaching the retina was as equal as possible for both montages with the aim of equalizing any effects of TACS on the retina. Throughout the experiment, we did not observe an effect of TACS using the frontal montage on behavior, nor on phase-amplitude coupling with gamma band power, nor on the relationship between both. This clearly shows that effects of TACS in the current experiment cannot be explained by (subthreshold-) entrainment of the retina.

Conclusion

The aim of this study was to test the specific hypothesis that the phase of slower oscillations, in the alpha band, modulate sensory processing, as reflected by stimulus-induced gamma-band power (Bastos et al., 2015; Fries, 2015) by means of pulsed inhibition (Klimesch et al., 2007; Jensen and Mazaheri, 2010). We found that TACS suppresses overall bottom-up gamma-band power. Additionally, we showed that this suppression was phasic in nature, in that gamma-band power was coupled to TACS phase. Furthermore, this resulted in decreased performance on a rotation detection task. Importantly,

the magnitude of the effect of TACS on performance was correlated to the amount of coupling between gamma-band power and TACS phase. We therefore show that pulsed-inhibition can be implemented with TACS and thereby recreate the functional effects of alpha oscillations on sensory processing.

Given the broad and still increasing use of TACS and TDCS to non-invasively modulate neuronal activity and thereby cognitive function and behavioral performance, recent methodological criticism has put the entire field into question. Indeed, the doubts raised with respect to the replicability of TDCS effects outside the motor cortex (Horvath et al., 2014, 2015), the question whether tDCS and TACS at common current intensities are actually capable at all of modulating neuronal activity in the human brain (Buzsaki, 2016, CNS meeting, NYC, however, see Kar et al., 2017), and the possibility of peripheral (e.g., retinal) entrainment as a major confound (Schutter, 2015), called the credibility of the entire field into question. While we fully agree that the field will benefit from increased methodological scrutiny, multiple studies (Pogosyan et al., 2009; Joundi et al., 2012; Polania et al., 2012; Brittain et al., 2013; Santarnecchi et al., 2013; Helfrich et al., 2014; Cecere et al., 2015; Alekseichuk et al., 2016) have provided behavioral evidence that TACS can indeed affect the human brain. However, despite pioneering TACS-EEG work (Helfrich et al., 2014) and proof-of-feasibility TACS-MEG studies (Neuling et al., 2015; Witkowski et al., 2015), strong evidence for a phase-dependent effect of TACS on neuronal activity during the stimulation is still lacking due to its occlusion by the presence of massive TACS artifacts. By providing direct evidence that TACS is capable of modulating visually-induced gamma power in a behaviorally relevant manner and ruling out retinal entrainment as alternative explanation, we here demonstrate that TACS can directly modulate the excitability of visual cortex.

Methods

Participants

All participants were recruited from a database of the Radboud University Nijmegen. In total, 17 participants (5 males, 12 females, age: 24.3 ± 0.7 (mean ± SEM)) with normal, or corrected-to-normal vision by contacts only, were included in the study. All participants conformed to standard inclusion criteria for MRI, MEG, and TACS. Written informed consent was obtained prior to start of the experiment according to the Declaration of Helsinki. The study was approved by the local ethics committee. Participants were financially compensated at 10 euros per hour. Data are reported from 15 participants; two participants had to be excluded since we could not detect a visual stimulus-induced gamma-band response even during TACS-free periods.

Procedure

Participants took part in two experimental sessions on two separate days (with all experimental conditions tested at both days). Additionally, a structural MRI was obtained on a separate day. On the beginning of the first session participants were familiarized with the experimental task. Otherwise, both experimental sessions followed the same procedures: After TCS and ECG electrodes were applied, participants were familiarized with the stimulation and the stimulation intensity was determined. Then, he participants were seated in the MEG and four minutes of resting state data were collected (two minutes eyes-open, two minutes eyes-closed) before they performed a rotation-detection task in blocks of 10 minutes with short breaks in between (Figure 1A). The total MEG time was 90 min per session.

Rotation detection task

Participants performed a rotation detection task in which they had to indicate by button-press the direction of rotation of an asterisk in the center of an inward moving high-contrast grating (Figure 1A). Participants were instructed to fixate a white dot on grey background in the center of the screen. Each trial started with a 1.5 s period in which participants were allowed to blink. Participants were asked to refrain from blinking as soon as the fixation dot turned grey. A 'baseline' period of two seconds followed after which an inward-moving (0.8 degree/second) black-and-white high contrast grating with concentric circles (2.5 cycles/degree) appeared on screen covering 8 degrees of visual angle (adapted from Hoogenboom et al., 2006) for 3.4 seconds. In the center of the inward moving grating an asterisk was present that slowly rotated either clock or counter-clock wise. The rotation rate was continuously updated after each trial using an adaptive-staircase procedure (Watson and Pelli, 1983) so that participants were roughly 80% correct in guessing the rotation direction. The goal of the task was to keep the participants fixated and assure a stable level of attention throughout the experiment and to assess effects of stimulation on foveal detection accuracy. Participants completed ~700 trials in total, divided over two sessions, pseudo-randomized to ensure that an equal amount of trials of each condition was completed after every session.

TACS

TACS was applied using a battery-driven NeuroConn DC+ stimulator (neuroConn GmbH, Ilmenau, Germany) attached to three 5 x 5 cm, conductive, non-ferromagnetic, rubber electrodes attached to the scalp following the international 10-20 system creating an occipital montage (Oz-Cz) and a frontal montage (Fpz-Cz), sharing electrode Cz (Figure 1B). The surface area of the scalp was thoroughly cleaned using alcohol and Nuprep skin preparation gel (Weaver and Company, Aurora, CO, USA) prior to attaching the electrodes using conductive Ten20 paste (Weaver and Company, Aurora, CO,

USA) ensuring no paste was applied outside of the contact area of the electrodes (cf. (Marshall et al., 2016)). One electrode was placed over Oz (10% of the inion-nasion distance, anterior to the inion), another electrode was placed over Cz, at the vertex and a final electrode was placed over FPz (10% of the inion-nasion distance, posterior to the nasion). The four electrode cables were connected to the electrodes in a manner that minimized the size of the current loop on the scalp. Cables for the Oz-Cz montage were connected to the anterior side of electrode Oz, and to the posterior side of electrode Cz. For the FPz-Cz montage, cables were connected to the posterior side of electrode FPz, and the anterior side of electrode Cz. Due to the stickiness of the paste no further mounting aids were required. Impedances were kept below 5 kOhm.

Several steps were taken to minimize the artifacts produced by the presence of additional material in the magnetically shielded room (MSR). First, all electrodes and cables, including connectors, were checked for ferromagnetic properties by moving the items inside the helmet while inspecting the effects on the MEG signal. Second, a CAT6 electronically shielded cable was used to attach the electrodes to the stimulator, which was located outside of the MSR. The cable was fixed to the chair in the MSR to minimize movement. Third, the cables attached to the scalp were twisted, per montage, so that the resulting current-loop was as small as possible. The cables attached to the scalp ran left of the subject, fixed to the shoulder, downwards towards the chair, away from the helmet.

Stimulation frequency was adjusted per participant based on the individual alpha frequency. To this end the individual alpha frequency (IAF) was determined, with a resolution of 0.2 Hz, at the beginning of each session as the peak frequency of the difference in power spectra between an eyes-closed and eyes-opened resting state session (10.31 ± 0.41 Hz, mean ± SD across subjects). During the experiment, stimulation frequency was set for each trial to either IAF -4Hz, IAF, or IAF +4 Hz (Figure 1C). These two flanker frequencies at 4 Hz below and above IAF were chosen to explore the frequency specificity of the stimulation while still being sufficiently close to the alpha-band not to target neighboring functionally relevant frequency bands (i.e., the theta- or beta-band).

Stimulation intensity was titrated at the beginning of each session to 90% of the individual retinal phosphene threshold, separately per montage (peak-to-peak TACS amplitude for Oz-Cz: 963 ± 319 μA and Fpz-Cz: 231 ± 114 μA; mean ± SD, range for Oz-Cz: 450 – 1750 μA, for FPz-Cz: 50 – 550 μA). Retinal phosphene threshold was determined by increasing the current strength of TACS at IAF from 100 mA in steps of 100 mA until the participants started to perceive retinal phosphenes. Stimulation intensity was adjusted per montage, because the goal of the frontal montage was to control for retinal stimu-

lation effects by increasing the proximity to the retina, while decreasing the proximity to the occipital pole, ensuring that the current effectively stimulating the retina was comparable between montages. The choice of subthreshold intensity ensured that no visual phosphene perception interfered with (i) the transcranial stimulation effects, (ii) the visual stimulus-induced gamma responses, and (iii) the detection task performance.

During each trial (except for the stimulation-free NoStim trials), TACS was applied for ~5.4 s at one of the three frequencies (IAF -4Hz, IAF, or IAF +4 Hz) and via one of the two montages (occipital Oz-Cz or frontal Fpz-Cz) (Figure 1C). Stimulation started 1 s before the baseline period to allow for a build-up of potential entrainment effects and continued throughout the 2 s baseline period into the visual stimulus presentation period. The stimulation was turned off 2.4 seconds into the visual stimulation period after completing a full number of cycles at the particular stimulation frequency. I total, 600 TACS trials (and 100 stimulation-free trials) were acquired per subject, distributed over two sessions, resulting in a total stimulation time of 27 min per session.

MEG data acquisition

Whole-head MEG was recorded using a 275-channel axial gradiometer CTF system (CTF MEG systems, VSM MedTech Ltd.) sampling at 1200 Hz, with a hardware low pass filter at 300 Hz. Head localization coils were placed on the nasion, and in the left- and right-ear canals. The position of the head was recorded at the beginning of the experiment and was monitored, and adjusted if head motion exceeded 3 mm, during breaks using online head-position tracking (Stolk et al., 2013). Eye-tracking was conducted throughout the experiment using an EyeLink 1000 eyetracker (SR Research Ltd, Ottawa, Canada), sampling at 2 kHz. Electrocardiogram (ECG) was recorded using two electrodes in a bipolar montage placed on the left collarbone, and right hip.

Data Analysis

Preprocessing

Data analyses was conducted using the FieldTrip toolbox (Oostenveld et al., 2011) and custom Matlab scripts for Matlab 2014b (Mathworks, Nattick, USA). First, trials that included blinks during the baseline- or visual stimulation period were detected by bandpass filtering the horizontal, and vertical motion eye-tracker channels between 1 and 15 Hz (4^{th} order, two-pass, Butterworth). Trials that exceeded a z-score of 5 were rejected. Second, trials that included SQUID-jumps were detected by first high-pass filtering the data at 30 Hz (4^{th} order, two-pass, Butterworth) to attenuate the stimulation artifact. Trials of which the first-order temporal derivative exceeded a z-score of 25

were rejected. This resulted in an average of 9% ± 8% (Mean ± SD) rejected trials per subject. The data were down-sampled to 600 Hz and epoched into trials from -3.4 to 3.6 seconds after onset of the gamma-inducing visual stimulus.

DICS beamforming

A single-shell head model (Nolte, 2003) was created from the individual MRIs. Next, an equally-spaced grid with 0.5 mm^3 based on a standard MNI template MRI with 0.1 mm^3 resolution was created. This template grid was subsequently warped to each individual subject's anatomy to easily average and compare voxels across and between subjects. The aim of the intended spatial filter was to maximize the sensitivity to the expected gamma-band response produced by the visual stimulation. To this end we selected the trials without stimulation and epoched the trials into a baseline period of -2.0 until -0.001 s and an activation period from 0.4 to 2.399 s after visual stimulus onset to create two epochs of 2.0 s length. After removing linear trends, we then calculated the cross-spectral density (CSD) matrix for both baseline as well as activation epochs and data from both epochs combined, at 60 Hz, with 15 Hz frequency smoothing using a multi-taper approach resulting in an analyzed frequency band of 45 – 75 Hz. A common spatial filter was calculated using a Dynamic Imaging of Coherent Sources (DICS) beamformer (Gross et al., 2001) on the CSD of the combined baseline and activation data using 5 % regularization. Note that the spatial filter was calculated on TACS-free trials. The resulting spatial filter was then applied to the activation and baseline data separately. To find the voxels showing the maximal increase in gamma-band power in response to visual stimulation, the relative gamma-power change from baseline was calculated by dividing for each voxel in source space the absolute change from baseline by the baseline gamma power.

LCMV virtual channels

To enhance the sensitivity to the visually induced gamma-band response, we used Linear Constrained Minimum Variance (LCMV) beamforming (Van Veen et al., 1997) to extract virtual channel time courses from the voxels which showed the strongest gamma-band power increase from baseline in each participant (Figure 1D) and were located inside the visual cortex (method adapted from Marshall et al. (2016); visual cortex defined by AAL atlas (Tzourio-Mazoyer et al., 2002) mask including all striate and extra-striate regions). From these data, we created a new grid with 10 voxels. After bandpass-filtering (40 – 70 Hz) to maximize spatial filter sensitivity to the gamma-band, the covariance matrix was calculated for epochs from -2.3 to 2.3 s relative to visual stimulus onset on TACS-free trials, and spatial filters were calculated using 5% regularization. The raw sensor-level data was multiplied by the resulting spatial filters to obtain virtual channel time courses for each of the 10 voxels in the grid. For each subsequent

analysis, we first analyzed each of the time courses separately and per subject, averaged over the 10 time courses.

FFT interpolation

The main focus of the study was the effect of TACS in the alpha frequency-range on visually-induced gamma-band oscillations. Therefore, our original strategy was to ignore the artifact-loaded signal at the stimulation frequency itself and only analyze the gamma-band power modulation with respect to the known TACS phase. However, while TACS was applied at lower frequencies (range: 5 – 16 Hz) and thus well outside the stimulus-induced gamma-band of interest (i.e., 45 – 75 Hz), the magnitude of the TACS artifact in the MEG signal was orders of magnitude larger than the magnetic fields produced by the brain and the higher harmonics of the TACS frequency still affected the gamma-band frequencies of interest (Supplementary Figure S1C). TACS artifacts and their harmonics could not be sufficiently suppressed by bandstop filters alone. LCMV spatial filters have previously been used to extract the brain signal of interest while effectively attenuating the TCS artifact due to the suppression of correlated sources (e.g. Neuling et al., 2015; Marshall et al., 2016). Unfortunately, we could not follow this approach, since LCMV spatial filter calculation based on TACS trials did not only suppress TACS artifacts, but also the stimulus-induced gamma-band response of interest. In fact, only 3 out of 17 participants still showed a clear gamma-band response, even during TACS-free trials, after this procedure, while with the current procedure we only observed 2 out of 17 subjects without a visible gamma-band response while the gamma-response is known to be very reliable (Hoogenboom et al., 2006; Scheeringa et al., 2009; Scheeringa et al., 2011). We therefore calculated LCMV spatial filters on TACS-free trials only, with the priority of preserving gamma-band responses in the visual cortex, while still attenuating TACS artifacts, though to a lesser degree. In addition, we employed an FFT interpolation approach (Figure S1CD) previously used to attenuate line-noise in ECG recordings (Mewett et al., 2001) to effectively suppress the TACS frequency and its harmonics in all conditions. Data were transformed to the Fourier domain using a fast-Fourier transform (FFT) with 0.2 Hz frequency resolution (after zero-padding each trial to 5 s). Then, for each TACS trial the magnitude spectrum was interpolated from -2 to 2 Hz around the TACS frequency, and each of its harmonics up until the Nyquist frequency, while the phase spectrum remained intact. The interpolated frequency domain data was then transformed back into the time domain using an inverse FFT. As the effect of overall magnitude attenuation of the signal depended on the TACS frequency, we generated appropriate control conditions by applying the same FFT interpolation approach to copies of the TACS-free trials. The resulting frequency-specific TACS-free control conditions thus ensured fair comparisons even if harmonics inside the gamma frequency-band were interpolated.

Time-Frequency Analysis

To assess visual stimulus-induced gamma-band responses we calculated time-frequency representations (TFRs) of power by means of a sliding window FFT. For each trial, a sliding time window of 500 ms was moved in steps of 20 ms over the entire trial. The sliding time window was multiplied with a sequence of tapers (discrete prolate slepian sequence; dpss) to achieve a frequency smoothing of 10 Hz. Frequencies between 30 Hz and 100 Hz were analyzed in steps of 1 Hz. The data was zero-padded up to 10 seconds to achieve an artificial frequency resolution of 0.1 Hz. The mean and any linear trend were removed prior to calculating the FFT. The gamma-band response is usually best represented as relative change from baseline to account for its comparably low amplitude. During TACS trials, however, any residual noise in the baseline may thereby result in spuriously low ratios. We thus first subtracted the baseline (-1 to -0.2 s) from the activation period, effectively removing any residual frequency- and montage-specific TACS-related artifacts (which are per design identical in baseline and visual activation periods of the same condition), and then divided all conditions by the same average baseline period that was derived from all TACS-free trials and is thus unaffected by TACS-artifacts (ensuring a fair comparison of the gamma-band response relative to TACS-free trials). Gamma peak frequency was estimated by first calculating, for all conditions, the relative change in gamma power from a TACS free baseline. Subsequently, a 23rd order polynomial was fitted to the average over all conditions and the largest peak within a range from 40 – 90 Hz was extracted using Matlab's 'findpeaks' function. Gamma power extracted at these individual peak frequencies were used for all subsequent analyses. For each experimental condition, relative power at individual gamma peak frequency was extracted between 0.5 and 1.5 s and used for subsequent statistics. Note that the attenuation of gamma power differs between frequency conditions based on the number of TACS harmonics in the gamma-band range that had to be interpolated within the FFT for artifact removal. However, the same procedure was applied to the TACS-free trials, to guarantee a fair comparison. We used one-sample t-tests to test for significant gamma power responses relative to baseline, and repeated-measures ANOVAs (no correction for non-sphericity was necessary) on the baseline- and surrogate-corrected data, followed by paired-sample t-tests were appropriate, to compare values between TACS montage and frequency conditions.

Phase-Amplitude Coupling

A different approach for assessing the extent to which TACS phasically modulates the gamma-band response is to calculate phase-amplitude coupling (PAC). We used Tort's Modulation Index (MI) by calculating the normalized Kullback-Leibler (KL) divergence of the histogram of TACS phase-binned gamma amplitude to a uniform distribution (Tort et al., 2010). In case of PAC, the histogram diverges from a uniform distribution. To this

end, the gamma-band amplitude was determined by convolving the virtual channel data during the 0.5 and 1.5 s period with a 5-cycle moving time window multiplied with a Hanning taper for frequencies from 30 Hz to 100 Hz in steps of 1 Hz, while a 1 second time window was used for estimating the phase of the TACS signal similarly to the gamma-band magnitude. As for TACS peak-locked TFRs, we randomly subsampled the data for each condition 500 times using a sample size equal to the lowest number of trials across conditions, to prevent any bias due to unequal trial numbers between conditions. MIs were calculated for each random subsample and then averaged. As control, PAC was also estimated for surrogate data, for which the phase-providing TACS signal was randomly phase-shifted to create frequency-specific surrogate PAC values for each TACS condition. We used one-sample t-tests to test for significant PAC after subtracting PAC values at baseline and respective visual-stimulation induced changes in surrogate PAC values. We used repeated-measures ANOVAs (no correction for non-sphericity was necessary) on the baseline- and TACS-corrected data, followed by paired-sample t-tests were appropriate, to compare PAC between TACS montage and frequency conditions.

Alpha Peak-Locked TFRs

To assess whether TACS phasically modulated the power of the visually-induced gamma-band response, we evaluated the gamma-band power dynamics in TACS peak-locked TFRs. To this end, we first calculated TFRs of each trial as described in the previous paragraph, but decreased the size of the sliding time window to 0.1 s to be more sensitive to transient changes in the gamma-band across the TACS cycle. Also, this time data were normalized per trial to allow robust single-trial assessment of phasic gamma power modulation for subsequent TACS-phase-gamma-amplitude-coupling analyses. To take variations in signal-to-noise ratio into account (e.g., due to residual artifacts), TFRs were z-normalized trial-by-trial by subtracting the mean and dividing by the standard deviation of the trial's baseline, resulting in an estimate of time-locked power that is relatively robust against noisy trials and extreme values (see Grandchamp and Delorme (2011)).

Next, we detected the peaks of the TACS cycle in the output copy of the TACS signal as provided by the stimulation device, using Matlab's *findpeaks* function. Peaks were defined as the local maxima on the z-transformed stimulation signal with a minimum width of a quarter cycle of the stimulation signal, a minimum height of 1, and a minimum distance of 0.9 cycles. The data were epoched into segments around each peak with a duration of 4 cycles of the respective TACS frequency. For each TACS frequency, a comparable segmentation was also applied to the TACS-free trials, however, using randomly chosen stimulation signals from one of the respective TACS trials. This resulted in a specific TACS-free control condition for each TACS frequency, effectively providing

a surrogate distribution of gamma power values relative to the TACS cycle. Finally, averages were created for each of the TACS frequencies and respective TACS-free surrogates. As the number of epochs depends on the number of cycles (being higher for higher frequencies), we applied a random subsampling approach to create unbiased averages. We first determined the stimulation frequency with the smallest number of epochs and then averaged 500 randomly drawn subsamples of that size per condition. To allow direct comparison between TACS frequencies and averaging across subjects (with individualized IAF), we transformed the time-axis to radians by adjusting the step size during TFR calculation accordingly. Importantly, TACS peak-locked TFRs were calculated for both baseline and visual stimulation period. Since the baseline period does not contain any visually-induced gamma-band responses, but may contain residual TACS artifacts, it serves as an excellent control against TACS artifact-related spurious phase-amplitude coupling.

Supplementary tables

Table S1

One Sample T-Test	Mean	SE	t	df	p
Occipital: IAF - 4 Hz	0.129	0.030	4.243	14	< .001
Occipital: IAF	0.087	0.019	4.530	14	< .001
Occipital: IAF + 4 Hz	0.042	0.012	3.622	14	0.003
Frontal: IAF - 4 Hz	0.176	0.044	4.017	14	0.001
Frontal: IAF	0.122	0.027	4.534	14	< .001
Frontal: IAF + 4 Hz	0.058	0.015	3.972	14	0.001
TACS free: IAF - 4 Hz	0.222	0.051	4.393	14	< .001
TACS free: IAF	0.141	0.033	4.274	14	< .001
TACS free: IAF + 4 Hz	0.071	0.017	4.279	14	< .001

Table S1. *Mean relative change from TACS free baseline.* Table contains mean (+/- SEM) relative change values from TACS free baseline. Right columns contain t-statistics and p-values for the one-sample t-tests for the mean against zero. All means were significantly different from zero indicating an increase in gamma-band power from a TACS free baseline was observed for all conditions.

Table S2

Paired Samples T-Test			t	df	p
Occipital: IAF - 4 Hz	-	TACS free: IAF - 4 Hz	-2.733	14	0.016
Occipital: IAF	-	TACS free: IAF	-2.276	14	0.039
Occipital: IAF + 4 Hz	-	TACS free: IAF + 4 Hz	-2.471	14	0.027
Frontal: IAF - 4 Hz	-	TACS free: IAF - 4 Hz	-3.255	14	0.006
Frontal: IAF	-	TACS free: IAF	-1.879	14	0.081
Frontal: IAF + 4 Hz	-	TACS free: IAF + 4 Hz	-2.894	14	0.012

Table S2. *Difference from TACS free data.* Table contains paired-samples t-tests between gamma power at peak gamma frequency for TACS and TACS free data. Right columns contain t-statistics and p-values for the paired-sample t-tests of the difference between pairs. All apart from 'Frontal: IAF' were significantly lower indicating a decrease in gamma-band power from TACS free trials for all conditions.

Supplementary Figures

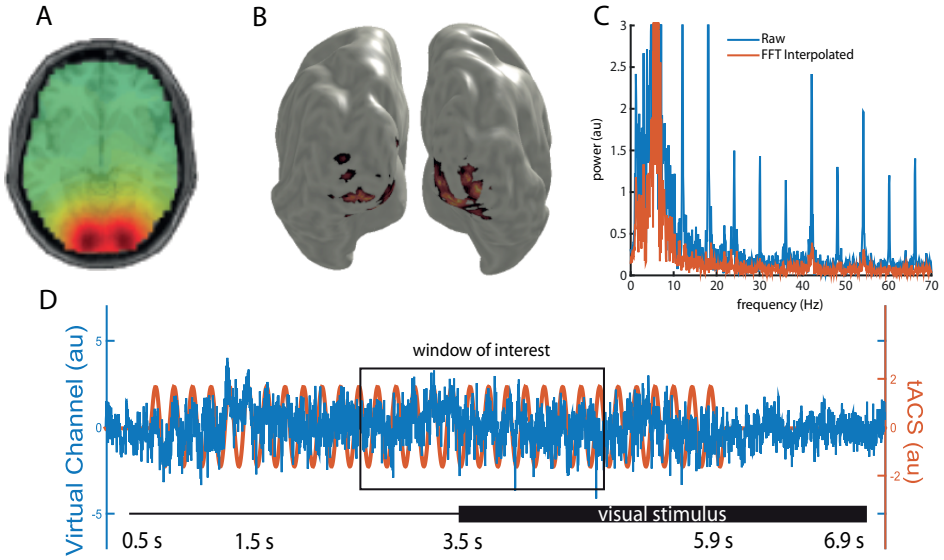

Figure S1. Voxel selection and cleaning. **A,** Virtual channels were extracted at the 10 voxels, in the visual cortex, showing the highest increase in gamma-band power from baseline due to visual stimulation. Warm colors in the transversal slice indicate areas showing increased gamma-band activity due to visual stimulation. **B,** Group heat map indicating the voxels selected from A. **C,** power spectrum for a subject from a 6 Hz TACS trial before (Raw; blue trace) and after (FFT interpolated; red trace) FFT interpolation. **D,** Example trial of a virtual channel time-course (blue trace) with the stimulation signal (red trace) overlaid. The analyzed epochs during TACS is indicated by a black box.

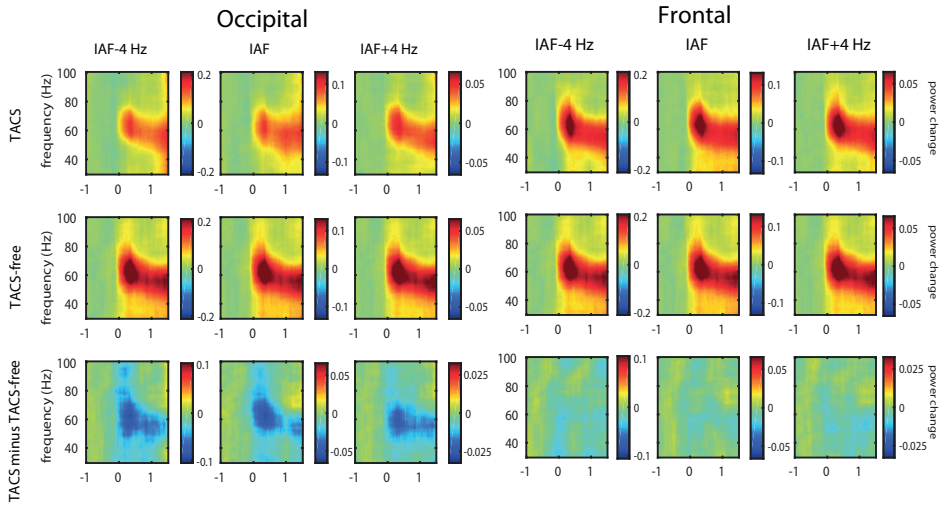

Figure S2. Occipital TACS suppresses visually-induced gamma-band response. TFRs show the visually-induced gamma-band responses for occipital, as well as frontal stimulation, for all stimulation frequencies, including corresponding stimulation free data. The bottom row represents the difference between stimulation and stimulation free data. Note the different scaling of color values per TACS frequency condition.

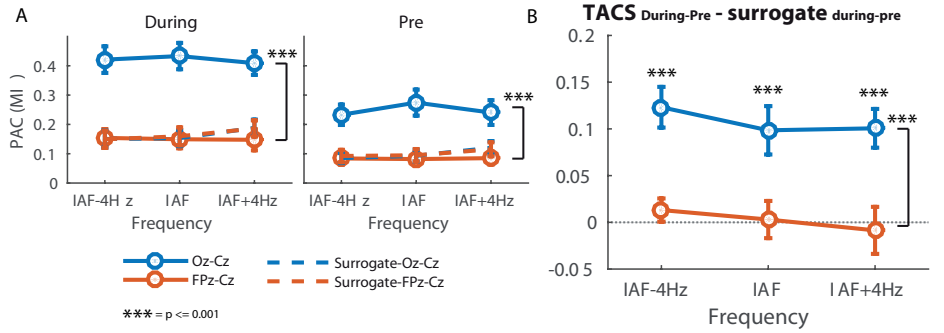

Figure S3. Gamma-band activity phase-coupled to TACS for occipital stimulation. **A,** Modulation index (MI) analyses showed increased phase-amplitude coupling (PAC) for occipital, but not for frontal stimulation compared to baseline and surrogate data. Importantly, frontal stimulation did not differ significantly from the surrogate data. **B,** Difference in PAC between periods during visual stimulation and baseline, with surrogate data (also during visual stimulation minus baseline) subtracted. Subtracting baseline PAC values, and surrogate data ensures correction for any artefactual coupling due to the presence of TACS.

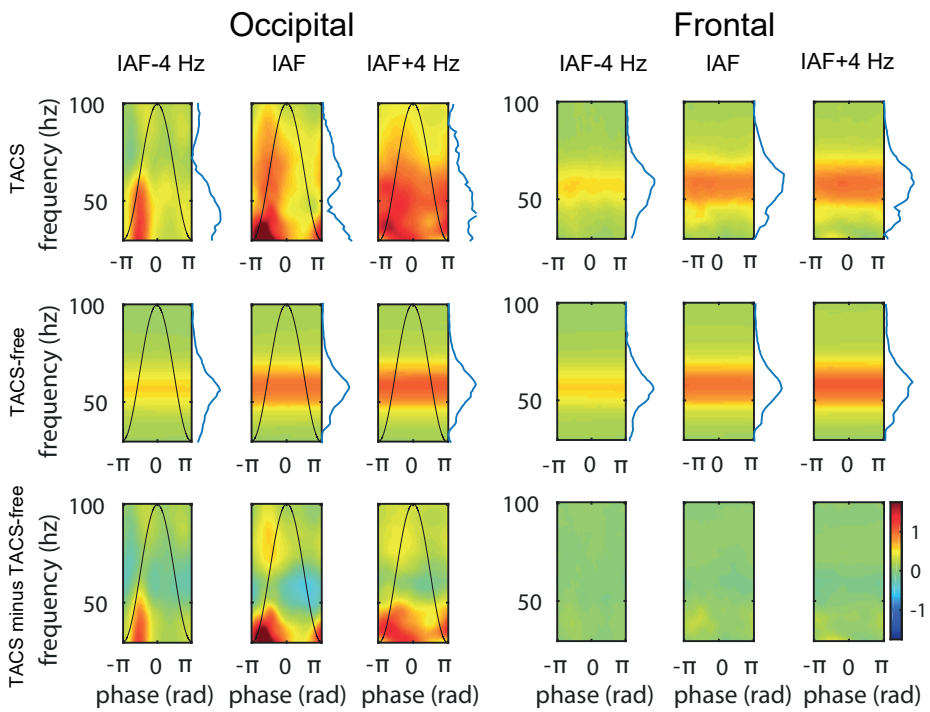

Figure S4. Occipital TACS phasically modulates visually-induced gamma-band response. TACS peak-locked TFRs show gamma-band amplitude sorted according to phase of TACS. Note that some of the apparent differences between TFRs for different frequencies (cf. columns for middle row representing TACS-free trials) are partially due to the different cycle length (i.e. time window) that had been normalized into radians as longer segments are accompanied with less frequency smoothing. Only occipital stimulation shows a clear modulation of gamma-band amplitude according to TACS phase. The bottom row represents the difference between the TACS and stimulation free data.

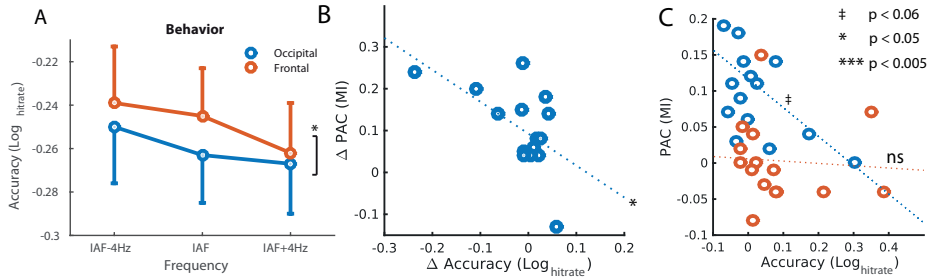

Figure S5. TACS decreases performance on rotation discrimination task. **A,** only occipital TACS significantly reduces performance on the rotation discrimination task. Error bars represent standard error of the mean (SEM). **B,** The difference in modulation index values for occipital versus frontal stimulation correlate with the difference in performance for occipital versus frontal stimulation. Both A, and B, show that subjects showing stronger coupling of gamma-band activity with TACS show a larger decrease in performance on the rotation discrimination task. **C,** Modulation index (MI) correlates with accuracy on the rotation discrimination task only for occipital, but not for frontal stimulation.

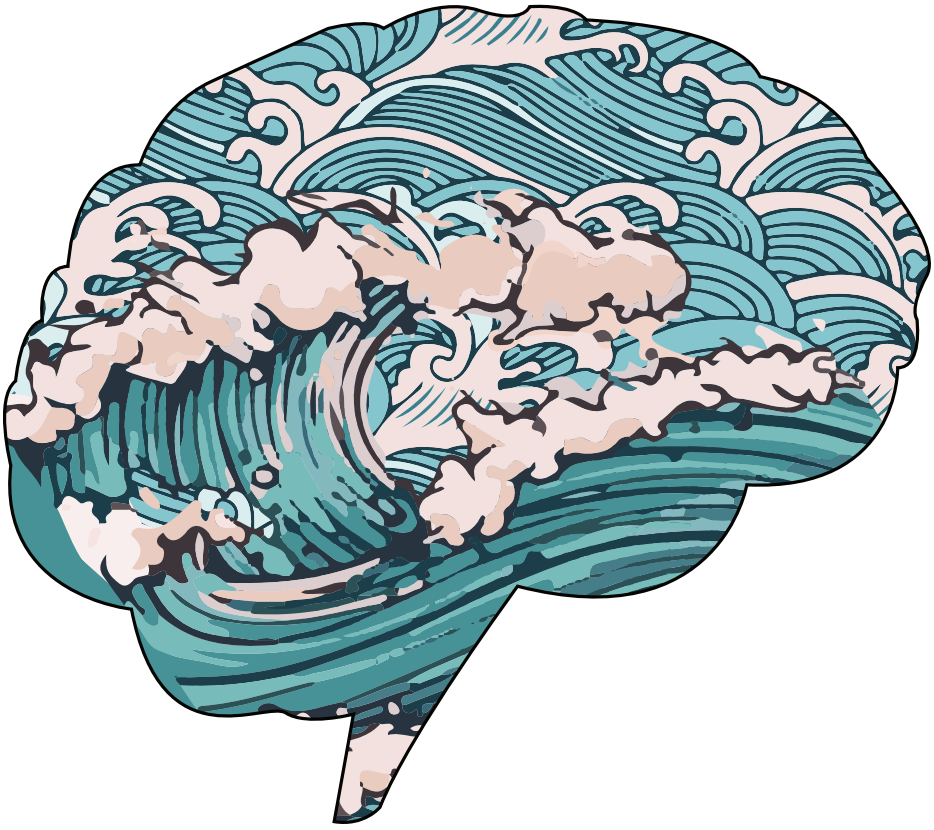

CHAPTER 5

Probing cortical excitability by rapid frequency tagging

Adapted from:

Herring, J.D., Herpers, J., Bergmann, T.O., & Jensen, O. (2017) Probing cortical excitability by rapid frequency tagging (in preparation) & Herpers, J. (2017) Frequency tagging at high frequencies in downstream areas under influence of attention (Master's thesis)

Abstract

Frequency tagging has been widely used to study the role of selective attention on stimulus processing. Presenting a stimulus at a specific frequency generates so-called steady-state visually evoked responses. Neuronal oscillations have been shown to play an important role in gating information flow in the brain. Frequency tagging would lend itself to study how neuronal oscillations modulate sensory processing. However, frequency tagging is mostly done at frequencies in the range of neuronal oscillations. Technical limitations have limited the frequency range used in frequency tagging studies. In the current study, we used a new projector that is able to present images at up to 1440 Hz. We asked participants to perform a cued spatial attention task in which they had to detect changes in face or house stimuli (tagged at 63 Hz or 78 Hz) while measuring whole-head magnetoencephalography. We found posterior sensors to show a strong response at the tagged frequency. Additionally, this response was enhanced by spatial attention. Furthermore, the spectral power time course of the tagged stimulus was modulated in the alpha band. We therefore provide proof-of-principle for the use of high-frequency tagging to study sensory processing in the brain and the role of neuronal oscillations therein.

Introduction

Frequency tagging has been successfully used to study selective stimulus processing in EEG studies. e.g. (Müller et al., 1998; Müller et al., 2003; Müller et al., 2006; Vialatte et al., 2010). It has been applied in MEG studies to investigate visual perception (Parkkonen et al., 2008) as well as the engagement of representational selective areas in the ventral stream (Baldauf and Desimone, 2014). With frequency tagging, a stimulus (usually visual or auditory) is presented at a fixed frequency, which then produces robust steady-state visually evoked potentials or fields (respectively SSVEPs or SSVEFs for EEG and MEG), with power at the tagged frequency (Vialatte et al., 2010). These responses are enhanced by attention (Morgan et al., 1996; Müller et al., 2006) and reflect subjective perception in a bistable perception task (Parkkonen et al., 2008). Typically, frequency tagging is applied at lower frequencies (<30 Hz). This creates a problem when relating frequency tagging to neuronal oscillations in e.g. the alpha (8 – 13 Hz) and beta band (15 – 30 Hz) since the frequency tagging is likely to entrain spontaneous neuronal oscillations as well (Keitel et al., 2014; Spaak et al., 2014). In this study, we make use of new projector technology that allow us to perform frequency tagging at high frequencies (e.g. 60 – 80 Hz). As we will demonstrate, this allows us to study neuronal excitability and visual attention in relation to naturally occurring oscillations in the alpha band.

Neuronal oscillations have been shown to play a key role in the processing of sensory information by synchronizing neuronal firing and modulating synaptic input (Schroeder and Lakatos, 2009). For example, alpha oscillations have been hypothesized to support active inhibition of brain regions processing task-irrelevant, and possibly distracting, stimuli (Klimesch et al., 2007; Jensen and Mazaheri, 2010; Foxe and Snyder, 2011). This is underscored by the findings that posterior alpha oscillations are strongly modulated by spatial attention (Worden et al., 2000; Händel et al., 2011). Additionally, the phase of alpha has been shown to modulate perception (Mathewson et al., 2011; VanRullen et al., 2011) and cortical excitability (Dugue et al., 2011; Scheeringa et al., 2011; Spaak et al., 2012).

In this study, we apply frequency tagging in the 60 – 80 Hz band in order to probe neocortical excitability in relation to alpha oscillations. A previous study by Christoph Hermann (Herrmann, 2001) has shown that with a rapidly flickering LED, neuronal responses in humans as measured by EEG can be driven and measured up to around 100 Hz. Intracranial recordings in monkeys and humans have demonstrated that neuronal spiking in visual regions is entrained by the refresh rate of a CRT computer monitor (~60 Hz) (Sandström et al., 1997; Krolak-Salmon et al., 2003; Williams et al., 2004). We applied frequency tagging above 60 Hz using a projector supporting presentation rates up to

1440 Hz while recording whole-head MEG while subjects attended to flickering face and house stimuli in a cued spatial attention paradigm. The aim was to determine if cortical excitability as modulated by spatial attention could be estimated using rapid frequency tagging. A second aim was to investigate the relationship between alpha band oscillations and the cortical excitability assessed by rapid frequency tagging.

Methods

Participants

Participants were recruited from a participant database from the Radboud University Nijmegen. Twenty-three healthy (17 Females, Age: 26 +/- 10; Mean +/- SD) participants in the study, two of the subjects were excluded due excessive amounts of rejected trials. Written informed-consent was acquired before enrollment in the study. All subjects conformed to standard inclusion criteria for MRI, and MEG experiments. Subjects had normal, or corrected-to-normal vision. The study was approved by the local ethics committee (CMO region Arnhem/Nijmegen) and was performed according to the declaration of Helsinki. Subjects received financial compensation at a rate of 8 euros per hour or were compensated in course credits.

Procedure

The study consisted of one experimental MEG session. On a separate occasion a structural MRI was acquired for subsequent source localization of the MEG data. In the experimental session subjects were first prepared for MEG recordings by changing into clothes free of ferromagnetic materials. Following, the head shape of the participants was digitized using a 3D digitizer (Polhemus, Colchester, USA). Next, participants were brought into the magnetically shielded room and placed in the MEG at a distance of 75 cm in front of the screen. An Eyelink 1000 eyetracker (SR Research, Ottowa, Canada) was used to monitor the gaze of the participants. After calibrating the eye-tracker participants were familiarized with the experimental task. The spatial attention task was performed in 4 blocks of about 15 minutes per block with short breaks in between. In total, the task lasted 60 minutes.

Attention Task

Participants performed a spatial attention task in which they had to allocate attention to either the left, or the right visual hemifield, depending on a cue presented at the start of each block (see Figure 1). Each trial started with a brief arrow indicating the direction participants had to attend to, while fixating on the center of the screen. After 350 ms stimuli appeared in both the left as well as the right visual hemifield for 1500

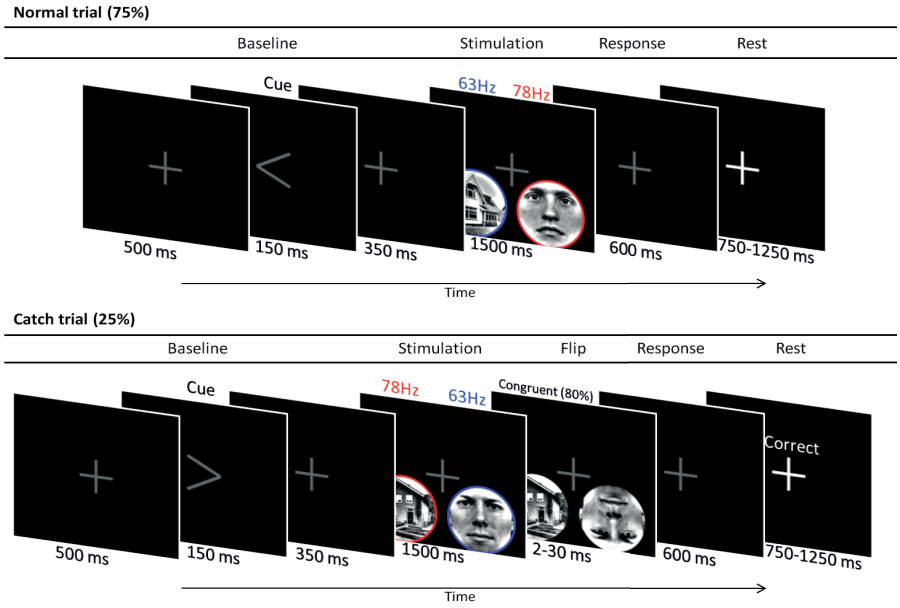

Figure 1. *The experimental paradigm*. Whole-head MEG (CTF, 275-channels, 1200 Hz) was recorded while participants (19 Females, Age: 26 +/- 2; Mean +/- SEM) were presented with a cue, indicating the image most probable to flip. A face and house were presented at 63 and 78 Hz. In 25% of the trials, one of the images was flipped vertically. In 80% of these catch trials, the flip was congruent to the cue direction and participants had to respond to the position of the flip. In the other 20% of the catch trials, the flip was incongruent to the cue and participants had to ignore this event. The direction of the cue, the position of the stimuli, the position of the frequencies and whether the flip was congruent or incongruent was manipulated in a semi-random manner during the experiment. Fixation was monitored throughout the experiment using an Eyelink 1000 eyetracker (SR Research, Ottawa Canada). Note that size of fixation cross, cue, and stimulus have been enlarged for clarity of the figure.

ms. Participants had to detect a vertical flip of the attended stimulus, which could occur in 25% of trials after 1500 ms. Participants had to indicate by button-press (right index finger for left, right middle finger for right) the location of the flipped stimulus. The duration of the flipped stimulus was adjusted using a QUEST adaptive staircase procedure (Watson and Pelli, 1983) set to reach a level of 80% correct responses. Starting at 10 ms, presentation duration of the flipped image varied between 2-30 ms. After stimulus presentation, participants had 0.6 s to respond followed by a rest period. Participants were given written feedback on the screen for correct ("CORRECT"), incorrect ("INCORRECT"), and missed ("MISS") responses. The task was presented using MATLAB 2014b (Mathworks Inc, Natrick, USA) and the Psychophysics Toolbox 3.0.11 (Kleiner et al., 2007).

On each trial two stimuli were presented in the lower left and lower right visual field (8.3 degrees eccentricity). Stimuli were circular face and house stimuli (10 degrees visual angle in diameter) normalized for luminance using the SHINE Toolbox for MATLAB (Willenbockel, 2010). The two stimuli were always of a different type (i.e. there was always a face and a house). One of the stimuli was presented at a rate of 63 Hz, while the other was presented at 78 Hz. The presentation rate was achieved by modulating the transparency of the stimulus with a sinusoid at the target frequency, phase-locked across trials. Focus of attention, stimulus type, and tagged frequency were randomly intermingled throughout the experiment.

Projector

To achieve the high presentation rate, we used a GeForce GTX960 2GB graphics card with a refresh rate of 120 Hz was used in combination with a PROPixx DLP LED projector (VPixx Technologies Inc., Saint-Bruno-de-Montarville, Canada). This specific projector allows for a refresh-rate up to 1440 Hz by dividing each frame received from the graphics card (at 120 Hz) into multiple smaller frames, which are presented in rapid succession. To this end the projector divides each received frame (1920 x 1200 pixels) into four equally sized quadrants (960 x 600 pixels), allowing for a fourfold increase in refresh rate. For each quadrant, the values from each of the three color channels (red, green, blue) are extracted and processed as separate greyscale images, multiplying the refresh rate further by three producing a refresh rate of 1440 Hz and a resolution 960 x 600 pixels.

MRI Data Acquisition

A high-resolution T1-weighted image (TR = 2300 ms, TE = 3.03 ms, TI = 1100 ms, 1.0 mm^3 isotropic resolution, 192 sagittal slices) was acquired using a 3T MAGNETOM Skyra (Siemens Healthcare, Erlangen, Germany)

MEG Data Acquisition

MEG was acquired using a 275-channel axial gradiometer CTF system (CTF MEG systems, Coquitlam, Canada). Sampling was done at 1200 Hz with a 300 Hz hardware lowpass filter. The participants head position was constantly monitored throughout the experiment using three head-localization coils placed on the nasion and both periauricular points (Stolk et al., 2013).

MEG Data Analysis

Preprocessing

The MEG data were analyzed using Matlab 2014b (The Matworks) and the Fieldtrip toolbox (Oostenveld et al., 2011). The MEG data were preprocessed blind to the experimental conditions. The data were epoched into segments from in -1 – 1.5 s intervals centered at the stimulus onset. Trials in which eye blinks were detected during stimulus presentation or in the baseline period, were rejected in addition to trials in which MEG sensors jumps occurred (determined by z-scoring the data and rejecting trials exceeding a z-score of 150). This resulted in rejection of 23 % of trials on average (+/- 12 SD). Following, the data were down sampled to 600 Hz (following at ~150 Hz low pass filter). ICA unmixing matrices were calculated using Runica (Makeig et al., 1996) on the first 90 principal components of the data. Prior to performing the ICA, the data was down-sampled to 300 Hz to conserve memory. The resulting unmixing matrices were applied to the data sampled at 600 Hz. Components containing topographies and time courses clearly matching cardiobalistic activity, line noise, or eye-movements/blinks were rejected from the data.

Channel-level analysis

Event-related fields (ERFs) were calculated by averaging the gradiometer data over trials, per condition. Synthetic planar gradients were calculated to ease interpretation of the topography of power measurements (Bastiaansen and Knösche, 2000). Power at frequencies from 1 – 100 Hz, in steps of 1 Hz was calculated for each condition separately by calculating the FFT on epochs from 0.5 to 1.5 seconds after stimulus onset multiplied by a Hanning taper.

To estimate the effect of attention on power at the tagged frequencies and to normalize across subjects, an Attention Modulation Index (AMI) was calculated, for each voxel, for each of the tagged frequencies. The effect of spatial attention was calculated as follows:

$$AMI = \frac{Power_{attend\ left} - Power_{attend\ right}}{Power_{attend\ left} + Power_{attend\ right}}$$

Using this formula, we expect positive values for right hemisphere sensors, or voxels, where the power at the tagged frequency is higher for attention to a stimulus on the left versus attention to a stimulus on the right (and vice versa for left hemisphere sensors or voxels).

To determine whether activity at the tagged frequency was modulated in amplitude by low-frequency oscillations, we calculated time-frequency representations (TFRs) with a moving time-window of 3-cycles at the tagged frequency, multiplied by a Hanning taper. The resulting power envelope was then analyzed by performing an FFT analysis of the power envelope zero-padded to two seconds. The resulting power spectrum reflects the spectral content of the envelope modulation of the frequency-tagged signal.

Statistical comparisons

Unless specified otherwise, conditions were compared using dependent-samples t-tests. On the channel-level, correction for multiple comparisons was applied by correcting for False Discovery Rate (FDR; Benjamini and Hochberg (1995)).

Results

Subjects performed a cued spatial attention task in which they had to report the location (left or right) of a stimulus that flipped along the horizontal axis. In each trial both a face and house stimulus appeared throughout a 1.5 second period in respectively the left and right visual hemifield (Figure 1). Each stimulus was flickering at either 63 Hz or 78 Hz. The location of the face and house stimulus (left or right hemifield) and flicker frequency (63 or 78 Hz), and cued direction of attention was randomly intermingled throughout the experiment.

Behavior

Behavioral results show participants performed the task as required; they were able to detect flips in the attended hemifield while ignoring flips in the uncued hemifield. The average hit rate was 0.73 +/- 0.1 (mean +/- SD). The false alarm rate was 0.24 +/- 0.15 (mean +/- SD), both significantly different from chance level of 0.5 (hit rate: $t_{23} = 11.1$, $p < 0.001$, false alarm rate: $t_{23} = -8.3$, $p < 0.001$). Reaction times to hits were on average 396 +/- 30 ms (mean +/- SD).

Spatial attention modulates responses of frequency-tagged stimuli.

To investigate the response in the early visual cortex to the flickering stimuli, we calculated time-locked averages of the event-related fields. We pooled over stimulus type (face, house) and direction of attention (left, right). Visual stimulation at the tagged frequencies produced clear steady-state visual evoked fields (SSVEFs) in occipital channels of the grand average (see Figure 2). The SSVEFs lasted for the entire stimulation period and were markedly larger for 63 Hz, than for 78 Hz as evident by a significant main effect of tagged frequency ($F_{1,22} = 249.77$, $p < 0.0001$) in a 2x2 WS-ANOVA with

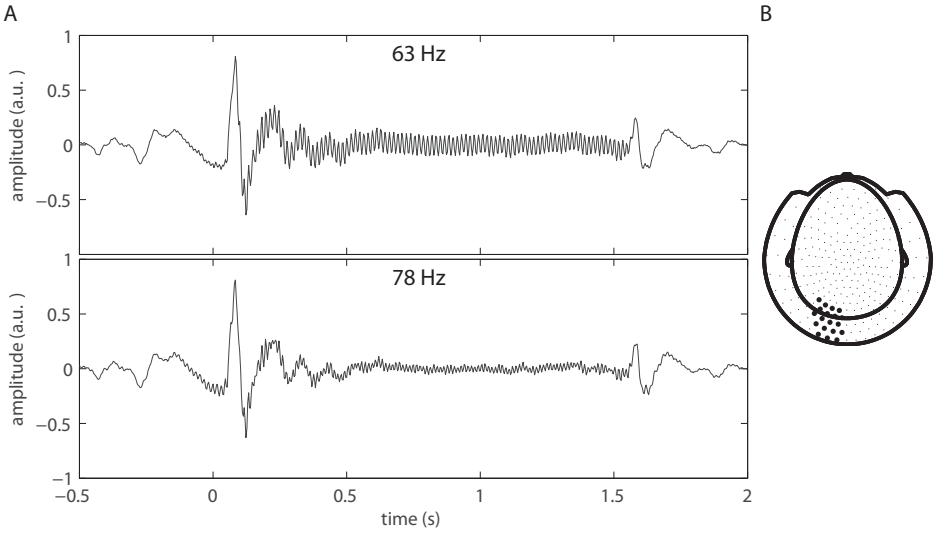

Figure 2. *Event-related field shows clear response at tagged frequency.* **A.** The top row shows group-average ERFs for 63 Hz stimulus for the left occipital sensors highlighted in panel B. The steady-state visual evoked fields start after 100 ms and lasts until stimulus offset 1.5 s later. The bottom row shows the ERF for a 78 Hz stimulus. As for 63 Hz, the onset of the SSVEF is around 100 ms after stimulus onset. The amplitude for the 78 Hz stimulus is weaker compared to the 63 Hz stimulus. As in each trial both a 63 Hz and a 78 Hz stimulus are presented, a notch filter between 77 and 79 Hz was applied for displaying the ERF at 63 Hz and a 62 to 64 Hz filter was applied for displaying the ERG at 78 Hz. **B.** The MEG sensors for which the ERF was plotted are highlighted in black.

factors channel (average of Left Occipital & average of Right Occipital channels) and tagged frequency (63 Hz & 78 Hz).

To investigate the effect of spatial attention on the tagged stimuli, we calculated power spectra in the interval of 0.5 to 1.5 seconds after stimulus onset to exclude the initial evoked response to the onset of the visual stimulus (as seen ~100-200 ms in Figure 2). We calculated the spatial attention modulation index (see Methods) for frequencies between 0 and 100 Hz.

Spatial attention produced a clear enhancement of power at the tagged frequency for the hemisphere contralateral to the locus of attention (see Figure 3A for the modulation spectrum for left occipital channels). The attentional modulation of the tagged stimuli is localized over posterior sensors. As expected, responses at the tagged frequencies (for both 63 Hz as well as 78 Hz) were larger in the hemisphere contralateral to the site of attention. Only 78 Hz differed significantly between attentional conditions, although the topography of the attentional modulation was similar to that at 63 Hz. Interestingly,

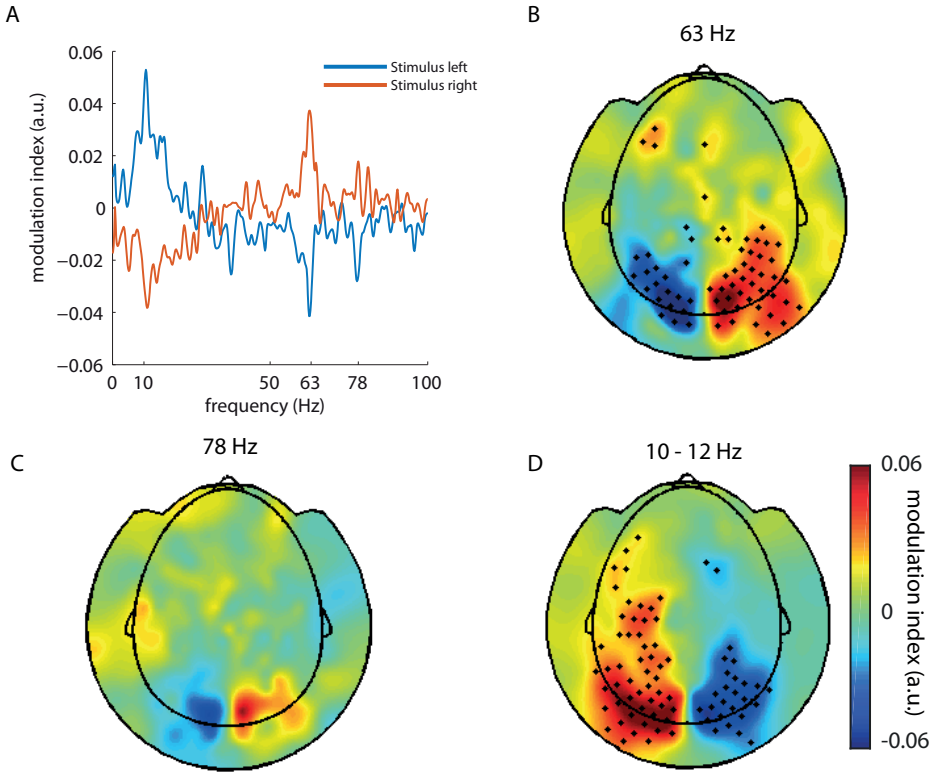

Figure 3. *Attention modulates power at tagged frequency.* **A.** Spatial attention modulation indices (Power $_{\text{attend left}}$ – Power $_{\text{attend right}}$) / (Power $_{\text{attend left}}$ + Power $_{\text{attend right}}$) for frequencies between 0 and 100 Hz for left occipital channels (see Figure 2B). It is clear that attention modulates power in the alpha band (10-12 Hz) as well at the tagged frequencies (63 and 78 Hz). **B.** Spatial attention modulation indices for all channels for 63 Hz. **C.** Same as in B for 78 Hz. **D.** Same as in C for the alpha band (10 – 12 Hz). Sensors showing a modulation index significantly different from zero are marked by a black dot (corrected for multiple comparisons by correcting for false discovery rate, FDR; Benjamini and Hochberg (1995))

a larger response for left versus right attention was found in left frontal sensors for 63 Hz as well as the alpha band. It is unclear whether this effect might relate to frontal regions driving top-down attention. As could be seen in Figure 2, the response to 78 Hz (see Figure 3A, C) was smaller in magnitude than the response to 63 Hz (see Figure 3A, B; $t_{22} = -57.25$, $p < 0.0001$), however, the effect at 78 Hz (Figure 3C) was in-line with that at 63 Hz (Figure 3B) albeit none of the channels survived multiple-comparisons correction. In sum, the frequency tagged signal increases in magnitude with respect to spatial attention.

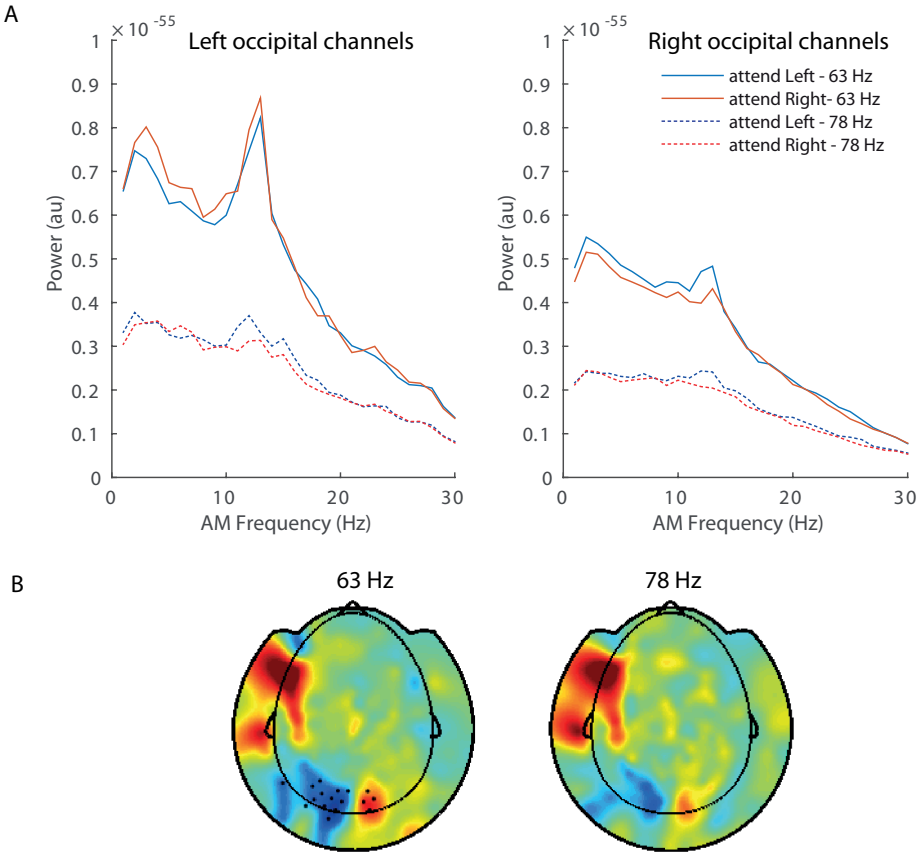

Figure 4. *Slow frequency modulation of the tagged stimulus.* **A.** Power spectra of the envelope of the tagged stimuli, for 63 Hz (blue and red lines), and 78 Hz (dotted blue and dotted red lines), show a clear peak in the alpha band indicating amplitude modulation in the alpha band. **B.** Topographical representation of the attention modulation index (AMI) of envelope amplitude modulation power for 63 Hz (left plot) and 78 Hz (right plot). Sensors showing a modulation index significantly different from zero are marked by a black dots (corrected for multiple comparisons by correcting for false discovery rate, FDR; Benjamini and Hochberg (1995))

In contrast, alpha-band oscillations (10 – 12 Hz) during stimulus processing were larger in the hemisphere ipsilateral to the site of attention than in the contralateral hemisphere (Figure 4D; $t_{22} = 6.70$, $p < 0.0001$). Thus, is similar to the classical modulation of alpha band oscillations as reported in numerous studies (Worden et al., 2000; Thut et al., 2006a; Foxe and Snyder, 2011; Händel et al., 2011; van Ede et al., 2011). We conclude that the typical pattern of alpha band modulation with spatial attention is relatively undisturbed by the rapid frequency tagging.

Power time-course of tagged-stimulus modulated by alpha oscillations

To investigate the relationship between low-frequency alpha-band oscillations and the tagged signals, we calculated spectral power of the envelope at the tagged frequency. We found a strong modulation of the power envelope of the signal in the alpha band, as evident by a clear peak in the power spectrum (Figure 4A). The peaks were more pronounced for 63 Hz than for 78 Hz as evident by a significant main effect of tagged frequency ($F_{1,22}$ = 3277, $p < 0.0001$; 63 Hz vs 78 Hz: t_{22} = -57.25, $p < 0.0001$) in a 2x2 WS-ANOVA with factors channel (average of Left Occipital & average of Right Occipital channels) and tagged frequency (63 Hz & 78 Hz), but they were visible for both. These findings suggest that alpha oscillations modulate the tagged signals rhythmically.

The modulation of the tagged signal amplitude in the alpha-band was modulated by spatial attention: the modulation was positive in sensors contralateral to the focus of attention (Figure 4A&B). The attention modulation index (AMI; see Methods) was significantly different from zero in occipital channels (see Figure 4B for channels showing significant difference from zero; paired-samples t-tests; $p < 0.05$; corrected for false discovery rate) for 63 Hz, where the amplitude modulation in the alpha band was stronger for right channels when attention was focused to stimuli on the left, and stronger for left channels when attention was focused to stimuli on the right. Interestingly, similarly to the attentional modulation of the tagged stimuli and the alpha band (cf. Figure 3B,C & D), the topographies of the attention modulation of the amplitude envelope of the tagged stimuli showed a modulation in left frontal sensors.

The visual stimulus itself did not contain a spectral component in the alpha band. The amplitude modulation in the alpha band can neither be explained by an interaction between the presence of both a 63 Hz, and a 78 Hz stimulus. It is possible that a 15 Hz component might results from such an interaction (78 Hz – 63 Hz = 15 Hz). However, the peak of the alpha band component was at 12 Hz and not at 15 Hz and is therefore unlikely to be a confound.

Discussion

We here demonstrate that frequency-tagging of visual stimuli at rapid frequencies (up to 78 Hz) can entrain neuronal responses in early visual cortex. Spatial attention towards a tagged stimulus produced stronger responses at the tagged frequency contralateral to the focus of attention compared to the unattended stimulus. As such, the tagged signal reflects the gain of neuronal excitability with spatial attention. Posterior alpha band oscillations decreased in magnitude in posterior regions contralateral to the focus

of attention while increasing ipsilateral to the focus of attention; i.e. the alpha oscillations appeared relatively undisturbed by the tagging signal. Moreover, the spectral envelope at the tagged signal was modulated by the phase of the alpha oscillations.

Proof of principle: using rapid frequency-tagging to probe neocortical excitability

The current study provides proof of principle that rapid frequency frequency-tagging can be used as a method to study processing of visual stimuli with high SNR. Previous studies have shown that it is possible to elicit responses in early visual cortex by use of flickering LEDs at high frequencies up to 100 Hz (Herrmann, 2001). Additionally, steady-state visually evoked potentials have been shown to distribute over a wide range of cortical regions in studies using intracranial EEG (Srinivasan et al., 2006; Srinivasan et al., 2007; Yan and Gao, 2011; Xu et al., 2013; Zhang et al., 2013). However, the use of complex stimuli in such paradigms has been technically challenging due to the physical limitations of computer monitors and projectors. In the current study, we used a state-of-the-art LED projector that was capable of presenting stimuli at a refresh rate of 1440 Hz. The use of this projector allowed us to sinusoidally modulate the luminance of the to-be-tagged stimulus at frequencies up until the Nyquist frequency of the projector (720 Hz). As in the study of Herrmann (2001), we observed lower response magnitudes for stimuli tagged at 78 Hz compared to 63 Hz, although both were modulated with the same amplitude. This is most like explained by an attenuation resulting from the synaptic drives in the early visual stream. The time course of the post-synaptic potentials are in the order of ~10 ms (Koch et al., 1996), which effectively creates a ~100 Hz low pass filter. This factor should be taken into consideration in future studies.

Attention enhances neural response to tagged stimulus

One assumption underlying the use of frequency-tagging as a tool to study sensory processing in the brain is that the EEG/MEG signal at the tagged frequency reflects underlying sensory processing. We have shown here that spatial attention modulates power at the tagged frequency in the expected direction; the response at the tagged frequency was enhanced when attention was directed towards the stimulus and suppressed when attention was directed away. This suggests that the gain increase associated with the allocation of spatial attention results in increased neuronal excitation, which in turn is reflected by the power of the frequency-tagged MEG signal.

Alpha oscillations are unperturbed by rapid frequency tagging

The increase in response with spatial attention has also been shown for frequency-tagged stimuli at lower frequencies as well (e.g. Müller et al., 2006; Toffanin et al., 2009). However, frequency tagging done at lower frequencies (0.5- 30 Hz) is likely to interfere

with naturally occurring oscillations. Most frequency tagging experiments had to limit themselves to frequency bands below 30 Hz (e.g. Müller et al., 2006; Toffanin et al., 2009). This raises the possibility that the stimulus interacts and potentially 'entrains' these oscillations (Thut et al., 2011a; Spaak et al., 2014). In entrainment, an external drive (the visual stimulus) drives the internal rhythm (e.g., alpha band oscillations) at the frequency of the external drive (see (Keitel et al., 2014) for a Discussion). This is especially evident given that frequency tagging, in the visual domain, is most successful at frequencies between 12 Hz and 18 Hz (Kuś et al., 2013).

In our study, posterior alpha band oscillations were relatively undisturbed by the rapid frequency tagging. This was evident by the spatial attention modulation of the alpha oscillations. Alpha power increased ipsilateral to the focus of attention while alpha power decreased contra-laterally, during visual stimulus processing. From the current study, it is evident that the frequency tagging did not interfere, or entrain, lower frequency oscillations. Applying frequency tagging at higher frequencies therefore makes is possible to study the role of lower-frequency oscillations on sensory processing.

Does the rapid frequency tagging entrain neuronal gamma oscillations?

There are studies that have attempted to stimulate at frequencies in the gamma-band in an attempt to entrain natural gamma-band oscillations (30 – 90 Hz). This is important as gamma band oscillations have been proposed to play an important role of orchestrating neuronal computation (Varela et al., 2001; Fries et al., 2007; Jensen et al., 2007). Bauer et al. (2009) showed that attention could be captured by stimuli flickering subliminally at 50 Hz. However, follow-up studies have shown that these effects could be explained by effects unrelated to the flicker (Van Diepen et al., 2010). Manipulating visual perceptual integration by manipulating phase of externally driven gamma frequency stimulation has proven difficult (Bauer et al., 2012). In future work, it would be interesting to explore to what extend the neuronal activity elicited by rapid frequency tagging entrain naturally occurring gamma oscillations. This could for instance be done my pharmacological means. It is well established that GABAergic inhibition from interneurons plays a crucial role for generating gamma oscillations (Traub et al., 1999). In support of this notion, we recently demonstrated that visual gamma oscillations in humans increase when the GABergic agonist Lorazepam is applied (Lozano-Soldevilla et al., 2014). If rapid frequency-tagging entrains natural gamma oscillations, this results in the hypothesis that rapid-frequency tagging in the gamma band should increase with the application of GABAergic agonists.

The frequency tagged signal is phasically modulated by alpha oscillations

We have shown that the power envelope at the tagged frequency was modulated in the alpha band (Figure 5). This suggests that stimulus processing, as reflected by the power time course of the tagged frequency, is modulated by alpha oscillations. This is in line with previous evidence showing that alpha band oscillations modulate neuronal firing in a phasic manner (Bollimunta et al., 2011; Haegens et al., 2011b; Snyder et al., 2015). In such a framework, posterior alpha band oscillations serve as a mechanism to group visual information in packets of information (cycles of gamma), which are sorted and segmented by the alpha cycle, reflecting shifting states of excitability (Gips et al., 2016). However, it remains to be seen whether this modulation can be linked to an actually observable alpha oscillation.

Interestingly, the magnitude of the amplitude modulation as reflected by power in the alpha band of the tagged stimulus' power envelope was significantly modulated by attention in the sensors contralateral to the focus of attention showed a stronger modulation of the frequency tagged signal in the alpha band compared to when attention was directed to the other hemifield. These results both highlight the role of alpha oscillations in (i) inhibiting task-irrelevant areas as well as (ii) modulating ongoing stimulus processing.

Conclusion

We set out to investigate the feasibility of using rapid frequency-tagging of visual stimuli to study the role of sensory processing in the visual cortex. We found that it is indeed possible to measure responses at the tagged frequency and that these responses increase with the allocation of spatial attention. More importantly, we found these responses to be modulated in amplitude in the alpha band, which highlights the role of alpha band oscillations in modulating ongoing stimulus processing. In short, we have successfully shown that frequency-tagging at high frequencies is a useful tool in studying the interaction of neuronal oscillations with ongoing sensory processing.

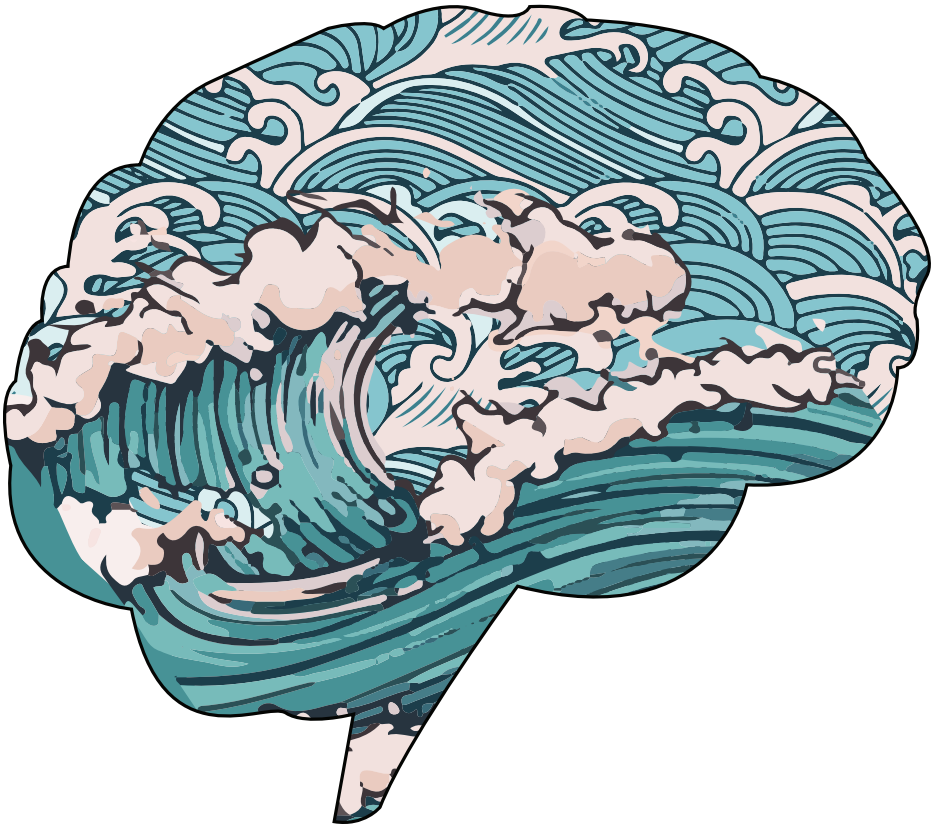

CHAPTER 6

General discussion

General discussion

On a daily basis, the brain is overloaded with sensory information. To cope with this, the brain must apply a mechanism to prioritize bottom-up sensory input. Irrelevant information has to be blocked, while at the same time important, salient stimuli should be allowed access. As in the example from the introduction, to focus on working on your manuscript, you have to block out irrelevant auditory input while at the same time still be able to process relevant, salient, stimuli such as your crying child. Additionally, relevant sensory input has to be grouped, or bound, low in the visual hierarchy, while segregated on a higher level. With this thesis, I hoped to gain important insights into the role of posterior alpha band oscillations in this process (Figure 1). More specifically, I aimed to answer the following questions:

1. Are cortical alpha oscillations an intrinsic property of the visual system?
2. Do cortical alpha oscillations serve as a mechanism of functional inhibition by phasically modulating visual processing?
3. Can rapid frequency tagging be used as a tool to study the role of neuronal oscillations in visual information processing?

Cortical oscillations are an intrinsic property of the visual system

In **chapter 2** I combined TMS with EEG to investigate whether it is possible to use TMS as a tool to study the causal role of alpha band oscillations in visual processing. I initially set out to investigate whether studies claiming to 'entrain' alpha oscillations were not merely generating a series of evoked responses at the rate of stimulation (i.e. alpha). However, during piloting I quickly discovered single TMS pulses were sufficient to produce alpha-like responses. This so-called 'alpha-ringing' was previously observed by Rosanova et al. (2009) who reported oscillatory resonance following TMS depending on the natural frequency of the stimulated region. This suggests oscillations are indeed a fundamental property of neuronal circuits. However, it was not clear whether these oscillatory responses reflected the same underlying mechanisms as spontaneous alpha oscillations. To investigate this, I asked participants to perform a cross-modal attention task in which they had to attend to auditory or visual stimuli, while I applied TMS to the left early visual cortex. By concurrently measuring EEG I was able to establish that cross-modal attention indeed modulated the TMS-locked alpha ringing similarly as in spontaneous alpha oscillations. TMS-locked alpha ringing was enhanced when subjects attended to the auditory modality, while TMS-locked alpha ringing was suppressed when participants attended to the visual modality. Furthermore, I discovered that this effect was dependent on the participant's ability to modulate their alpha power at baseline. Participants who were better able to modulate their alpha power at baseline, also showed stronger modulation of TMS-locked alpha in response to allocation of at-

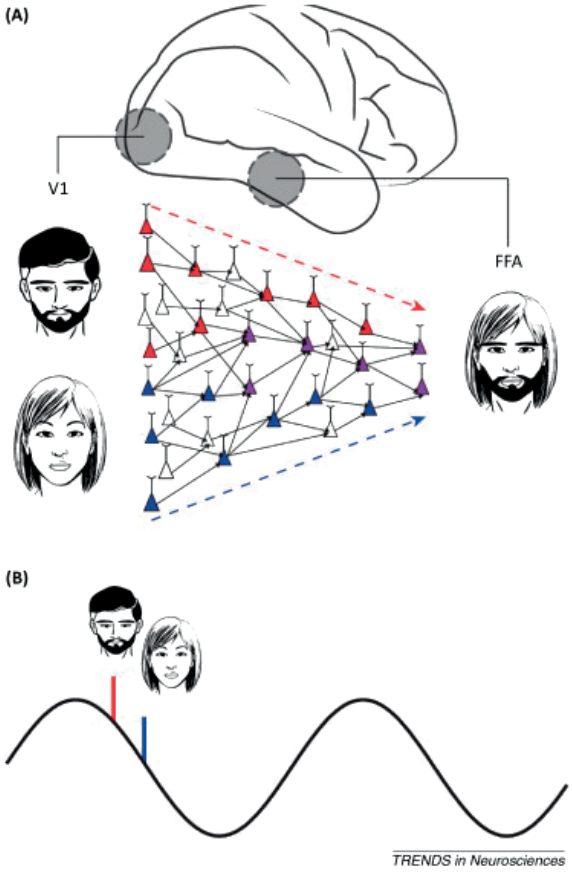

Figure 1. *Alpha oscillations as a mechanism to sort distinct streams of information.* **A.** The visual system is hierarchical in nature. In the early visual cortex representations of the visual field are organized retinotopically, while higher up in the hierarchy representations become more abstract. For example, face selective regions (Reddy and Kanwisher, 2006) high in the visual hierarchy might code for distinct faces, while partly sharing the same neuronal representation. Although this causes an information overload problem, the visual system is usually able to cope and distinguish between two faces. **B.** Phase coding is proposed by *(Jensen et al., 2014)* as a possible mechanism to cope with the problem of information overload by temporally segregating distinct representations according to the phase of alpha oscillations. *Reproduced with permission from Jensen et al. (2014).*

tention to the auditory modality. In addition, I found an early TMS-evoked component, the N40, that was enhanced by visual attention thereby reflecting the current state of cortical excitability.

In **chapter 3** I followed up on the study from **chapter 2** by investigating *perceptual echoes,* as they were named by VanRullen and Macdonald (2012). *Perceptual echoes* are oscillatory responses extracted from the EEG by cross-correlating the EEG in response

to random flickering visual stimuli with the visual stimulus time course. Mathematically this should result in the *Impulse Response Function* of the brain. However, this approach relies on the assumption that the brain is a linear system, which it most likely is not. *Perceptual echoes* have a characteristic alpha-like component that is very similar to the TMS-locked alpha ringing I observed in **chapter 2**. Contrary to the TMS-locked alpha oscillations observed in **chapter 2**, in the study by VanRullen and Macdonald (2012) *perceptual echoes* were enhanced by visual attention, not suppressed. In **chapter 2,** a cross-modal attention paradigm was applied whereas in the study by VanRullen and Macdonald (2012) spatial attention was modulated. I was therefore interested to see whether cross-modal attention would produce similar results as in **chapter 2** and show an enhancement of perceptual echoes with increased alpha power when attention is directed towards the auditory modality. I therefore adapted the study by VanRullen and Macdonald (2012) in the MEG while participants performed a cross-modal attention task. I found reliable *perceptual echoes* in all participants localized to posterior sources. Unfortunately, *perceptual echoes* were not modulated reliably by attention in either direction. I did, however, find alpha power both at baseline, as during visual stimulation, to be enhanced with low visual attention (i.e. attention to the auditory modality). Additionally, I found an early N70 component to be correlated to participant's performance on the visual detection task akin to the N40 component in **chapter 2**. This led me to further explore the data as the similarities between the *perceptual echoes* in **chapter 3** and the TMS-locked alpha oscillations in **chapter 2** might not be so straightforward as I had initially expected. An important difference between *perceptual echoes* and TMS-locked alpha oscillations is that only TMS-locked alpha oscillations are produced by directly stimulating visual cortex. *Perceptual echoes*, on the other hand, are produced by indirect, visual stimulation via the retina. The effects of attention and the interaction with alpha oscillations might therefore not be straightforward. Although the *perceptual echo* might reflect endogenous alpha oscillations, when alpha is high, it is thought to reflect inhibition of sensory input (Jensen and Mazaheri, 2010) and therefore suppress the inducing effect of the visual stimulation. I tested this complex interplay with a hypothetical model including both attention as well as alpha oscillations to predict the magnitude of the modulation in the perceptual echo and found that indeed individual variability in the level of both attention as well as spontaneous alpha oscillations predicted perceptual echo magnitude (see chapter 3- Figure 6B). At moderate levels of visual attention, baseline alpha power predicted perceptual echo magnitude. While at high levels of visual attention, attention predicted perceptual echo magnitude as visual input was enhanced. Very high levels of alpha power at baseline, however, resulted in decreased perceptual echo magnitude, possibly due to suppression of visual input. However, this model is purely speculative and post-hoc and therefore should be further explored in future studies.

The exact nature of *perceptual echoes* (and perhaps TMS-locked alpha oscillations) is unclear. In **chapter 2** I argued that TMS-locked alpha oscillations might arise by triggering a new alpha oscillation in the stimulated population, which would be independent of global alpha oscillations at the time of stimulation. Alternatively, TMS could reset ongoing alpha, but only in the stimulated region. In both cases, the amplitude of the TMS-locked alpha oscillation would be modulated similarly as spontaneous alpha oscillations. The *perceptual echoes*, reported in **chapter 3** are thought to be the *Impulse Response Function* of the brain. In other words, the brain's response to a single stimulus (flash). According to VanRullen and Macdonald (2012) previous literature dating back to the middle of the 20th century reported on repetitive *afterdischarges* at a rate of approximately 10 Hz (Bishop and O'Leary, 1938; Adrian, 1941; Fleming and Evarts, 1959). Additionally, VanRullen and Macdonald (2012) notes that *perceptual echoes* could be linked to intrinsic properties of thalamocortical circuits producing augmented responses with 10 Hz input. This appears to be related to cortical entrainment (Thut et al., 2011a) as it has recently been shown that the visual system responds well to quasi-rhythmic (i.e. a frequency band, rather than a fixed frequency) stimulation (Keitel et al., 2017).

Finally, the functional relevance of perceptual echoes as well as TMS-locked alpha oscillations remains to be clarified. According to VanRullen and Macdonald (2012), perceptual echoes could reflect immediate sensory, or "iconic" memory as they allow the visual system to retain sensory information for extended periods of time (up to 1 s). However, both perceptual echoes as well as TMS-locked alpha oscillations seem to reflect oscillatory properties of the stimulated neuronal populations. It is therefore unlikely they are functionally distinct from these neuronal oscillations. According to a framework of pulsed-inhibition (Klimesch et al., 2007; Jensen and Mazaheri, 2010) both reflect the visual system shifting between stated of excitability and inhibition.

Importantly, both perceptual echoes as well as TMS-locked alpha oscillations allow us to study neuronal oscillatory dynamics in a controlled way. For both perceptual echoes, as well as TMS-locked alpha oscillations, the alpha component is predictable on a subject-by-subject basis. This allows future studies to easily test theories on the functional role of alpha oscillations, such as importance of phase (e.g. Jensen et al., 2014).

Both **chapter 2** and **chapter 3** show that alpha oscillations are an intrinsic property of the visual system. By perturbation using TMS as well visual stimulation, alpha band oscillations emerged. I have also shown that these oscillations behave similarly to endogenous alpha oscillations in response to top-down attention although the effect of attention on perceptual echoes was rather complex. In the next paragraph, I hope to shed light on the function of alpha oscillations in sensory processing.

Cortical alpha oscillations serve as a mechanism of functional inhibition by phasically modulating behaviorally relevant neuronal activity

In **chapter 4** I attempted to reproduce the functional properties attributed to endogenous alpha band oscillations by externally applying weak currents at alpha frequency while concurrently measuring MEG. I had participants perform a modified detection task that was known to induce reliable, bottom-up, gamma-band oscillations (Hoogenboom et al., 2006), while I applied TACS at Cz, according to the international 10-20 system, at individual alpha frequency and neighboring frequencies. To control for the effects of retinal stimulation (Schutter, 2015) I also applied stimulation in a control montage targeting FPz. I found visually induced gamma-band oscillations to be suppressed more so when stimulating Oz, than FPz.

Additionally, this suppression appeared to be phasic as gamma-band power was phasically modulated by TACS as apparent by significant phase-amplitude coupling of gamma-band power with TACS phase only for Oz stimulation. This phasic suppression resulted in a slight, but significant, reduction in performance on the visual detection task. Interestingly, frequency of stimulation did not seem to matter. As neighboring frequencies differed only 4 Hz from individual alpha frequency it is possible I forced endogenous alpha oscillations to lock to our external stimulation, regardless of frequency (Ali et al., 2013). Alternatively, if alpha oscillations functional properties are 'merely' the result of shifting between states of excitability and inhibition by fluctuations in resting membrane potentials, it could also be our external stimulation was merely replacing this effect usually produced by the mechanisms underlying spontaneous alpha oscillations. Regardless, I have shown in **chapter 4** that oscillatory network behavior can indeed provide functionally relevant changes in bottom-up sensory processing, in a phasic manner, with subsequent consequences for behavior.

In **chapter 5** I used rapid frequency tagging to study sensory processing and the role of neuronal oscillations in this. I showed that the power envelope of the tagged stimulus was modulated in the alpha band, suggesting phasic modulating of sensory processing of the stimuli. In both **chapter 4** and **chapter 5** I show that alpha oscillations appear to phasically inhibit bottom-up sensory processing. This apparent coupling between the phase of slow oscillations (alpha) and bottom-up gamma-band power has been observed previously and is thought to play an important role in information processing (Jensen and Colgin, 2007; Canolty and Knight, 2010). One role is the prioritizing of sensory processing (Lisman and Jensen, 2013; Jensen et al., 2014). As is illustrated in Figure 1B, incoming sensory input is prioritized and processed according to saliency along the phase of alpha, thereby avoiding sensory overload and perceptually combining distinct objects (see right-most face in Figure 1B for such an example). However,

chapter 4 and **chapter 5** do not provide sufficient evidence to show that bottom-up input is indeed prioritized. It would be interesting to investigate whether future studies could use rapid frequency tagging to show a phase difference in the power envelope of two tagged face-stimuli. Here the expectation would be that the face with the highest saliency (the attended stimulus) will be prioritized over a face with lower saliency (the unattended face) resulting in a unidirectional phase delay. This unidirectional phase delay would switch when attention increases saliency of the other face.

To conclude, in **chapter 4** I show that we were able to implement pulsed inhibition with TACS and reproduce the functional aspects of alpha oscillations. In **chapter 5** I provide additional evidence of bottom-up sensory processing being phasically modulated in the alpha band.

A note on individual variability

It is important to note that in light of recent critique on non-invasive brain stimulation studies (e.g. Horvath et al., 2014, 2015) on the lack of consistent effects, individual variability has to be taken into account. Indeed, although the study in **chapter 3** did not include brain stimulation, **chapter 2, chapter 3** as well as **chapter 4** report effects that have taken individual variability (e.g. in the ability to modulate alpha power at baseline) into account. In studies where we do not expect large but meaningful effects, we should try to reduce unexplained variance by taking individual differences into account. Horvath et al. (2015) mention the lack of consistency in effects could be due to a dependency of the efficacy of TMS on brain states. If this is the case, it might be helpful for future studies to include some measurement of the individual's brain state (such as the ability to modulate alpha power at baseline) into the analysis to account for individual variability.

Rapid frequency tagging is a promising tool to study sensory processing and the role of neuronal oscillations herein

In **chapter 5** I investigated whether frequency tagging at high frequencies (> 60 Hz) can be used to study sensory processing in the brain and the role of neuronal oscillations in its coordination. To this end I presented participants with bilateral pictures of faces and houses. Participants were required to attend to a picture in one hemifield, while ignoring the other. Both pictures were flickering at fixed frequencies (resp. 63 and 78 Hz). Previous studies with LEDs in humans (Herrmann, 2001), as well as animals (Rager and Singer, 1998) have shown it to be possible to elicit responses to flashed of up to ~100 Hz. The use of a new projector with the capability of presenting stimuli at rates of up to 1440 Hz allowed us to achieve this with complex stimuli. While participants were performing this task I concurrently measured MEG. I found strong steady-state visually

evoked potentials (SSVEPs) to the tagged stimuli. Additionally, these responses were enhanced when attention was directed towards the tagged stimulus. As noted previously by (Herrmann, 2001), the response at the higher frequency (78 Hz) was much weaker than that at the lower frequency (63 Hz).

This opens up new possibilities to study the role of neuronal oscillations in sensory processing. In **chapter 5**, I found that the power time course of the tagged stimulus was modulated in the alpha band. However, what is not clear from this is whether this modulation is tightly linked to endogenous alpha band oscillations and would indicate whether one stimulus is gated to down-stream regions over another. More specifically, if one were to be presented with two faces (Figure 1A) tagged at different frequencies. Would posterior alpha oscillations be phase-locked to the power time course of the attended stimulus? Interestingly, modulation of the power time course of the tagged stimulus appeared to be larger in the hemisphere contralateral to the focus of attention (**chapter 5**). Speculatively, this suggests an important role for alpha-band oscillations in gating, not only task-irrelevant, but relevant input.

In sum, in **chapter 5** I have provided proof-of-principle to use rapid frequency tagging to probe cortical excitability. Using rapid frequency tagging, I was able to distinguish processing of two concurrently presented stimuli and study the effect of top-down attention on them. Additionally, I was able to show that the sensory input from both stimuli was modulated in the alpha band. Together with the fact that posterior alpha oscillations remained intact during visual stimulation, makes rapid frequency tagging a promising tool to study sensory processing and the role of neuronal oscillations herein.

Conclusion

In summary, the studies reported in this thesis confirm neuronal alpha band oscillations to be a fundamental property of the visual system. In general, this thesis highlights the role of alpha band oscillations in inhibiting irrelevant stimuli. More specifically, I have provided evidence that this inhibition is phasic in nature and has consequences for behavior. Importantly, both non-invasive brain stimulation as well as rapid frequency tagging have been shown to be a valuable tool in studying the (causal) role of neuronal oscillations in sensory processing.

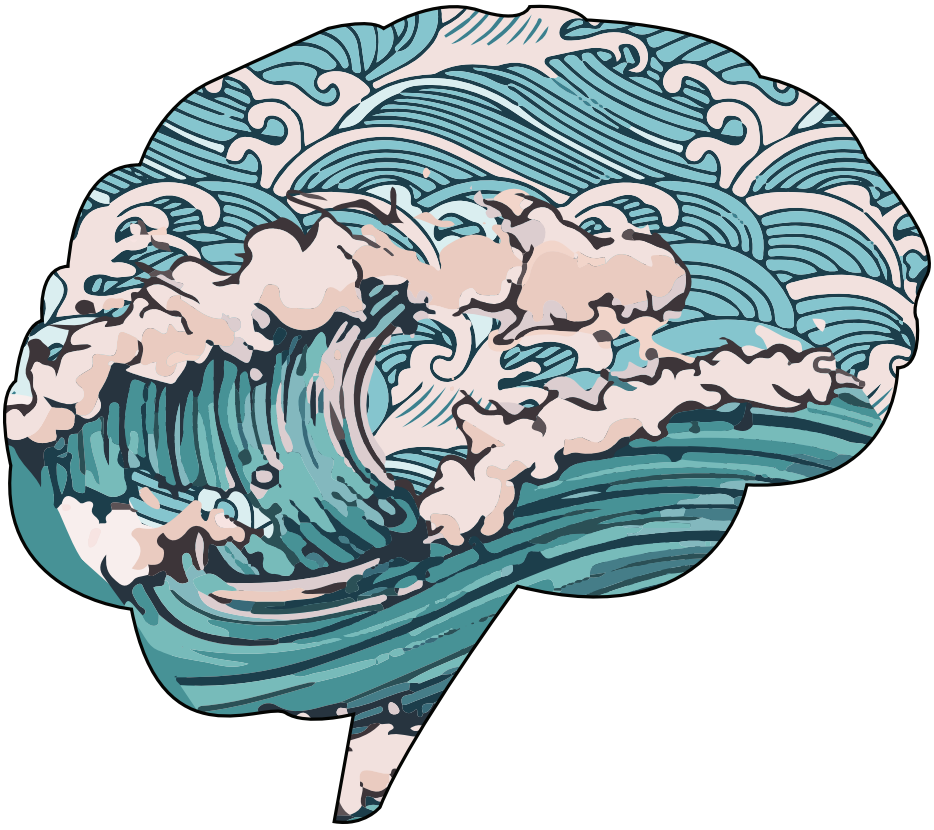

APPENDIX

References

Adrian ED (1941) Afferent discharges to the cerebral cortex from peripheral sense organs. The Journal of physiology 100:159.

Adrian ED (1944) Brain Rhythms. Nature 153:360-362.

Adrian ED, Matthews BH (1934) The Berger rhythm: potential changes from the occipital lobes in man. Brain 57:355-385.

Alekseichuk I, Turi Z, Amador de Lara G, Antal A, Paulus W (2016) Spatial Working Memory in Humans Depends on Theta and High Gamma Synchronization in the Prefrontal Cortex. Curr Biol.

Ali MM, Sellers KK, Fröhlich F (2013) Transcranial alternating current stimulation modulates large-scale cortical network activity by network resonance. Journal of Neuroscience 33:11262-11275.

Baldauf D, Desimone R (2014) Neural mechanisms of object-based attention. Science 344:424-427.

Bastiaansen MC, Knösche TR (2000) Tangential derivative mapping of axial MEG applied to event-related desynchronization research. Clinical Neurophysiology 111:1300-1305.

Bastos AM, Vezoli J, Bosman CA, Schoffelen JM, Oostenveld R, Dowdall JR, De Weerd P, Kennedy H, Fries P (2015) Visual areas exert feedforward and feedback influences through distinct frequency channels. Neuron 85:390-401.

Bauer F, Cheadle SW, Parton A, Müller HJ, Usher M (2009) Gamma flicker triggers attentional selection without awareness. Proceedings of the National Academy of Sciences 106:1666-1671.

Bauer M, Akam T, Joseph S, Freeman E, Driver J (2012) Does visual flicker phase at gamma frequency modulate neural signal propagation and stimulus selection? Journal of vision 12:5-5.

Benjamini Y, Hochberg Y (1995) Controlling the False Discovery Rate: A Practical and Powerful Approach to Multiple Testing. Journal of the Royal Statistical Society Series B (Methodological) 57:289-300.

Berger H (1929) Über das elektrenkephalogramm des menschen. European Archives of Psychiatry and Clinical Neuroscience 87:527-570.

Bergmann TO, Karabanov A, Hartwigsen G, Thielscher A, Siebner HR (2016) Combining non-invasive transcranial brain stimulation with neuroimaging and electrophysiology: current approaches and future perspectives. NeuroImage 140:4-19.

Bergmann TO, Molle M, Schmidt MA, Lindner C, Marshall L, Born J, Siebner HR (2012) EEG-Guided Transcranial Magnetic Stimulation Reveals Rapid Shifts in Motor Cortical Excitability during the Human Sleep Slow Oscillation. J Neurosci 32:243-253.

Bishop G, O'Leary J (1938) Potential records from the optic cortex of the cat. Journal of Neurophysiology.

Bollimunta A, Mo J, Schroeder CE, Ding M (2011) Neuronal mechanisms and attentional modulation of corticothalamic alpha oscillations. Journal of Neuroscience 31:4935-4943.

Bonnefond M, Kastner S, Jensen O (2017) Communication between Brain Areas Based on Nested Oscillations. eNeuro 4:ENEURO. 0153-0116.2017.

Brittain JS, Probert-Smith P, Aziz TZ, Brown P (2013) Tremor suppression by rhythmic transcranial current stimulation. Curr Biol 23:436-440.

Busch NA, Dubois J, VanRullen R (2009) The phase of ongoing EEG oscillations predicts visual perception. Journal of Neuroscience 29:7869-7876.

Buzsaki G, Draguhn A (2004) Neuronal oscillations in cortical networks. Science 304:1926-1929.

Canolty RT, Knight RT (2010) The functional role of cross-frequency coupling. Trends in cognitive sciences 14:506-515.

Cecere R, Rees G, Romei V (2015) Individual differences in alpha frequency drive crossmodal illusory perception. Curr Biol 25:231-235.

Drewes J, VanRullen R (2011) This is the rhythm of your eyes: the phase of ongoing electroencephalogram oscillations modulates saccadic reaction time. Journal of Neuroscience 31:4698-4708.

Dugue L, Marque P, Vanrullen R (2011) The Phase of Ongoing Oscillations Mediates the Causal Relation between Brain Excitation and Visual Perception. J Neurosci 31:11889-11893.

Engel AK, Fries P (2010) Beta-band oscillations--signalling the status quo? Curr Opin Neurobiol 20:156-165.

Fleming TC, Evarts EV (1959) Multiple response to photic stimulation in cats. American Journal of Physiology--Legacy Content 197:1233-1236.

Foxe JJ, Snyder AC (2011) The role of alpha-band brain oscillations as a sensory suppression mechanism during selective attention. Frontiers in psychology 2:154.

Foxe JJ, Simpson GV, Ahlfors SP (1998) Parieto-occipital ~10Hz activity reflects anticipatory state of visual attention mechanisms. Neuroreport 9:3929-3933.

Fries P (2005) A mechanism for cognitive dynamics: neuronal communication through neuronal coherence. Trends in cognitive sciences 9:474-480.

Fries P (2015) Rhythms for Cognition: Communication through Coherence. Neuron 88:220-235.

Fries P, Nikolić D, Singer W (2007) The gamma cycle. Trends in neurosciences 30:309-316.

Fu KM, Foxe JJ, Murray MM, Higgins BA, Javitt DC, Schroeder CE (2001) Attention-dependent suppression of distracter visual input can be cross-modally cued as indexed by anticipatory parieto-occipital alpha-band oscillations. Brain Res Cogn Brain Res 12:145-152.

Garcia JO, Grossman ED, Srinivasan R (2011) Evoked potentials in large-scale cortical networks elicited by TMS of the visual cortex. J Neurophysiol 106:1734-1746.

Gilbert CD, Li W (2013) Top-down influences on visual processing. Nature Reviews Neuroscience 14:350-363.

Gips B, Eerden JP, Jensen O (2016) A biologically plausible mechanism for neuronal coding organized by the phase of alpha oscillations. European Journal of Neuroscience 44:2147-2161.

Grandchamp R, Delorme A (2011) Single-trial normalization for event-related spectral decomposition reduces sensitivity to noisy trials. Front Psychol 2:236.

Gross J, Kujala J, Hamalainen M, Timmermann L, Schnitzler A, Salmelin R (2001) Dynamic imaging of coherent sources: Studying neural interactions in the human brain. Proc Natl Acad Sci U S A 98:694-699.

Haegens S, Händel BF, Jensen O (2011a) Top-down controlled alpha band activity in somatosensory areas determines behavioral performance in a discrimination task. Journal of Neuroscience 31:5197-5204.

Haegens S, Luther L, Jensen O (2012) Somatosensory anticipatory alpha activity increases to suppress distracting input. J Cogn Neurosci 24:677-685.

Haegens S, Nácher V, Luna R, Romo R, Jensen O (2011b) α-Oscillations in the monkey sensorimotor network influence discrimination performance by rhythmical inhibition of neuronal spiking. Proceedings of the National Academy of Sciences 108:19377-19382.

Haegens S, Cousijn H, Wallis G, Harrison PJ, Nobre AC (2014) Inter- and intra-individual variability in alpha peak frequency. NeuroImage 92:46-55.

Händel BF, Haarmeier T, Jensen O (2011) Alpha oscillations correlate with the successful inhibition of unattended stimuli. Journal of cognitive neuroscience 23:2494-2502.

Hanslmayr S, Matuschek J, Fellner M-C (2014) Entrainment of prefrontal beta oscillations induces an endogenous echo and impairs memory formation. Current Biology 24:904-909.

Hanslmayr S, Gross J, Klimesch W, Shapiro KL (2011) The role of alpha oscillations in temporal attention. Brain research reviews 67:331-343.

Hayes AF (2013) Introduction to mediation, moderation, and conditional process analysis: A regression-based approach: Guilford Press.

Helfrich RF, Schneider TR, Rach S, Trautmann-Lengsfeld SA, Engel AK, Herrmann CS (2014) Entrainment of brain oscillations by transcranial alternating current stimulation. Curr Biol 24:333-339.

Herring JD, Thut G, Jensen O, Bergmann TO (2015) Attention modulates TMS-locked alpha oscillations in the visual cortex. Journal of Neuroscience 35:14435-14447.

Herrmann CS (2001) Human EEG responses to 1–100 Hz flicker: resonance phenomena in visual cortex and their potential correlation to cognitive phenomena. Experimental brain research 137:346-353.

Herrmann CS, Rach S, Neuling T, Struber D (2013) Transcranial alternating current stimulation: a review of the underlying mechanisms and modulation of cognitive processes. Front Hum Neurosci 7:279.

Hoogenboom N, Schoffelen J-M, Oostenveld R, Parkes LM, Fries P (2006) Localizing human visual gamma-band activity in frequency, time and space. NeuroImage 29:764-773.

Horvath JC, Forte JD, Carter O (2014) Evidence that transcranial direct current stimulation (tDCS) generates little-to-no reliable neurophysiologic effect beyond MEP amplitude modulation in healthy human subjects: A systematic review. Neuropsychologia 66C:213-236.

Horvath JC, Forte JD, Carter O (2015) Quantitative Review Finds No Evidence of Cognitive Effects in Healthy Populations From Single-session Transcranial Direct Current Stimulation (tDCS). Brain stimulation 8:535-550.

İlhan B, VanRullen R (2012) No counterpart of visual perceptual echoes in the auditory system. PloS one 7:e49287.

Ilmoniemi RJ, Kicic D (2010) Methodology for Combined TMS and EEG. Brain Topogr 22:233-248.

Jaegle A, Ro T (2014) Direct control of visual perception with phase-specific modulation of posterior parietal cortex. Journal of cognitive neuroscience 26:422-432.

Jensen O, Colgin LL (2007) Cross-frequency coupling between neuronal oscillations. Trends in cognitive sciences 11:267-269.

Jensen O, Mazaheri A (2010) Shaping functional architecture by oscillatory alpha activity: gating by inhibition. Frontiers in human neuroscience 4:186.

Jensen O, Kaiser J, Lachaux J-P (2007) Human gamma-frequency oscillations associated with attention and memory. Trends in neurosciences 30:317-324.

Jensen O, Gelfand J, Kounios J, Lisman JE (2002) Oscillations in the alpha band (9–12 Hz) increase with memory load during retention in a short-term memory task. Cerebral cortex 12:877-882.

Jensen O, Gips B, Bergmann TO, Bonnefond M (2014) Temporal coding organized by coupled alpha and gamma oscillations prioritize visual processing. Trends Neurosci 37:357-369.

Joundi RA, Jenkinson N, Brittain JS, Aziz TZ, Brown P (2012) Driving oscillatory activity in the human cortex enhances motor performance. Curr Biol 22:403-407.

Kar K, Duijnhouwer J, Krekelberg B (2017) Transcranial Alternating Current Stimulation Attenuates Neuronal Adaptation. Journal of Neuroscience 37:2325-2335.

Keitel C, Quigley C, Ruhnau P (2014) Stimulus-driven brain oscillations in the alpha range: entrainment of intrinsic rhythms or frequency-following response? Journal of Neuroscience 34:10137-10140.

Keitel C, Thut G, Gross J (2017) Visual cortex responses reflect temporal structure of continuous quasi-rhythmic sensory stimulation. NeuroImage 146:58-70.

Klimesch W, Sauseng P, Gerloff C (2003) Enhancing cognitive performance with repetitive transcranial magnetic stimulation at human individual alpha frequency. Eur J Neurosci 17:1129-1133.

Klimesch W, Sauseng P, Hanslmayr S (2007) EEG alpha oscillations: the inhibition-timing hypothesis. Brain research reviews 53:63-88.

Koch C, Rapp M, Segev I (1996) A brief history of time (constants). Cerebral cortex 6:93-101.

Krolak-Salmon P, Hénaff MA, Tallon-Baudry C, Yvert B, Guénot M, Vighetto A, Mauguière F, Bertrand O (2003) Human lateral geniculate nucleus and visual cortex respond to screen flicker. Annals of neurology 53:73-80.

Kuś R, Duszyk A, Milanowski P, Łabęcki M, Bierzyńska M, Radzikowska Z, Michalska M, Żygierewicz J, Suffczyński P, Durka PJ (2013) On the quantification of SSVEP frequency responses in human EEG in realistic BCI conditions. PloS one 8:e77536.

Lisman JE, Jensen O (2013) The theta-gamma neural code. Neuron 77:1002-1016.

Loftus GR, Masson MEJ (1994) Using confidence intervals in within-subject designs. Psychonomic bulletin & review 1:476-490 %@ 1069-9384.

Lozano-Soldevilla D, ter Huurne N, Cools R, Jensen O (2014) GABAergic modulation of visual gamma and alpha oscillations and its consequences for working memory performance. Current Biology 24:2878-2887.

Luck SJ (2005) An introduction to the event-related potential technique. Cambridge, Mass.: MIT Press.

Makeig S, Bell AJ, Jung T-P, Sejnowski TJ (1996) Independent component analysis of electroencephalographic data. Advances in neural information processing systems:145-151.

Marshall TR, Bergmann TO, Jensen O (2015) (Accepted) Fronto-parietal structural connectivity mediates the top-down control of neuronal synchronization associated with selective attention. PLOS Biology.

Marshall TR, Esterer S, Herring JD, Bergmann TO, Jensen O (2016) On the relationship between cortical excitability and visual oscillatory responses - A concurrent tDCS-MEG study. NeuroImage 140:41-49.

Massimini M, Ferrarelli F, Esser SK, Riedner BA, Huber R, Murphy M, Peterson MJ, Tononi G (2007) Triggering sleep slow waves by transcranial magnetic stimulation. Proc Natl Acad Sci U S A 104:8496-8501.

Mathewson KE, Gratton G, Fabiani M, Beck DM, Ro T (2009) To see or not to see: prestimulus α phase predicts visual awareness. Journal of Neuroscience 29:2725-2732.

Mathewson KE, Lleras A, Beck DM, Fabiani M, Ro T, Gratton G (2011) Pulsed out of awareness: EEG alpha oscillations represent a pulsed-inhibition of ongoing cortical processing. Frontiers in psychology 2.

Mazaheri A, van Schouwenburg MR, Dimitrijevic A, Denys D, Cools R, Jensen O (2014) Region-specific modulations in oscillatory alpha activity serve to facilitate processing in the visual and auditory modalities. NeuroImage 87:356-362.

Mewett DT, Nazeran H, Reynolds KJ (2001) Removing power line noise from recorded EMG. In: Engineering in Medicine and Biology Society, 2001. Proceedings of the 23rd Annual International Conference of the IEEE, pp 2190-2193: IEEE.

Moliadze V, Zhao Y, Eysel U, Funke K (2003) Effect of transcranial magnetic stimulation on single-unit activity in the cat primary visual cortex. J Physiol 553:665-679.

Moreno-Duarte I, Gebodh N, Schestatsky P, Guleyupoglu B, Reato D, Bikson M, Fregni F, Cohen Kadosh R (2014) Transcranial electrical stimulation: Transcranial direct current stimulation (tDCS), transcranial alternating current stimulation (tACS), transcranial pulsed current stimulation (tPCS) and transcranial random noise stimulation (tRNS). The stimulated brain: Cognitive enhancement using noninvasive brain stimulation:35-59.

Morgan S, Hansen J, Hillyard S (1996) Selective attention to stimulus location modulates the steady-state visual evoked potential. Proceedings of the National Academy of Sciences 93:4770-4774.

Müller M, Andersen S, Trujillo N, Valdes-Sosa P, Malinowski P, Hillyard S (2006) Feature-selective attention enhances color signals in early visual areas of the human brain. Proceedings of the National Academy of Sciences 103:14250-14254.

Müller MM, Malinowski P, Gruber T, Hillyard S (2003) Sustained division of the attentional spotlight. Nature 424:309-312.

Müller MM, Picton TW, Valdes-Sosa P, Riera J, Teder-Sälejärvi WA, Hillyard SA (1998) Effects of spatial selective attention on the steady-state visual evoked potential in the 20–28 Hz range. Cognitive Brain Research 6:249-261.

Neuling T, Ruhnau P, Fusca M, Demarchi G, Herrmann CS, Weisz N (2015) Friends, not foes: Magnetoencephalography as a tool to uncover brain dynamics during transcranial alternating current stimulation. NeuroImage 118:406-413.

Nolte G (2003) The magnetic lead field theorem in the quasi-static approximation and its use for magnetoencephalography forward calculation in realistic volume conductors. Phys Med Biol 48:3637-3652.

Oostenveld R, Fries P, Maris E, Schoffelen J-M (2011) FieldTrip: open source software for advanced analysis of MEG, EEG, and invasive electrophysiological data. Computational intelligence and neuroscience 2011:1.

Opitz A, Falchier A, Linn GS, Milham MP, Schroeder CE (2017) Limitations of ex vivo measurements for in vivo neuroscience. Proc Natl Acad Sci U S A.

Opitz A, Falchier A, Yan CG, Yeagle EM, Linn GS, Megevand P, Thielscher A, Deborah AR, Milham MP, Mehta AD, Schroeder CE (2016) Spatiotemporal structure of intracranial electric fields induced by transcranial electric stimulation in humans and nonhuman primates. Sci Rep 6:31236.

Osipova D, Hermes D, Jensen O (2008) Gamma power is phase-locked to posterior alpha activity. PloS one 3:e3990.

Parkkonen L, Andersson J, Hämäläinen M, Hari R (2008) Early visual brain areas reflect the percept of an ambiguous scene. Proceedings of the National Academy of Sciences 105:20500-20504.

Paus T, Sipila PK, Strafella AP (2001) Synchronization of neuronal activity in the human primary motor cortex by transcranial magnetic stimulation: an EEG study. J Neurophysiol 86:1983-1990.

Perrin F, Pernier J, Bertrand O, Echallier JF (1989) Spherical splines for scalp potential and current density mapping. Electroencephalography and Clinical Neurophysiology 72:184-187.

Perrin F, Pernier J, Bertrand O, Echallier JF (1990) Corrigenda: EEG 02274. Electroencephalography and Clinical Neurophysiology 76:565-566.

Pfurtscheller G, Stancak A, Neuper C (1996) Event-related synchronization (ERS) in the alpha band—an electrophysiological correlate of cortical idling: a review. International journal of psychophysiology 24:39-46.

Pogosyan A, Gaynor LD, Eusebio A, Brown P (2009) Boosting cortical activity at Beta-band frequencies slows movement in humans. Curr Biol 19:1637-1641.

Polania R, Nitsche MA, Korman C, Batsikadze G, Paulus W (2012) The Importance of Timing in Segregated Theta Phase-Coupling for Cognitive Performance. Curr Biol.

Premoli I, Castellanos N, Rivolta D, Belardinelli P, Bajo R, Zipser C, Espenhahn S, Heidegger T, Müller-Dahlhaus F, Ziemann U (2014) TMS-EEG signatures of GABAergic neurotransmission in the human cortex. The Journal of Neuroscience 34:5603-5612.

Rager G, Singer W (1998) The response of cat visual cortex to flicker stimuli of variable frequency. European Journal of Neuroscience 10:1856-1877.

Rajagovindan R, Ding M (2011) From prestimulus alpha oscillation to visual-evoked response: an inverted-U function and its attentional modulation. The Journal of Cognitive Neuroscience 23:1379-1394.

Reddy L, Kanwisher N (2006) Coding of visual objects in the ventral stream. Current opinion in neurobiology 16:408-414.

Riela AR (1990) Topographic brain mapping of EEG and evoked potentials: Edited by Dr. K. Maurer. 576 pages. Dm 198.00. Berlin: Springer-Verlag, 1989. In: Elsevier.

Romei V, Gross J, Thut G (2010) On the role of prestimulus alpha rhythms over occipito-parietal areas in visual input regulation: correlation or causation? Journal of Neuroscience 30:8692-8697.

Romei V, Gross J, Thut G (2012) Sounds reset rhythms of visual cortex and corresponding human visual perception. Curr Biol 22:807-813.

Romei V, Rihs T, Brodbeck V, Thut G (2008a) Resting electroencephalogram alpha-power over posterior sites indexes baseline visual cortex excitability. Neuroreport 19:203-208.

Romei V, Driver J, Schyns PG, Thut G (2011) Rhythmic TMS over parietal cortex links distinct brain frequencies to global versus local visual processing. Current Biology 21:334-337.

Romei V, Brodbeck V, Michel C, Amedi A, Pascual-Leone A, Thut G (2008b) Spontaneous fluctuations in posterior alpha-band EEG activity reflect variability in excitability of human visual areas. Cereb Cortex 18:2010-2018.

Rosanova M, Casali A, Bellina V, Resta F, Mariotti M, Massimini M (2009) Natural frequencies of human cortico-thalamic circuits. J Neurosci 29:7679-7685.

Ruzzoli M, Soto-Faraco S (2014) Alpha stimulation of the human parietal cortex attunes tactile perception to external space. Curr Biol 24:329-332.

Sandström M, Lyskov E, Berglund A, Medvedev S, Mild KH (1997) Neurophysiological effects of flickering light in patients with perceived electrical hypersensitivity. Journal of Occupational and Environmental Medicine 39:15-22.

Santarnecchi E, Polizzotto NR, Godone M, Giovannelli F, Feurra M, Matzen L, Rossi A, Rossi S (2013) Frequency-dependent enhancement of fluid intelligence induced by transcranial oscillatory potentials. Curr Biol 23:1449-1453.

Sauseng P, Klimesch W, Stadler W, Schabus M, Doppelmayr M, Hanslmayr S, Gruber WR, Birbaumer N (2005) A shift of visual spatial attention is selectively associated with human EEG alpha activity. European Journal of Neuroscience 22:2917-2926.

Sauseng P, Klimesch W, Heise KF, Gruber WR, Holz E, Karim AA, Glennon M, Gerloff C, Birbaumer N, Hummel FC (2009) Brain oscillatory substrates of visual short-term memory capacity. Curr Biol 19:1846-1852.

Scheeringa R, Mazaheri A, Bojak I, Norris DG, Kleinschmidt A (2011) Modulation of visually evoked cortical FMRI responses by phase of ongoing occipital alpha oscillations. Journal of Neuroscience 31:3813-3820.

Scheeringa R, Petersson KM, Oostenveld R, Norris DG, Hagoort P, Bastiaansen MC (2009) Trial-by-trial coupling between EEG and BOLD identifies networks related to alpha and theta EEG power increases during working memory maintenance. NeuroImage 44:1224-1238.

Schroeder CE, Lakatos P (2009) Low-frequency neuronal oscillations as instruments of sensory selection. Trends Neurosci 32:9-18.

Schutter DJ (2015) Cutaneous retinal activation and neural entrainment in transcranial alternating current stimulation: A systematic review. NeuroImage.

Snyder AC, Morais MJ, Willis CM, Smith MA (2015) Global network influences on local functional connectivity. Nature neuroscience 18:736-743.

Soekadar SR, Witkowski M, Cossio EG, Birbaumer N, Robinson SE, Cohen LG (2013) In vivo assessment of human brain oscillations during application of transcranial electric currents. Nature communications 4:2032.

Spaak E, de Lange FP, Jensen O (2014) Local entrainment of alpha oscillations by visual stimuli causes cyclic modulation of perception. Journal of Neuroscience 34:3536-3544.

Spaak E, Bonnefond M, Maier A, Leopold DA, Jensen O (2012) Layer-Specific Entrainment of Gamma-Band Neural Activity by the Alpha Rhythm in Monkey Visual Cortex. Curr Biol.

Srinivasan R (2004) Internal and external neural synchronization during conscious perception. International Journal of Bifurcation and Chaos 14:825-842.

Srinivasan R, Bibi FA, Nunez PL (2006) Steady-state visual evoked potentials: distributed local sources and wave-like dynamics are sensitive to flicker frequency. Brain topography 18:167-187.

Srinivasan R, Russell DP, Edelman GM, Tononi G (1999) Increased synchronization of neuromagnetic responses during conscious perception. Journal of Neuroscience 19:5435-5448.

Srinivasan R, Fornari E, Knyazeva MG, Meuli R, Maeder P (2007) fMRI responses in medial frontal cortex that depend on the temporal frequency of visual input. Experimental brain research 180:677-691.

Stolk A, Todorovic A, Schoffelen J-M, Oostenveld R (2013) Online and offline tools for head movement compensation in MEG. NeuroImage 68:39-48.

Thut G, Schyns P, Gross J (2011a) Entrainment of perceptually relevant brain oscillations by non-invasive rhythmic stimulation of the human brain. Frontiers in psychology 2:170.

Thut G, Miniussi C, Gross J (2012) The functional importance of rhythmic activity in the brain. Curr Biol 22:R658-663.

Thut G, Nietzel A, Brandt SA, Pascual-Leone A (2006a) Alpha-band electroencephalographic activity over occipital cortex indexes visuospatial attention bias and predicts visual target detection. The Journal of neuroscience : the official journal of the Society for Neuroscience 26:9494-9502.

Thut G, Nietzel A, Brandt SA, Pascual-Leone A (2006b) Alpha-band electroencephalographic activity over occipital cortex indexes visuospatial attention bias and predicts visual target detection. J Neurosci 26:9494-9502.

Thut G, Veniero D, Romei V, Miniussi C, Schyns P, Gross J (2011b) Rhythmic TMS Causes Local Entrainment of Natural Oscillatory Signatures. Curr Biol 21:1176-1185.

Toffanin P, de Jong R, Johnson A, Martens S (2009) Using frequency tagging to quantify attentional deployment in a visual divided attention task. International Journal of Psychophysiology 72:289-298.

Tononi G, Srinivasan R, Russell DP, Edelman GM (1998) Investigating neural correlates of conscious perception by frequency-tagged neuromagnetic responses. Proceedings of the National Academy of Sciences 95:3198-3203.

Tort AB, Komorowski R, Eichenbaum H, Kopell N (2010) Measuring phase-amplitude coupling between neuronal oscillations of different frequencies. Journal of neurophysiology 104:1195-1210.

Traub RD, Jefferys JG, Whittington MA (1999) Fast oscillations in cortical circuits: MIT press.

Tuladhar AM, Huurne Nt, Schoffelen JM, Maris E, Oostenveld R, Jensen O (2007) Parieto-occipital sources account for the increase in alpha activity with working memory load. Human brain mapping 28:785-792.

Tzourio-Mazoyer N, Landeau B, Papathanassiou D, Crivello F, Etard O, Delcroix N, Mazoyer B, Joliot M (2002) Automated anatomical labeling of activations in SPM using a macroscopic anatomical parcellation of the MNI MRI single-subject brain. NeuroImage 15:273-289.

Underwood E (2016) Cadaver study casts doubts on how zapping brain may boost mood, relieve pain. Sciencemag org.

Van Diepen RM, Born S, Souto D, Gauch A, Kerzel D (2010) Visual flicker in the gamma-band range does not draw attention. Journal of neurophysiology 103:1606-1613.

Van Dijk H, Schoffelen J-M, Oostenveld R, Jensen O (2008) Prestimulus oscillatory activity in the alpha band predicts visual discrimination ability. Journal of Neuroscience 28:1816-1823.

van Ede F, Köster M, Maris E (2012) Beyond establishing involvement: Quantifying the contribution of anticipatory α-and β-band suppression to perceptual improvement with attention. Journal of neurophysiology 108:2352-2362.

van Ede F, de Lange F, Jensen O, Maris E (2011) Orienting attention to an upcoming tactile event involves a spatially and temporally specific modulation of sensorimotor alpha-and beta-band oscillations. Journal of Neuroscience 31:2016-2024.

Van Veen BD, van Drongelen W, Yuchtman M, Suzuki A (1997) Localization of brain electrical activity via linearly constrained minimum variance spatial filtering. IEEE Trans Biomed Eng 44:867-880.

VanRullen R, Koch C (2003) Is perception discrete or continuous? Trends Cogn Sci 7:207-213.

VanRullen R, Macdonald JS (2012) Perceptual echoes at 10 Hz in the human brain. Current biology 22:995-999.

VanRullen R, Busch N, Drewes J, Dubois J (2011) Ongoing EEG phase as a trial-by-trial predictor of perceptual and attentional variability. Frontiers in psychology 2:60.

Varela F, Lachaux J-P, Rodriguez E, Martinerie J (2001) The brainweb: phase synchronization and large-scale integration. Nature reviews neuroscience 2:229-239.

Vialatte F-B, Maurice M, Dauwels J, Cichocki A (2010) Steady-state visually evoked potentials: focus on essential paradigms and future perspectives. Progress in neurobiology 90:418-438.

Watson AB, Pelli DG (1983) QUEST: A Bayesian adaptive psychometric method. Attention, Perception, & Psychophysics 33:113-120.

Williams PE, Mechler F, Gordon J, Shapley R, Hawken MJ (2004) Entrainment to video displays in primary visual cortex of macaque and humans. Journal of Neuroscience 24:8278-8288.

Witkowski M, Cossio EG, Chander BS, Braun C, Birbaumer N, Robinson SE, Soekadar SR (2015) Mapping entrained brain oscillations during transcranial alternating current stimulation (tACS). NeuroImage.

Worden MS, Foxe JJ, Wang N, Simpson GV (2000) Anticipatory biasing of visuospatial attention indexed by retinotopically specific-band electroencephalography increases over occipital cortex. J Neurosci 20:1-6.

Xu P, Tian C, Zhang Y, Jing W, Wang Z, Liu T, Hu J, Tian Y, Xia Y, Yao D (2013) Cortical network properties revealed by SSVEP in anesthetized rats. Scientific reports 3:2496.

Yan Z, Gao X (2011) Functional connectivity analysis of steady-state visual evoked potentials. Neuroscience letters 499:199-203.

Zhang Y, Xu P, Huang Y, Cheng K, Yao D (2013) SSVEP response is related to functional brain network topology entrained by the flickering stimulus. PloS one 8:e72654.

Nederlandse samenvatting

Stel je voor dat je 's avonds op de bank zit en druk bezig bent op je laptop. Je bent je erg aan het concentreren omdat je nog wat werk gedaan moet krijgen. Je partner zit naast je en kijkt televisie. Je probeert alle geluiden uit de omgeving te negeren en je te concentreren op je taak. Plotseling hoor je dat je kind jouw naam roept vanaf zijn slaapkamer. Hoewel de stem van je kind zachter is dan de geluiden van de televisie, grijpt het meteen je aandacht. Je rent naar boven en hij vertelt dat hij een nachtmerrie heeft gehad. Je stelt je kind gerust, gaat weer naar beneden en gaat verder met werken.

Hoe komt het dat je de geluiden van de tv kon negeren maar toch je kind kon horen? We denken dat bepaalde hersengolven, zogenaamde alfa golven, een rol spelen bij het blokkeren van irrelevante informatie (het geluid van de tv) waarbij er nog ruimte over gelaten wordt om informatie te verwerken die wel van belang is (het roepen van je kind).

Hersengolven worden geproduceerd door hersencellen. Pas als een grote groep hersencellen tegelijk actief worden, is het signaal zo groot dat we het kunnen meten. Het elektrisch signaal wat hierbij geproduceerd wordt, kunnen we meten met behulp van elektro-encefalografie (EEG). Dit elektrisch signaal, produceert tevens een magnetisch signaal. We kunnen dit magnetisch signaal meten met magneto-encefalografie (MEG). In mijn proefschrift heb ik beide meetmethodes gebruikt. Ik onderzocht in mijn proefschrift of we hersengolven konden manipuleren met behulp van hersenstimulatietechnieken. In het eerste experiment heb ik transcraniële magnetische stimulatie (TMS) gebruikt. TMS is een techniek waarbij een sterke magnetische puls een elektrische stroom in het brein opwekt. In het derde experiment heb ik transcraniële wisselstroom gebruikt (TACS). Hierbij dien ik zwakke stroom op de schedel toe, die de hersengolven moeten nabootsen.

Als groepen hersencellen vervolgens gelijktijdig afwisselend meer en minder vuren, spreken we van hersengolven. Deze hersengolven kenmerken zich door de frequentie waarmee meer en minder vuren zich afwisselen. De alfa golven, bijvoorbeeld, hebben een frequentie tussen de 8 en 14 Hz (8-14 golven per seconde). In het verleden is aangetoond dat deze golven in verband staan met aandacht. Als je je aandacht richt op je laptop, terwijl je de geluiden van de televisie probeert te negeren worden alfa golven sterken in het hersengebied waar geluiden verwerkt worden. Anderzijds zijn er weinig alfa golven te ontdekken in het hersengebied waar visuele informatie verwerkt wordt (zie Figuur 1). Verder wijst onderzoek uit dat ook bij sterke alfa golven (Figuur 1, blauwe golf) geluiden verwerkt kunnen worden. Als je naar Figuur 1 kijkt, kun je je voorstellen

dat een alfa golf de mate van inhibitie weergeeft. Als de golf zich in een piekje bevindt, is er veel inhibitie en kan er dus weinig verwerkt worden en als de golf zich in een dal bevindt, is de mate van inhibitie hetzelfde als in de visuele cortex en kan er wel dus wat verwerkt worden. Bijvoorbeeld, als je partner wat tegen je zegt een piekje van een alfa golf, zou het kunnen zijn dat het plaatje niet waargenomen wordt terwijl presentatie tijdens een dal van een alfa golf wel tot waarneming kan leiden.

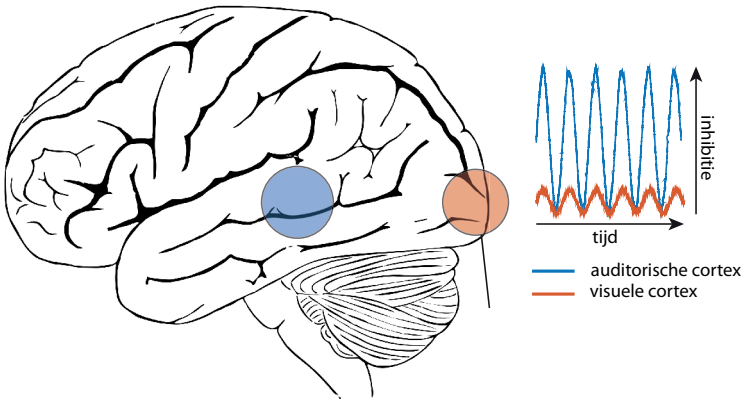

Figuur 1. *Alfa golven blokkeren irrelevante input.* In dit schematische voorbeeld zie je de sterkte van alfa golven in de visuele cortex (rood) en in de auditorische cortex (blauw). De mate van inhibitie wordt gerepresenteerd door de sterkte van de alfagolven. Je kunt zien dat de mate van inhibitie binnen een alfa golf afwisselt. Op sommige momenten is er weinig inhibitie in zowel visuele als auditorische cortex.

In mijn proefschrift heb ik deze alfa golven onderzocht en laat verschillende manieren zien hoe we met behulp van verschillende stimulatietechnieken aan kunnen tonen dat alfa golven een belangrijke rol spelen in het verwerken van informatie. In een eerste experiment heb ik gekeken of we alfa golven kunnen beïnvloeden met behulp van TMS. In dit experiment moesten deelnemers hun aandacht richten op plaatjes of geluiden terwijl we regelmatig TMS-pulsen toedienden. Tegelijkertijd hebben we met behulp van EEG hun hersenactiviteit gemeten. We vonden dat het toedienen van een TMS-puls ervoor zorgde dat er een aantal alfa golven opgewekt werden. Tevens zagen we dat deze alfa golven sterker waren als proefpersonen hun aandacht richtten op de geluiden. Omdat we weten dat alfa golven normaal gesproken groter zijn in hersengebieden die onderdrukt zijn, namen we hierdoor aan dat we met TMS instaat waren het mechanisme te stimuleren wat verantwoordelijk is voor het opwekken van alfa golven. Dit liet ons dus zien dat TMS een uitstekende methode is om alfa golven te bestuderen.

In een vervolgexperiment onderzocht ik of we soortgelijke effecten konden opwekken met behulp van visuele stimulatie. Je zou namelijk kunnen zeggen dat de reactie op

TMS vergelijkbaar is met een hele sterke visuele flits. Om dit te testen hebben we proefpersonen naar flikkerende rondjes laten kijken. Belangrijk hierbij is om te weten dat het flikkeren geen bepaald ritme had maar volledig willekeurig was. Hierbij hebben we de hersenactiviteit met behulp van MEG gemeten. Deelnemers moesten wederom hun aandacht richten op plaatjes of geluiden. We gebruikten vervolgens een wiskundige techniek om de reactie van het brein op een simpele flits te meten. We zagen dat ook hier een alfa golf werd opgewekt. Alhoewel de resultaten niet zo duidelijk waren als in het eerste experiment, leken de opgewekte alfa golven ook hier sterker als deelnemers zich op de geluiden probeerden de concentreren.

In het derde experiment keken we of we met behulp van TACS alfa golven konden opwekken en of we met deze stroompjes de effecten van alfa golven konden nabootsen. Hierbij keken we naar het effect van de stimulatie op hersenactiviteit die opgewekt wordt bij het kijken naar plaatjes. Deze plaatjes veroorzaken specifieke hersenactiviteit die we vervolgens probeerden te veranderen met behulp van elektrische stimulatie. Hierbij maten we hersenactiviteit met behulp van MEG. We stimuleerden het brein op verschillende frequenties en verwachtten dat alleen stimulatie in de alfa frequentie de effecten van alfa golven na konden bootsen. We zagen echter dat het niet zoveel uitmaakte met welke frequentie we stimuleerden. Bij alle frequenties zagen we een vermindering in de hersenactiviteit, net als bij toenemende alfa activiteit. Proefpersonen presteerden hierbij slechter op de gedragstaak. Tevens zagen we dat de hersenactiviteit fluctueerde afhankelijk van de positie binnen in de golf van stimulatie. Hersenactiviteit was anders tijdens een piek van een golf van stimulatie, dan in een dal. Elektrische stroom kan dus inderdaad gebruikt worden om alfa golven te bestuderen. Omdat de stimulatiefrequentie niet van belang was, was het niet duidelijk of wij bestaande alfa golven aan het aansturen waren, of dat we simpelweg de effecten van alfa golven met de stimulatie aan het nabootsen waren.

In het laatste experiment keken we hoe we de rol van alfa golven tijdens visuele verwerking kunnen bestuderen. Alfa golven nemen af in kracht tijdens visuele verwerking. Toch denken we dat ze een belangrijke rol spelen in het verwerken van visuele informatie, met name in het onderdrukken van irrelevante visuele informatie. Het is echter lastig een zwak signaal te meten. Tevens spelen er zich een hoop processen in het brein gelijktijdig af waardoor het vaak ingewikkeld is door de bomen het bos te zien. Een techniek die hierbij kan helpen is 'frequency tagging'. Bij deze techniek laat je een proefpersoon naar een plaatje kijken wat met een specifieke snelheid knippert. Vervolgens kijk je naar de hersenactiviteit die precies dezelfde 'knippersnelheid' laat zien waarbij je dan vrijwel zeker kunt zijn dat het met het verwerken van dat specifieke plaatje te maken heeft.

Ten eerste vonden we een mooi signaal in het brein op de knippersnelheid van de plaatjes. Tevens vonden we dat dit signaal sterker was als deelnemers hun aandacht op het plaatje richtten. We concludeerden hierbij dat het signaal de verwerking van het plaatje representeerde. Vervolgens zagen we dat de sterkte van het signaal fluctueerde in lijn met een alfa golf, wat dus suggereert dat alfa golven een rol spelen bij visuele verwerking. We concludeerden dus dat deze techniek uitermate geschikt is om alfa golven te bestuderen.

In mijn proefschrift heb ik verschillende technieken laten zien die gebruikt kunnen worden om alfa golven te bestuderen. Ik hoop hierbij dat het een bijdrage zal leveren om een beter begrip te verkrijgen wat de exacte rol is van alfa oscillaties in aandacht en visuele verwerking.

Deutsche Zusammenfassung

Du sitzt abends auf dem Sofa und beschäftigst dich mit deinem Laptop. Da du noch arbeitest, musst du dich stark konzentrieren. Dein Partner sitzt neben dir und schaut Fernsehen. Du versuchst um alle Geräusche auszublenden und dich nur auf deine Arbeit zu konzentrieren. Plötzlich hörst du, dass dein Kind aus seinem Schlafzimmer deinen Namen ruft. Obwohl die Stimme deines Kindes viel leiser ist als die Geräusche des Fernsehers, hat die Stimme deines Kindes sofort deine Aufmerksamkeit geweckt. Du läufst schnell nach oben und dein Kind sagt dir, dass es einen Albtraum hatte. Du beruhigst dein Kind und gehst wieder runter um weiterzuarbeiten.

Wie kommt es, dass du die Geräusche des Fernsehers ignorieren kannst, aber dein Kind dennoch hörst? Wir glauben, dass bestimmte Gehirnwellen, so genannte Alpha-Wellen, eine Rolle beim Blockieren irrelevanter Informationen spielen (die Geräusche des Fernsehers), aber trotzdem Raum lassen für die Verarbeitung von wichtigen Informationen (die Rufe deines Kindes).

Gehirnwellen werden von Neuronen produziert. Erst wenn eine große Gruppe von Gehirnzellen gleichzeitig aktiviert wird, ist das Signal groß genug, dass wir es messen können. Das hierbei erzeugte elektrische Signal kann mittels Elektroenzephalographie (EEG) gemessen werden. Dieses elektrische Signal erzeugt auch ein magnetisches Signal. Wir können dieses magnetische Signal mit Magnetoenzephalographie (MEG) messen. In meiner Dissertation habe ich beide Messmethoden verwendet. Ich untersuchte in meiner Dissertation, ob wir Gehirnwellen mit Gehirnstimulationstechniken manipulieren können. Im ersten Experiment habe ich transkranielle Magnetstimulation (TMS) verwendet. TMS ist eine Technik, bei der ein starker magnetischer Puls einen elektrischen Strom im Gehirn erzeugt. Im dritten Experiment habe ich transkraniellen Wechselstrom (TACS) verwendet. Hiermit habe ich den Schädel mit schwachen Strömen stimuliert, die die Gehirnwellen nachahmen sollten.

Wenn sich eine großen Gruppe Gehirnzellen gleichzeitig und abwechselnd Signale abfeuern, spricht man von Gehirnwellen. Diese Gehirnwellen zeichnen sich durch die Frequenz aus, mit der sich die abgefeuerten Signale abwechseln. Alpha-Wellen haben beispielsweise eine Frequenz zwischen 8 und 14 Hz (8-14 Wellen pro Sekunde). Vorrangegangene Studien haben gezeigt, dass diese Wellen mit Aufmerksamkeit zusammenhängen. Wenn du dich auf deinen Laptop konzentrierst, während du versuchst die Geräusche des Fernsehers zu ignorieren, werden Alpha-Wellen in dem Gehirnbereich stärker, wo Geräusche verarbeitet werden. Andererseits gibt es nur wenige Alpha-Wellen im Gehirnbereich, in denen visuelle Informationen verarbeitet werden.

Aktuelle Forschungsergebnisse haben erwiesen, dass auch bei starken Alpha-Wellen (Abbildung 1, blaue Welle) Geräusche verarbeitet werden können. Wenn man sich Abbildung 1 anschaut, kann man sich vorstellen, dass eine Alpha- Welle das Ausmaß der Unterdrückung von Informationen darstellt. Auf dem Lokalem Maximum der Welle wird Aufmerksamkeit am stärksten unterdrückt und es können nur wenige Informationsquellen verarbeitet werden. Wenn die Welle aber an einem Lokalem Minimum ist, ist das Ausmaß der Unterdrückung am niedrigsten. Zum Beispiel, wenn dein Partner mit dir spricht während des Hochpunktes einer Alpha-Welle, könnte es sein, dass du sie nicht verstehst. Wenn sie aber während eines Tiefpunktes einer Alpha-Welle mit dir spricht kannst du sie verstehen.

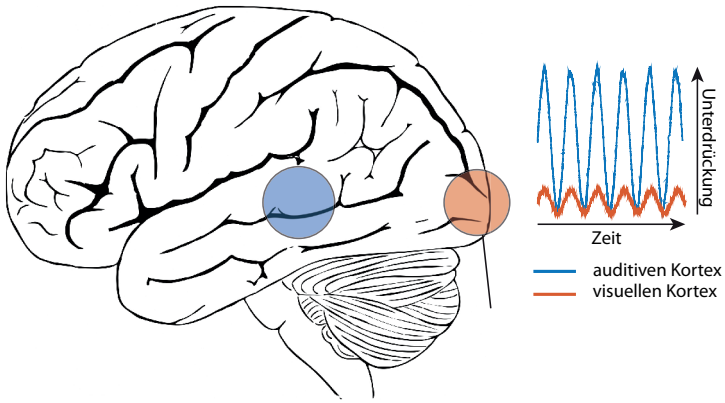

Figur 1. *Alpha-Wellen blockieren irrelevante zu verarbeitende Informationen.* In dieser Veranschaulichung ist die Amplitude der Alpha-Wellen im visuellen Kortex (rot) und im auditiven Kortex (blau) zu sehen. Das Ausmaß der Unterdrückung von Informationen wird durch die Amplitude der Alpha-Wellen bestimmt. Das Ausmaß der Unterdrückung von Informationen innerhalb einer Alpha-Welle fluktuiert. Zu bestimmten Zeitpunkten gibt es sowohl im visuellen als auch im auditiven Kortex wenig Unterdrückung.

In meiner Dissertation erforschte ich Alpha-Wellen und zeigte auf verschiedene Weisen wie wir mit Hilfe verschiedener Gehirnstimulationstechniken beweisen können, dass Alpha-Wellen eine wichtige Rolle bei der Verarbeitung von Information spielen. In einem ersten Experiment habe ich untersucht ob wir Alpha-Wellen mit TMS beeinflussen können. In diesem Experiment mussten Teilnehmer ihre Aufmerksamkeit auf Bilder oder Töne richten, während sie in regelmäßigen Abständen TMS-Impulse bekamen auf dem visuellen Kortex. Gleichzeitig haben wir ihre Gehirnaktivität mit EEG gemessen. Meine Ergebnisse haben gezeigt, dass die Stimulierung mit Hilfe eines TMS-Impulses mehrere Alpha-Wellen erzeugt haben. Wir sahen auch, dass diese Alpha-Wellen stärker waren, als die Teilnehmer ihre Aufmerksamkeit auf Töne fokussierten. Da wir bereits wissen, dass Alpha-Wellen stärker sind in Gehirngebieten die unterdrückt werden, nehme ich

an, dass ich die Erzeugung von Alpha-Wellen mit Hilfe von TMS anregen konnte. Dies zeigte mir, dass TMS eine hervorragende Methode ist um Alpha-Wellen zu erforschen.

In einem zweiten Experiment habe ich untersucht, ob wir mit visueller Stimulation ähnliche Effekte erzeugen können. Ich nahm an, dass die durch TMS-Impulse produzierte Reaktionen im EEG mit einem sehr starken visuellen Flackern vergleichbar ist. Um diese Vermutung zu überprüfen, ließen wir Teilnehmer flackernde Kreise betrachten. Es war hierbei besonders wichtig, dass das Flackern keinem bestimmten Rhythmus folgte, sondern völlig willkürlich war. Dabei haben wir die Gehirnaktivität mit MEG gemessen. Die Teilnehmer mussten sich entweder auf Bilder oder Töne konzentrieren. Wir stellten fest, dass gleichzeitig mit dem Flackern auch eine Alpha-Welle erzeugt wurde. Obwohl die Ergebnisse nicht so deutlich waren wie im ersten Experiment, schienen die erzeugten Alpha-Wellen auch hier stärker zu sein, wenn sich die Teilnehmer auf Töne konzentrierten.

Im dem dritten Experiment überprüfte ich, ob wir mit TACS Alpha-Wellen erzeugen können, und ob wir die Auswirkungen von Alpha-Wellen mit diesen Strömen nachahmen können. Hierbei untersuchte ich die Auswirkungen der Stimulation auf Gehirnaktivität, die bei der Verarbeitung von visuellen Informationen erzeugt wird. Die Bilder verursachten spezifische Gehirnaktivität, die wir dann mit elektrischer Stimulation versuchten zu verändern. Hierbei maßen wir die Gehirnaktivität mit MEG. Wir stimulierten das Gehirn mit verschieden frequentierten Stromwellen, wobei wir vermuteten, dass nur die Stimulation mit Stromwellen der Alpha-Frequenz die Effekte von Gehirn Alpha-Wellen nachahmen können. Allerdings haben wir herausgefunden, dass die Stimulationsfrequenz bedeutungslos war. Bei allen Frequenzstimulation sahen wir eine Abnahme in allgemeiner Gehirnaktivität, sowie zunehmender Alpha-Aktivität. Des Weiteren erfüllten Teilnehmer ihr Aufgabe während der Hirnstimulation schlechter. Wir fanden jedoch auch heraus, dass die Gehirnaktivität sich je nach Position innerhalb einer Stimulationswelle veränderte. Die Gehirnaktivität war während eines Hochpunktes anders als während eines Tiefpunktes. Wir schlussfolgern daher, dass wir elektrische Ströme verwenden können um Alpha-Wellen zu erforschen. Weil wir herausfanden, dass die Stimulationsfrequenz des Gehirns keine Auswirkungen hatte, war es nicht ersichtlich, ob wir vorhandene Alpha-Wellen beeinflussten oder neue Alpha-Wellen produzierten.

Im meinem letzten Experiment habe ich untersucht, wie man am besten die Funktion von Alpha-Wellen während der visuellen Verarbeitung untersucht. Alpha-Wellen sind während der visuellen Verarbeitung sehr schwach. Dennoch denken wir, dass sie eine wichtige Rolle bei der Verarbeitung visueller Informationen spielen, vor allem bei der

Unterdrückung irrelevanter visueller Informationen. Es ist jedoch schwierig ein schwaches Signal zu messen. Dabei gibt gleichzeitig auch noch viele andere Prozesse im Gehirn, die simultan aktiv sind, so dass es oft kompliziert ist die richtigen Prozesse zu erkennen. Eine Technik die dabei helfen kann ist ‚Frequenzerfassung'. Bei dieser Technik lassen wir Teilnehmer Bilder anschauen die sie in einer bestimmten gleichmäßigen Geschwindigkeit (Frequenz) zu sehen bekommen. Gleichzeitig betrachten wir die Gehirnaktivität die in genau der gleichen, gleichmäßigen Geschwindigkeit 'blinkt', da wir davon ausgehen, dass diese Frequenz mit der Verarbeitung der jeweiligen Bilder zusammenhängt. Wir entdeckten ein deutliches Signal im Gehirn in der gleichen Geschwindigkeit der blinkenden Bilder. Auch haben wir festgestellt, dass dieses Signal stärker war, wenn Teilnehmer ihre Aufmerksamkeit auf Bilder fokussierten als wenn sie ihre Aufmerksamkeit auf Töne fokussierten. Daraus schlussfolgerten wir, dass das Signal Aspekte der Verarbeitung der Bilder darstellte. Auch sahen wir, dass die Signalstärke der Gehirnaktivität, die mit der Verarbeitung der jeweiligen Bilder zusammenhängt, sich im Einklang mit einer Alpha-Welle veränderte, was darauf hindeutet, dass Alpha-Wellen eine Rolle bei der visuellen Verarbeitung spielen. Wir schlussfolgten daher, dass die angewendete Technik gut geeignet ist um Alpha-Wellen zu erforschen.

In meiner Dissertation legte ich verschiedene Techniken dar, die verwendet werden können um Alpha-Wellen zu erforschen. Diese Techniken werden in Zukunft helfen ein besseres Verständnis der Rolle von Alpha-Wellen im Zusammenhang mit Aufmerksamkeit und visueller Verarbeitung von Informationen zu erlangen.

Donders Graduate School for Cognitive Neuroscience

For a successful research Institute, it is vital to train the next generation of young scientists. To achieve this goal, the Donders Institute for Brain, Cognition and Behaviour established the Donders Graduate School for Cognitive Neuroscience (DGCN), which was officially recognized as a national graduate school in 2009. The Graduate School covers training at both Master's and PhD level and provides an excellent educational context fully aligned with the research program of the Donders Institute.

The school successfully attracts highly talented national and international students in biology, physics, psycholinguistics, psychology, behavioral science, medicine and related disciplines. Selective admission and assessment centers guarantee the enrolment of the best and most motivated students.

The DGCN tracks the career of PhD graduates carefully. More than 50% of PhD alumni show a continuation in academia with postdoc positions at top institutes worldwide, e.g. Stanford University, University of Oxford, University of Cambridge, UCL London, MPI Leipzig, Hanyang University in South Korea, NTNU Norway, University of Illinois, North Western University, Northeastern University in Boston, ETH Zürich, University of Vienna, etc. Positions outside academia spread among the following sectors: specialists in a medical environment, mainly in genetics, geriatrics, psychiatry and neurology. Specialists in a psychological environment, e.g. as specialist in neuropsychology, psychological diagnostics or therapy. Positions in higher education as coordinators or lecturers. A smaller percentage enters business as research consultants, analysts or head of research and development. Fewer graduates stay in a research environment as lab coordinators, technical support or policy advisors. Upcoming possibilities are positions in the IT sector and management position in pharmaceutical industry. In general, the PhDs graduates almost invariably continue with high-quality positions that play an important role in our knowledge economy.

For more information on the DGCN as well as past and upcoming defenses please visit: http://www.ru.nl/donders/graduate-school/phd/

Publications

Soekadar, S. R., **Herring, J. D.**, & McGonigle, D. (2016). Transcranial electric stimulation (tES) and NeuroImaging: the state-of-the-art, new insights and prospects in basic and clinical neuroscience. *NeuroImage*, Volume 140, 2016, Pages 1-3,

Herring, J. D., Thut, G., Jensen, O., & Bergmann, T. O. (2015). Attention modulates TMS-locked alpha oscillations in the visual cortex. *The Journal of Neuroscience, 35*(43), 14435-14447.

Marshall, T. R., Esterer, S., **Herring, J. D.,** Bergmann, T. O., & Jensen, O. (2015). On the relationship between cortical excitability and visual oscillatory responses—A concurrent tDCS–MEG study. *NeuroImage, 140*, 41-49.

de Graaf, T. A., **Herring, J.,** & Sack, A. T. (2011). A chronometric exploration of high-resolution 'sensitive TMS masking' effects on subjective and objective measures of vision. *Experimental brain research*, *209*(1), 19-27

In preparation

Herring, J.D., Esterer, S., Marshall, T.R., Jensen, O., & Bergmann, T.O. Low-frequency transcranial alternating current stimulation rhythmically suppresses stimulus-induced gamma-band oscillations in early visual cortex and impairs perceptual performance.

Herring, J.D., Herpers, J., Bergmann, T.O., & Jensen, O. Frequency Tagging at High Frequencies in Downstream Areas.

Herring, J.D., Chota, S., VanRullen, R., Bergmann, T.O., & Jensen, O. The Effect of Attention on Perceptual and Transcranial Evoked Cortical Echoes.

About the author

Jim was born on April 29th 1987 in the city of Kerkrade, the Netherlands. He obtained his high school diploma at the Graaf Huyn College in Geleen. After studying computer science for two years he started studying Psychology at Maastricht University. In his 2nd year he participated in a research project involving studying awareness using TMS under supervision of Tom de Graaf in the lab of Alex Sack. Jim enjoyed this project so much that he then started to work as a research assistant for Tom de Graaf. Little did Jim know that one project in collaboration with Gregor Thut from the University of Glasgow, would later be the topic of his PhD project in Nijmegen. As part of the research master program in Nijmegen, students were encouraged to perform their research internship at different universities. Jim discovered an excellent opportunity to perform his internship combining TMS with EEG at the Donders Institute under supervision of Til Bergmann and Ole Jensen. This internship lead to writing the grant proposal that funded Jim's PhD to study the phasic role of alpha oscillations using brain stimulation techniques. After finishing his thesis, Jim started as a post-doctoral researcher in the lab of Heleen Slagter at the University of Amsterdam.

Acknowledgements

In 1675, Sir Isaac Newton wrote a letter to Robert Hooke, who would later become his rival, in which he said "If I have seen further, it is by standing on ye shoulders of giants". My PhD project wouldn't have been possible without standing on the shoulders of giants, two bearded giants to be precise. **Ole** (a.k.a. bearded giant #1, also Ragnar Lodbrok the 2nd), without you my PhD project wouldn't have been possible in the first place. You taught me how to be pragmatic while at the same time maintaining a high level of research quality. I felt very welcome in your group and knew I could always knock on your door regardless of how busy you were. Also thanks to **Freya**, **Oskar**, and **Felix** for welcoming me whenever I was at your place.

Bearded giant #2, **Til**, thank you for taking me under your wing as a master student and later co-writing the grant proposal together with Ole that would pay for my PhD project. You taught me how to properly do experiments, mostly involving complicated combinations of brain stimulation and neuroimaging, and to be extremely meticulous. I doubt I will ever be as precise and meticulous as you but I've hopefully picked up a thing or two. I enjoyed piloting our various crazy projects in the lab, dealing with 'smelly caps', and the numerous discussions we had over a cup of coffee in the old library at the DCCN.

It goes without saying that my interest in brain stimulation research started at Maastricht University when I performed a TMS project supervised by **Tom de Graaf** in the 2nd year of my Psychology Bachelors program. **Tom**, thanks for supervising me so well and, together with **Alex Sack**, feeding my interest in brain stimulation and allowing me to work for you during my time in Maastricht.

During my time as a PhD student we thought up (and piloted) many crazy projects involving brain stimulation. Although only a few turned into real projects, none of these would have been possible without support from the excellent technical group at the DCCN lead by **Erik**. Most thanks go to **Uriel** for spending countless hours on designing and building many devices to suit our usually very specific needs. I enjoyed our discussions on these devices and learned a lot about circuit design and hardware programming in the process. I also liked our coffee-table discussions on the many fun things about being a parent. Many thanks to **Marek, Mike,** and their minions for keeping the IT infrastructure up to date and helping out during the many fieldtrip and brain stimulation toolkits.

Apart from technical support, no research project can be completed without a bunch of administrative work. For keeping that as streamlined as possible, I would like to thank **Nicole** and **Sandra** for dealing with my many administrative questions and dealing with my subjects' paperwork. Also, special thanks to **Tildie** for helping arranging the Fieldtrip and brain stimulation toolkits as well as always helping with travel arrangements.

A large part of my time as a PhD student was spent in the brain stimulation lab. **Tom**, and later **Sophie**, we've spent many hours together in the lab testing various different stimulation protocols, montages, phantom coils, etc., usually accompanied by many cups of tea and coffee. I enjoyed this very much and I learned the very important lesson that regardless how many hours you schedule for your pilot, you are always only able to record 10 minutes of data. Also, I learned that torturing subjects is fine, as long as they are your colleagues (sorry **Tom** ;-)). I'd also like to thank **Rocio** for helping during the TMS-EEG experiments.

When I started at the DCCN, the brain stimulation lab was just being revitalized in collaboration with the RUMC. I started at the best possibly moment as I felt I could help start-up the brain stimulation community at the DCCN. There now is a fantastic brain stimulation lab in place that I am proud of. I would, therefore, also like to thank the original brain stimulation crew for setting up this amazing lab and being part of the 'brain stimulation meeting', which **Til, Lennart, Tom,** and I set up. From the UMC, thanks to **Moniek, Arno, Sumientra,** and **Dick** for being part of the amazing brain stimulation community and joining the early brain stimulation meetings (unfortunately abbreviated to BS-meetings). Special thanks to **Lennart** for your contribution in setting up the BSM and brainstorming on how to best deal with TMS-EEG artifacts. Your work lay the foundation for the TMS-EEG artefact rejection pipeline.

Related to the above I would like to thank **Til** and **Lennart** for starting the brain stimulation toolkit series. I think we had an amazing combination of brain stimulation researchers which made it the perfect time to initiate such a toolkit. Thanks to **Ian, Dilene,** and **Tom** for later taking over organizing the toolkit after **Til** and **Lennart** left.

My thesis wouldn't have been possible without the help of two amazing master's students: **Sam Chota** and **Jerome Herpers**. Without your help, I'm sure I wouldn't be able to have finished on time and I would miss out on some very cool projects. I'm glad you both found very interesting PhD positions and hope to work with you in the future. Thanks!

My analyses wouldn't have been possible without the help of the awesome **FieldTrip** team. Special thanks to **Robert** and **Jan-Mathijs** for the interesting and fun discussions (and dinners & beers). My time as member of the FieldTrip team was very enjoyable and I learned a lot. Thanks to all of the Fieldtrip team members over the years!

My time at the DCCN would have been rather boring without the many coffee table and lunch discussions on different topics both related, and unrelated, to work. I particularly enjoyed the lunch and coffee breaks in the old library. In no specific order, I'd like to thank the following people for making these enjoyable: **Tom, Til, Lennart, Rene, Anke Marit, Flora, Ruben, Mirjam, Miriam, Stephen, Eelke, Sophie, Freek, Sebo, Annelies, Tim, Lisa, Vincent.** Special thanks also to **Verena** & **Eelco** for the many fun dinners and occasional babysitting Dante. Also thanks to **Nietzsche** for the fun dinners and helping painting our house!

Also, many thanks to the members of Ole's group over the years. Some might overlap with the lunch/coffee group (in the order stolen from the neuosc website); **Mathilde (+ Guillaume & Mia), Rene S, Jan, Tobias, Tom, Sara, Saskia, Niels, Marieke, Bart, Maarten, Linda, Cecillia, Lisa, Iske, Sam, Jerome, Madelon, Haiteng, Lin, Tzvetan, Sophie, Rene (ter Poorten), Mats, Anne, Rodolfo, Jörn**, **Eelke, Freek, Diego, Rocio, Verena, Ali B, Ester, Stephen, Johanna, and Til.**

I spent my time at the DCCN in four different offices. Starting as an intern in 0.98 moving one or two offices further as an RA in the office of **Racim** and **Peter K.**, onward to other side of the building as a PhD student sharing an office with **Daniel, Erik,** and **Peter S.** At the end of the DCCN rebuild I moved to my final office 2.214 and shared an office with **Silvy** and **Mieke**, and later **Bob.** Thanks to all of my office mates over the years for making my time as a PhD student more enjoyable. I'd also like to thank my new colleagues at the UvA for welcoming a Limburger into the scary Randstad.

Now, on to my dearest paranymphs. Ladies first, **Martine** we already were colleagues at the Donders Institute but we didn't know each other that well. If that were the case, I would've advised you already back then against starting a tACS study. Now you are my officemate and my paranymph I'll try my best to warn you in the future. Thanks for being my paranymph and I'm happy to have you as my officemate.
Jörn, back then we were the only two in Ole's group living in Kleve. When I helped you as Ole's RA we decided to try carpooling together. We soon became good friends and we still are even though Michelle and I moved all the way to Amstelveen. I'm glad to have met you and **Anne** and am thankful that you are my paranymph.

Uit het mooie Nirbik zou ik ook graag **Tom & Annebel** en **Roy & Eva (en Fin)** willen bedanken voor de vele leuke tijden. Het is natuurlijk jammer dat we niet meer bij elkaar in de buurt wonen maar ik hoop dat we ondanks dat nog lang vrienden zullen blijven.

Vanzelfsprekend zou ik ook graag mijn Belgische familie willen bedanken voor het verwelkomen van 'nen Hollander' in jullie familie. Bedankt **Opa, Oma, Billy, Jo, Anja Sandra, Danny, Xena,** en **Indi** en **Skylar.**
Jetzt möchte ich mich gerne noch bei meiner Deutschen Familie herzlich bedanken für alle Liebe und allen Spaß der letzten Jahren. Ich bin sehr gerne ein Teil eurer Familie und möchte mich auch bei euch bedanken für die Unterstützung in den letzten Jahren: **Beate, Ralf, Keshia, Opa Siegfried, Oma Waltraud, Tina, Detlef, Hella, Sieghard**, **Jana,** und **Marie.**
Many thanks as well to my family and friends overseas. If anything, you all provided a safe haven to relax during my, as well as Michelle's, stressful PhD period. Special thanks to **Dad, Leigh Ann, Grandpa, Grandma,** and of course **Aunt Laura, Uncle Ethan, Tracy, Dustin, Travis, Amelia, Uncle Barry, Aunt Angie, Uncle Reggie, Aunt Lisa, Aunt Robin, Brandy, Brystol, Josie, Tommy, Brady, Abby,** for welcoming us all into the family even though we do not see each other that often.
Also thanks to our friends from Philadelphia, **Denice, Cevin & K.C.,** and **Sally & Dave.**

Natuurlijk zou ik nooit zover gekomen zijn zonder alle liefde en ondersteuning vanuit mijn familie. **Mam, Ellie,** en **Jaime,** jullie zijn er altijd voor me geweest en daar ben ik enorm dankbaar voor. Weet dat ik er ook altijd voor jullie zal zijn, ook al woon ik zo ontzettend ver weg (dat is sarcastisch, 2 uur is niet zo ver weg). **Mam,** we hebben het vroeger niet altijd breed gehad. Toch heb jij er altijd voor gezorgd dat wij niks te klagen hadden (Natuurlijk klaagden wij, want we waren kinderen). Dank je om er altijd voor ons te zijn en het voor mij mogelijk te maken om nu uiteindelijk mijn proefschrift te verdedigen. **Ellie,** aller-een-van-mijn-twee-liefste zusje van mij, ik kan me nog goed herinneren dat ik een telefoonboek van jou tegen mij aangegooid kreeg. Gelukkig maken ze die tegenwoordig niet meer. Zoals het hoort tussen broer en zus maakten we af en toe ruzie, toch zou ik de tijd met jou niet willen missen en ben ik blij dat jij mijn zusje bent en **Hailey** mijn nichtje is! **Jaime,** jij bent er altijd voor ons geweest, ook al was je er niet. Je bent nog steeds vaker thuis dan ik alhoewel je de meeste tijd van het jaar ergens aan het cruisen bent. Ik ben ook heel dankbaar dat jij mijn zus bent en dat ik samen met **Ellie** het toch echt wel goed getroffen heb. **Romel,** Nagpapasalamat ako dahil ikaw ang aking naging bayaw at mabuting kabiyak ng aking kapatid na si **Jaime**. Ikinagagalak ko na naging bahagi ka ng aking pamilya at ganun din ako sa iyo. Batid ko na hindi madali ngunit sana ay magkaroon tayo nang mas madami pang pagkakataon na magkasama sama, makapagkulitan at tawanan. Maraming salamat pogi!

Ik heb regelmatig gezegd dat er niet veel rationele redenen zijn om kinderen te krijgen; ze kosten veel geld, moeite en bezorgen vaak slapeloze nachten. Toch zou ik niet meer zonder jou kunnen, **Dante**. Je bent nu nog te jong om dit te begrijpen maar door jou probeer ik een beter persoon en dus een goede vader te zijn. Ik kijk uit naar de komende jaren om je verder op te zien groeien (ondanks dat je zeker nog vaak het bloed onder mijn nagels vandaan gaat halen).

Michèlle, als er een iemand is die ik moet bedanken voor mijn tijd als PhD student dan ben jij het. Jij hebt mij uit mijn comfort zone getrokken en dankzij jou ben ik in Nijmegen begonnen en uiteindelijk in Amsterdam terecht gekomen. Door jou probeer ik het beste uit mezelf te halen en ik zie ook nog eens een beetje van de wereld. Ik schrijf dit nu vanuit onze hotelkamer in Las Vegas terwijl jij daar de Bronco's wedstrijd kijkt. Ik ben blij dat ik in jouw mentale ondersteuning heb gevonden en een reispartner (eerder reisleidster, laten we eerlijk zijn ☺) en ik ben zeker dat we samen nog een mooie toekomst tegenmoet gaan. **Michèlle,** ik hou van je!

I would like to end these acknowledgements with a quote that helped me through many boring moments during my PhD:

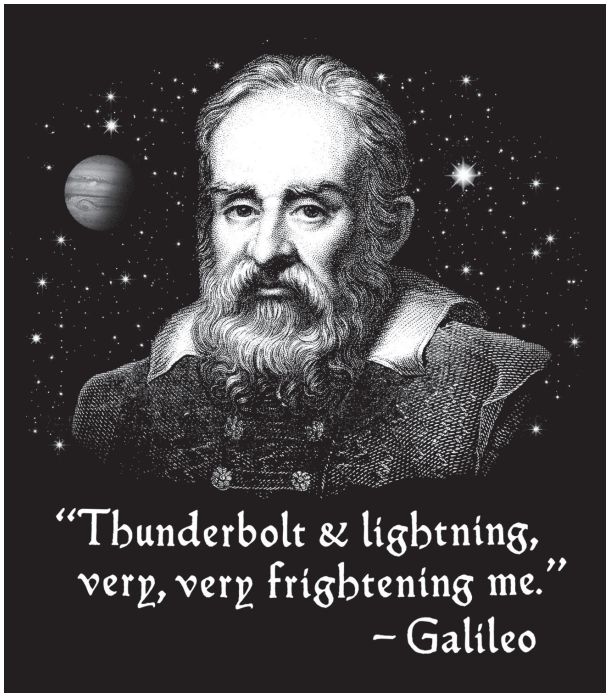

DONDERS
INSTITUTE

ISBN 978-94-6284-120-8

Radboud University Radboudumc